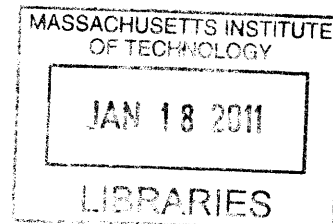# The Hemo-Neural Hypothesis: Effects of Vasodilation on Astrocytes in Mammalian Neocortex

by

Rosa Cao

B.A. Physics/Biology, University of Chicago, 2003

Submitted to the Department of Brain & Cognitive Sciences in Partial Fulfillment of the Requirements for the Degree of

DOCTOR OF PHILOSOPHY IN NEUROSCIENCE
AT THE
MASSACHUSETTS INSTITUTE OF TECHNOLOGY
FEBRUARY 2011

Author:_____

Department of Brain and Cognitive Sciences
January 7, 2010

Certified l _____

Christopher I. Moore
Associate Professor of Neuroscience
Thesis Supervisor

Accepted by:_____

Earl K. Miller
Picower Professor of Neuroscience
Director, BCS Graduate Program

The Hemo-Neural Hypothesis: Effects of Vasodilation on Astrocytes in Mammalian Neocortex

by

Rosa Cao

Submitted to the Department of Brain & Cognitive Sciences in
Partial Fulfillment of the Requirements for the Degree of Doctor of Philosophy in Neuroscience

ABSTRACT

Astrocytes play an important role in regulating neuronal activity and local brain states, in part by serving as intermediaries between neurons and vasculature. We postulate that neurons and astrocytes are sensitive to biophysical conditions in their local environment, in addition to their participation in traditional signaling networks with other neurons. Mechanically sensitive astrocytic endfeet ensheathe cerebral blood vessels, which change size in order to regulate blood flow.

We found that changes in local biophysical state caused by mechanical perturbations exerted through blood vessels can depolarize astrocytes and some neurons in slice. To test the hemoneural hypothesis in vivo, we developed a means of inducing dilation using the SUR2B receptor agonist pinacidil, which is specific to vascular smooth muscle. It was important to ascertain that pinacidil had no direct effect on astrocytes or neurons, and we confirmed this in whole cell recordings in cortical slices.

We then used two-photon imaging to visualize astrocytic calcium dynamics in vivo while manipulating vasodilation in vivo. Pinacidil caused a 10-20% dilation in most vessels, a degree of dilation of similar magnitude to those naturally evoked by persistent sensory stimulation (e.g. in fMRI studies). We found that increases in pial arteriole diameter could occasionally evoke traveling calcium waves in astrocytes. We also saw consistently slow increases (which took tens of seconds to onset, and persisted for minutes) in astrocytic calcium levels at both endfeet and soma in cortical layer 1, corresponding to vessel dilation. When vessels partially reconstricted due to pinacidil washout, calcium levels also showed a relative decrease. At short time scales (from 0.5 – 5 seconds) we saw strong correlations (>0.5) between small fluctuations in astrocytic calcium levels (1-3%) and vessel diameter (1-3%). Fluctuations in vessel diameter predicted similar fluctuations in astrocytic calcium, as often and as strongly as the reverse, suggesting feedback regulation between vascular diameter and astrocytic calcium activation levels.

Thesis supervisor: Christopher I. Moore
Title: Associate Professor of Neuroscience

Acknowledgements

Briefly, because those I wish to thank most know who they are and how much they've given in making it possible for me to finish this PhD:

My heartfelt thanks go to:

My advisor Chris Moore for generous open-mindedness, patience, and endless good humor; Josh Brumberg for opening doors to me and for me in his incredibly efficient (in every respect) lab; and Mriganka Sur for giving me an opportunity in the very beginning and making sure that I benefited from his excellent advice and support all the way to the end; Philip Haydon for teaching me about astrocytes before I ever thought to meet him in person, and Mark Bear, especially for making it to my defense in the middle of the holidays after a snowstorm.

Labmates who helped rather than hindered: for tolerance, teaching, Team Free Food, (especially Ulf Knoblich for his golden touch in making balky equipment lie down and purr, Jason Ritt for the care and feeding of old computers at critical junctures, and Alexis Bradshaw for her superogatory facilitation of lab function and improvement of lab life), and of course, friendship.

Raddy Ramos, Andrei Kozlov, Sava Sakadzic, James Schummers and everyone else who has given valuable time and scientific advice, as well as the many wonderful people I've learned from at MIT and elsewhere: Pawan Sinha, Yuri Ostrovsky, Ania Majewska (a fantastic role-model and teacher), Philip Ulinski, Ann Graybiel, Gadi Geiger, Gerald Schneider, Johannes Haushofer, Terra Barnes, Tom Byrne, Leon Trilling, Lana Ruvinskaya, Simon Overduin, Talia Konkle, Sam Cooke, and Nikhil Bhatla.

Lindy and Paymon for teaching me MATLAB, statistics, and how to stay up all night; Ana, my fellow traveler through graduate school, gym buddy, and friend; The Tech(ies), for all the awe-inspiring examples of how to get far too much done in far too little time; Matt (obscure papers in Harvard libraries), Barun and Kate (untangling me from the blue), KTSam, and Lizard, for a home away from home.

My parents, Evelyn, Marion and Sam for tough and not-so-tough love; Turbocat and her owner for so many things that words fail me, but every one of them appreciated; and Vera, my best friend who offered unstinting support through graduate school as through everything else.

Philosophers all for reminding me why neuroscience is the most exciting field in the world, especially William Wimsatt, Sean Kelly, Peter Godfrey-Smith, and Daniel Dennett.

Chapter 1

Introduction

Neuroscience is the study of neurons, but understanding the brain and its capacities requires more than the understanding of neurons alone. The brain also encompasses systems of glial cells and vasculature, which may be described as separate self-contained systems as a convenient simplification, but which clearly interact with neurons in meaningful ways. Vascular smooth muscle (VSM), astrocytes and neurons share many of the same functions, sensitivities and signaling molecules (Carmeliet 2003). Astrocytes have been shown over the last twenty years to be involved in interactions with neurons that impact almost every aspect of neural function, from plasticity to behavior.

Astrocytes regulate the stimulus-driven increase in blood flow known as functional hyperemia, in response to the activity and metabolic condition of the surrounding tissue. In that role, they may act as a buffer to protect neurons from fluctuations in biophysical variables induced by rapidly changing blood flow. While we do not yet understand the exact mechanism and significance of many of these interactions, it would be hard to deny that neurons live in an environment shaped by local conditions internal to the brain, to which they are sensitive as well as to the environment external to the body, and that part of the total environment is shaped by glia and vasculature.

This thesis will focus on the impact of blood flow on astrocytes, which has not previously been examined as a potential source of functional modulation in the brain (though not ignored in the context of ischemia or other pathological dysfunction). Because bidirectional interactions are a widespread (perhaps universal) feature of biological regulatory systems, we have reason to suspect that feedback from blood vessels may play a role in the modulation of astrocytic and neural activity.

That astrocytes physically bridge neurons and vasculature lends support to the hypothesis that they play a bidirectional role. On the neural side of this bridge, astrocytic processes surround

synapses, while on the vascular side, astrocytic endfeet ensheathe cerebral arteries and arterioles (Zonta 2002). On both sides, astrocytes have what might be called "receptors" and "effectors," allowing them to both sense the local environment and manipulate it. Astrocytes are thus positioned to act as transducers, allowing changes in blood flow to exert modulatory effects on neurons. To test whether they indeed function in such a capacity, we have to establish whether they are responsive to vascular dynamics. While the question of astrocytic sensitivity to the vasculature has its own intrinsic merit, discovering that astrocytes are responsive to vasculature is an important step towards demonstrating one way in which neurons could be impacted by vascular changes, given the already well-established sensitivity of neural function to astrocytic modulation.

Astrocyte-Neuron Interaction

Astrocytes are sensitive to neural activity through a variety of potential mechanisms, and can in turn regulate neurons through a variety of potential mechanisms. Astrocytes have glutamate receptors, allowing them to detect synaptic activity. They are able to modulate neural activity by releasing neuroactive substances, including glutamate (excitatory), adenosine (inhibitory), D-serine (inhibitory), and TNF-alpha (involved in homeostatic regulation of plasticity). Furthermore, at least some of these neuromodulatory effects have been shown to have behavioral consequences (Halassa 2010) It remains controversial whether the substances are released via vesicle fusion, as in exocytosis in neurons, or by another mechanism (Hamilton 2010). Astrocytes are also able to regulate neural transmission and plasticity by modulating their rate of neurotransmitter uptake: activity of astrocytic glutamate, GABA and glycine transporters are key determinants of the concentration of these transmitters in the synapse (Haydon 2001, Nedergaard 2003, Perea 2007).

Astrocyte-Vascular Interaction

Through their endfeet, astrocytes can act as vascular effectors. Endfeet are in direct communication with smooth muscle cells through the basal lamina, allowing them to control vascular tone, and release a variety of signaling molecules to which the smooth muscle is responsive. Vasodilators include prostaglandin PGE_2, the arachidonic acid metabolite EET, adenosine, vasoactive intestinal peptide (VIP), nitric oxide (NO), carbon monoxide (CO), and

release of potassium ions into the extracellular space. Vasoconstrictors include endothelin-3, thromboxane receptor agonists such as U46619, neuropeptide Y (NPY), somatostatin, other arachidonic acid metabolites such as 20-HETE, and other prostaglandins, such as PGF-2α (Haydon 2006, Iadecola 2007, Straub 2007, Koehler 2008).

Other agents appear to have effects whose polarity depends on the state of the tissue and vasculature. For example, the mGluR receptor agonist t-ACPD consistently raises calcium levels in astrocytes. However, the effect of the evoked astrocytic calcium increase depends on vascular tone (Blanco 2008). When vessels are already dilated, t-ACPD can cause constriction, whereas vessels pre-constricted to 30-40% of baseline show dilation. Gordon (2008) showed that the polarity of the vascular response to uncaging of calcium in astrocytic endfeet depends on the oxygen saturation level in the tissue. When pO_2 is low, endfoot activation results in vasodilation, whereas when pO_2 is high, endfoot activation results in vasoconstriction.

These results suggest that astrocytes may be functionally responsive to vascular dynamics and related local tissue state. However, they are also consistent with the hypothesis that vascular smooth muscle reactivity depends on pO_2 or vessel tone, rather than astrocytes. In this alternate scenario, the polarity reversing effects of astrocytes on the vasculature would be due to a difference in the vascular reactivity to astrocytic signaling, rather than due to a difference in the astrocytic signaling itself. In sum, astrocytes are able to control the vasculature in a state-dependent way, but it remains an open question whether this context-dependent impact reflects their integration of signals from the vasculature in astrocytes themselves.

In support of the scenario in which astrocytes modulate their signaling in response to local conditions, Girouard (2010) showed that the magnitude of calcium increase in an endfoot can also change the polarity of the vascular response. Whereas "modest" increases in calcium level (300-400 nM) cause vasodilation, larger increases (700-800 nM) caused vasoconstriction. These calcium amplitude effects appeared to be independent of whether calcium was raised by direct photolytic uncaging in the endfoot or indirectly by electric stimulation of nearby neurons.

Are Endfeet or Somata the Functional Units in Astrocytes and Astrocytic Networks?

Astrocytic activation and its downstream effects rely on elevation in internal calcium levels. Within a given astrocyte, calcium elevations propagate across adjacent processes, though they often do not involve the entire cell. As one example, more calcium activity has been observed in endfeet than in astrocytic soma following sensory stimulation in barrel cortex (Wang 2006). A possible cause of endfoot calcium increases could be signals resulting from vascular dilation, and/or internally generated signals meant to modulate the blood flow.

Inter-astrocyte signaling has also been observed in the form of traveling calcium waves, a robust phenomenon in brain slice and culture. Evidence indicates they propagate via extracellular ATP signaling (Arcuino 2002). There is dispute as to how often these waves occur *in vivo*, and whether they result from non-physiological conditions (e.g. photo damage from imaging) (Agulhon 2008). Astrocytes can also transfer ions and other molecules through selective connexin mediated gap junctions (Giaume 2010).

The varied effects of increases in astrocytic calcium levels appear to depend on the particular astrocytic compartment in which calcium rises. As one example, it is not known whether endfoot calcium increases are merely local control elements that interact only with the blood vessel, or whether the elevated calcium can propagate to the rest of the cell to affect neural activity at the synapse. Similarly, there may be astrocyte-to-astrocyte spread of calcium waves that do not propagate to the end of all astrocytic processes. If, however, there is functional communication between the vascular end of the astrocyte and the neuronal end, we should expect to see traveling waves that proceed from the endfeet to the somata, and we would predict an impact of vascular dynamics on neuronal function – i.e. hemoneural effects via astrocytes.

State of Understanding of Vascular-to-Astrocytic Signaling

The recent studies described above (Blanco 2008, Gordon 2008, as well as Newman 2006 in retina) suggest that astrocytes are functionally responsive to vascular and hemodynamically-controlled variables in the local tissue state, meaning there are "communication pathways" from vasculature to astrocytes. Thus far, none of the observations regarding astrocytic sensing of

vascular signals have been made *in vivo*, none have been made in the neocortex, and the impact of vascular events on calcium levels per se have not been tested. Most importantly, the impact of actual vasodilatory events—as opposed to static changes in dilation or oxygen tension levels—have not been assessed. As such, the relevance of functional hyperemia (or related faster time scale changes) per se has not been tested. Crucial to this question is the latency between vascular signals and subsequent astrocytic responses. Responses on the order of <1-2 seconds have the potential for impacting ongoing information processing, while slower ones are more likely to be involved in structural plasticity changes or metabolic regulation.

Many possible mechanisms could support vascular-to-astrocytic communication. One that has direct experimental support is a mechanosensitive pathway. Astrocytes express mechanosensitive channels (Niggel 2000), and mild mechanical stimulation reliably evokes calcium waves (Blomstrand 1999). It has been shown in the hippocampus (Angulo 2004) and olfactory bulb (Kozlov 2006) *in vitro*, that experimentally generated pressure waves in blood vessels increase the occurrence of slow inward and slow outward currents in astrocytes. As such, a mechanosensitive pathway appears to exist, though many other sensing mechanisms (e.g., of pO_2 levels) are implicated by prior data, and also serve as a potential means for vascular-driven calcium increases in local astrocytes.

One reason there are few studies thus far detailing astrocytic sensitivity to vascular signaling has been the lack of a conceptual framework predicting such interactions until recently (Filosa 2007; Moore 2008; Gordon 2008). A second impediment to progress on this topic has been the lack of adequate methods for independently manipulating the vasculature. As described in Chapter 2, I have developed and proven specific a means for this form of selective vascular control (Cao 2009).

Overview of Thesis and its Import

The goal of my thesis work has been to develop a detailed description of the hemo-neural hypothesis (Moore 2008), to develop means for testing this hypothesis (Cao 2009), and to test a key aspect of this broad proposal, the prediction that astrocytes can detect vascular motion, as indexed by astrocytic calcium levels.

While searching for a way to test the hypothesis, we found that almost all vasodilators (e.g. NO) and vasoconstrictors (e.g. chromakalim) are non-specific, either because they directly affect astrocytes and neurons as well as blood vessels, or because they affect vasculature by manipulating astrocytes and/or the whole brain environment (e.g. acidosis).

Pinacidil (N-cyano-N'-pyridin-4-yl-N''-(1,2,2-trimethylpropyl)guanidine) was the one exception we found, offering a way to induce hyperemia through independent control of vascular smooth muscle tone. Wahl (1989) showed that pinacidil dilates pial arterioles *in vivo*. Pinacidil exerts these effects through activation of the SUR2B subtype K_{ATP} channel, expressed only in vascular smooth muscle and possibly endothelial cells. The K_{ATP} channel expressed in neurons and astrocytes is the SUR1 subtype, and possibly the SUR2A subtype (Aguilar-Bryan 1998). Whereas SUR1 channels can only be driven by high pinacidil concentrations (in the millimolar range), SUR2B is activated by nanomolar concentration pinacidil. Opening potassium channels depolarizes vascular smooth muscle cells, causing vessel walls to relax and dilate under internal pressure. Using pinacidil, we were able to test whether astrocytes respond to the state of the vessels they are regulating.

Vascular-astrocytic interactions are interesting for two basic reasons. First, astrocytes can modulate neural activity on timescales relevant to plasticity and information processing. Unless there is some compelling reason to believe that astrocytes are functionally divided into vascular and neural compartments that have no effect on each other, we would expect that modulation of astrocytic activity would also lead, at least in some cases, to modulation of neural activity. Second, independent of (any) neuronal affects, the discovery of a new mode of communication from vasculature to astrocytes has implications for understanding homeostatic control of hemodynamics.

Outline

Chapter 2 of the thesis will describe the hemo-neural hypothesis in general, with a more specific elaboration of the literature review of astrocytic-vascular interactions and possible mechanisms. This was previously published as Moore (2008).

Chapter 3 of the thesis will report our method for controlling vasodilation in the brain using pinacidil, a pharmacological agent that does not have direct effects on astrocytes and neurons but that dilates cerebral arteries through modulation of smooth muscle. This work reflects *in vivo* optical imaging and *in vitro* slice physiology in neurons and astrocytes I conducted. This Chapter will derive in large part from Cao (2009).

Chapter 4 will report novel findings with respect to the effects of vasodilation on astrocytes using two-photon imaging to simultaneously record vascular dynamics and astrocytic calcium levels in distinct compartments (endfeet and somata). The data I have accumulated indicate that astrocytic calcium levels are impacted by vasodilatory events of a relevant (non-pathological) physiological size.

References

Carmeliet P. Blood vessels and nerves: common signals, pathways and diseases. *Nat Rev Genet* 4: 710–720, 2003.

Zonta M, Angulo MC, Gobbo S, Rosengarten B, Hossmann KA, Pozzan T, Carmignoto G. Neuron-to-astrocyte signaling is central to the dynamic control of brain microcirculation. *Nat Neurosci* 6: 43–50, 2002.

Halassa, M. and Haydon, Philip G. "Integrated brain circuits: astrocytic networks modulate neuronal activity and behavior," *Annual Review of Physiology* 72 (March 17, 2010): 335-355.

Hamilton, N. and Attwell D. Do astrocytes really exocytose neurotransmitters? *Nature Reviews Neuroscience* 11, 227-238 (April 2010)

Haydon, Philip G., Glia: listening and talking to the synapse. *Nat. Rev. Neurosci.* 2 (2001), pp. 185–193

V. M. Blanco, J. E. Stern, and J. A. Filosa, "Tone-dependent vascular responses to astrocyte-derived signals," *AJP: Heart and Circulatory Physiology* 294, no. 6 (2, 2008): H2855-H2863.

Gertrudis Perea and Alfonso Araque; Astrocytes Potentiate Transmitter Release at Single Hippocampal Synapses. *Science 317 (5841), 1083 (2007).*

Maiken Nedergaard, Bruce Ransomm, and Steven A. Goldman (2003). New roles for astrocytes: Redefining the functional architecture of the brain. *Trends in Neurosciences. Volume 26, Issue 10, Pages 523-530*

Philip G. Haydon and Giorgio Carmignoto; Astrocyte Control of Synaptic Transmission and Neurovascular Coupling. *Physiol. Rev. 86: 1009-1031, (2006).*

V. M. Blanco, J. E. Stern, and J. A. Filosa, "Tone-dependent vascular responses to astrocyte-derived signals," *AJP: Heart and Circulatory Physiology* 294, no. 6 (2, 2008): H2855-H2863.

Metea MR, Newman EA., "Glial Cells Dilate and Constrict Blood Vessels: A Mechanism of Neurovascular Coupling," *J. Neurosci.* 26, no. 11 (March 15, 2006): 2862-2870.

Gordon G., Choi, H., Rungta, R., Ellis-Davies G., & MacVicar, B., "Brain metabolism dictates the polarity of astrocyte control over arterioles," *Nature* 456, no. 7223 (December 11, 2008): 745-749.

Wang X, Lou N, Xu Q, Tian GF, Peng WG, Han X, Kang J, Takano T, Nedergaard M. Astrocytic Ca^{2+} signaling evoked by sensory stimulation in vivo. *Nat Neurosci* 9: 816–823, 2006

Arcuino G, Lin JH, Takano T, Liu C, Jiang L, Gao Q, Kang J, Nedergaard M. "Intercellular calcium signaling mediated by point-source burst release of ATP," *Proceedings of the National Academy of Sciences of the United States of America* 99, no. 15 (July 23, 2002): 9840-9845.

Agulhon C, Petravicz J, McMullen AB, Sweger EJ, Minton SK, Taves SR, Casper KB, Fiacco TA, McCarthy KD , "What Is the Role of Astrocyte Calcium in Neurophysiology?," *Neuron* 59, no. 6 (September 25, 2008): 932-946.

Giaume C, Koulakoff A, Roux L, Holcman D, Rouach N., "Astroglial networks: a step further in neuroglial and gliovascular interactions," *Nat Rev Neurosci* 11, no. 2 (February 2010): 87-99.

Angulo MC, Kozlov AS, Charpak S, Audinat E., "Glutamate Released from Glial Cells Synchronizes Neuronal Activity in the Hippocampus," *J. Neurosci.* 24, no. 31 (August 4, 2004): 6920-6927.

A.S. Kozlov, M.C. Angulo, E. Audinat and S. Charpak, Target cell-specific modulation of neuronal activity by astrocytes, *Proc. Natl. Acad. Sci. USA 103 (2006)*

Hua SZ, Gottlieb PA, Heo J, Sachs F, "A mechanosensitive ion channel regulating cell volume," *Am J Physiol Cell Physiol* 298, no. 6 (June 1, 2010): C1424-1430.

J. Niggel, W. Sigurdson, and F. Sachs, "Mechanically Induced Calcium Movements in Astrocytes, Bovine Aortic Endothelial Cells and C6 Glioma Cells," *Journal of Membrane Biology* 174, no. 2 (March 24, 2000): 121-134.

Blomstrand F, Khatibi S, Muyderman H, Hansson E, Olsson T, Rönnbäck L., "5-hydroxytryptamine and glutamate modulate velocity and extent of intercellular calcium signalling in hippocampal astroglial cells in primary cultures," *Neuroscience* 88, no. 4 (February 1999): 1241-1253.

Girouard H, Bonev AD, Hannah RM, Meredith A, Aldrich RW, Nelson MT., "Astrocytic endfoot Ca2+ and BK channels determine both arteriolar dilation and constriction," *Proceedings of the National Academy of Sciences* 107, no. 8 (February 23, 2010): 3811-3816.

Moore, C. I. and Cao, R. *The Role of Blood Flow in Information Processing*, Journal of Neurophysiology, May 2008

Cao, R., Higashikubo BT., Ramos, R., Nelson, MT, Brumberg, J., Moore, CI., *Pinacidil Provides a Selective Means for Induction of Vascular Dilation*, Cleveland Clinic Journal of Medicine, March 2009.

Michael Wahl, The effects of pinacidil and tolbutamide in feline pial arteries in situ. *Eur J. Phys 1989*

Aguilar-Bryan L, Clement JP 4th, Gonzalez G, Kunjilwar K, Babenko A, Bryan J., "Toward Understanding the Assembly and Structure of KATP Channels," *Physiol. Rev.* 78, no. 1 (January 1, 1998): 227-245.

Sato TR, Gray NW, Mainen ZF, Svoboda K., "The Functional Microarchitecture of the Mouse Barrel Cortex," *PLoS Biol* 5, no. 7 (July 10, 2007): e189.

Chapter 2

The Hemo-Neural Hypothesis:
On the Role of Blood Flow in Information Processing[a]

Abstract

Brain vasculature is a complex and interconnected network under tight regulatory control that exists in intimate communication with neurons and glia. Typically, hemodynamics are considered to exclusively serve as a metabolic support system. In contrast to this canonical view, we propose that hemodynamics also play a role in information processing through modulation of neural activity.

Functional hyperemia, the basis of the fMRI BOLD signal, is a localized influx of blood correlated with neural activity levels. Functional hyperemia is considered by many to be excessive from a metabolic standpoint, but may be appropriate if interpreted as having an activity-dependent neuro-modulatory function. Hemodynamics may impact neural activity through *direct* and *indirect* mechanisms. Direct mechanisms include delivery of diffusible blood-borne messengers, and mechanical and thermal modulation of neural activity. Indirect mechanisms are proposed to act through hemodynamic modulation of astrocytes, which can in turn regulate neural activity.

These hemo-neural mechanisms should alter the information processing capacity of active local neural networks. Here, we focus on analysis of neocortical sensory processing. We predict that hemodynamics alter the gain of local cortical circuits, modulating the detection and discrimination of sensory stimuli.

This novel view of information processing—that includes hemodynamics as an active and significant participant—has implications for understanding neural representation and the construction of accurate brain models. There are also potential medical benefits of an improved understanding of the role of hemodynamics in neural processing, as it directly bears on interpretation of and potential treatment for stroke, dementia and epilepsy.

Introduction

The brain contains a remarkably rich and inter-dependent network of neurons, whose activity is well correlated with information processing. The study of this network has been the focus of modern neuroscience (Ramon y Cajal 1996). The brain also contains a rich and inter-dependent vascular network, whose 'activity'—blood flow—is typically well correlated with neural activity. Based primarily on knowledge of anatomy, Aristotle believed that the vasculature was the biological system that manifested its activity in intelligence, emotion and action (Gross 1998). In contrast, the standard modern view of blood flow is that it serves a physiological function unrelated to information processing, such as bringing oxygen to active neurons, eliminating 'waste' generated by neural activity or regulating temperature. Except in extreme cases of cell damage or death, current hypotheses do not include blood flow as a contributor to shaping neural activity. Realistic computational models of brain function do not include blood flow as a component, and neurophysiologists do not consider it as a regressor to explain variance in their data.

In contrast to this canonical position, we propose the hypothesis that hemodynamics play a role in information processing, through modulation of neural activity by blood flow. We predict that functional hyperemia, the 'overflow' of blood to a brain region during neural activity, provides a spatially- and temporally-correlated source of regulation, modulating the excitability of the local circuit. This shaping of the neural response will, in turn, impact representation.

The goal of this paper is to describe this alternative view of information processing, and to argue for the importance of incorporating this potential class of mechanism into our understanding of how different systems in the brain act in a synthetic manner. We focus our comments on the role

that hemodynamics may play in sensory neocortex, as this brain region is widely studied with regard to its information processing role and a great deal is known about its hemodynamic regulation. This focus is not meant to detract from the potential importance of hemo-neural interactions for processing in other brain areas, or in other contexts, as noted throughout.

A 'Turing Test' for Biological Information Processing Systems

In what is commonly regarded as the 'Turing Test' (Turing 1950), the capacity of a computer for intelligent, autonomous thought is judged by whether the machine can lead a blinded human observer, unbiased by direct knowledge of the correspondent, to judge it as intelligent. Borrowing this logic to begin our argument, we provide a 'Turing Test' for biological information processing systems. We ask whether, given the following list of traits, a scientist would predict that this 'anonymous' system plays a role in representation in the brain. The traits of this system are as follows:

- The system possesses a complex anatomical network in the brain
  - o This system shows micro-scale structure in all brain areas
  - o This system shows regional anatomical specializations that reflect information processing, such as layer-specific localization of pathway density in different neocortical areas.

- Activity in this system is co-modulated synergistically with activity in the known information processing network—the major neuromodulators such as acetylcholine (ACh), serotonin (5-HT) and norepinephrine (NE), for example, are key regulators of this system, and almost all factors that impact activity in this system also impact neural activity.

- Fine regulation of activity in this network is not tightly coupled to metabolic need

- Fine regulation of activity in this network is tightly coupled to neural information processing:
  - o The spatial and temporal pattern of activity in this system shifts with perceptual input, motor output, attention and cognitive performance.

- The spatial resolution of differential activity in this system can be as precise as single cortical columns or olfactory glomeruli.
- The temporal onset of activity in this pathway is within hundreds of milliseconds of the onset of neural information processing, with a duration similar to the time scales for neural phenomena considered important for information processing such as adaptation and synaptic depression
  - o Localized damage in this system leads to specific and predictable information processing deficits

Without the predisposition to view hemodynamics as only a mechanism for meeting metabolic need or other physiologic function, this anonymous description suggests that the vascular system, and its 'activity' expressed as blood flow, is poised to play a role in information processing through the directed modulation of neural activity.

The validity of this hypothesis depends on three points. First, whether the anatomy and physiological regulatory mechanisms can position hemodynamic signals spatially and temporally to have an impact on neural activity. Second, whether there are known correlations between information processing and changes in blood flow. Third, whether there are mechanisms by which changes in hemodynamics in the normal range of function can impact neural activity. In the following sections, we suggest that these basic criteria are met, and begin to present hypotheses as to the information processing role that such regulation may play.

The Interleaved Anatomy and Physiology of Hemodynamic and Neural Systems

Anatomical Specificity

The vascular pathways that regulate blood flow are finely articulated and inter-digitated with the neural architecture. These anatomical vascular patterns are not uniform, and in many cases reflect the information processing functionality of the brain area. In the neocortex, capillary density shows specificity in the 'vertical' dimension through enhanced concentration in specific layers, such as layer IV of primary sensory areas (Patel 1983; Woolsey et al. 1996; Zheng et al.

1991), in contrast to the flat laminar profile in the entorhinal cortex (Michaloudi et al. 2005). Further, the system shows 'horizontal' specificity within a cortical area, such as the segmentation of capillary beds to the 'barrels' of rodent somatosensory cortex or 'blobs' and 'stripes' of V1 (Patel 1983; Riddle et al. 1993; Woolsey et al. 1996; Zheng et al. 1991). Subcortical structures show similar apparent principles of distribution, as the striatum of the basal ganglia shows enhanced capillary density in the matrix as compared to the striosomes (Feekes and Cassell 2006). The olfactory bulb also shows localization of capillary density in the glomeruli (Borowsky and Collins 1989). Peripheral nerves and vessels are known to follow anatomically similar paths (Vesalius), with recent studies showing that nerves and peripheral vascular supply employ similar developmental guidance mechanisms (Carmeliet 2003; Eichmann et al. 2005).

Overlapping Physiological Regulation

When local populations of neurons are active, they recruit increased blood flow and volume to the activated region, a process known as 'functional hyperemia' (Grubb et al. 1974; Hoge et al. 2005; Kong et al. 2004; Martin et al. 2006; Roy and Sherrington 1890). Functional hyperemia can be induced and modulated by a variety of mechanisms, with the relaxation of smooth muscle around arteries and arterioles a principal final common pathway leading to changes in blood flow and volume. As discussed below, astrocytes are believed to be a primary route for detecting neural activity and engaging the vasculature. Recent evidence has also implicated neurons in the direct control of blood flow. In neocortex, interneurons directly contact vascular processes, and intracellular electrical stimulation *in vitro* of interneurons adjacent to vessels can evoke dilation or constriction (Cauli et al. 2004; Hamel 2006; Hirase et al. 2004; Vaucher et al. 2000).

The mechanisms that induce functional hyperemia typically also impact neural activity. Almost all chemical factors that are known to modulate blood flow directly or indirectly regulate neuronal function. Prime examples of this overlap are the major brainstem neuromodulatory inputs, such as ACh, 5-HT and NE. Single cholinergic projections, for example, target pyramidal neurons, local interneurons (which in turn impact vasculature), astrocytes and smooth muscles around vasculature, and modulate activity in each within a restricted zone (see (Hamel 2006) for a review). Dopamine is believed to play a similar role in frontal and somatosensory neocortex, with contacts targeted to vasculature within the cortical mantle, implying local synergistic

19

regulation (Krimer et al. 1998). Other factors known to directly regulate both networks include the freely diffusing molecule nitric oxide (NO), which relaxes smooth muscle (Palmer et al. 1987) and modulates neural activity in a variety of ways (see below). Processes from single interneurons and from astrocytes contact and impact neighboring neurons and nearby microvascular processes (Hamel; Haydon and Carmignoto 2006; Oberheim et al.; Zonta et al. 2003). These examples of local co-regulation imply fine-scale synergy in the function of neural and vascular networks.

These observations, that the anatomical organization of vascular networks map to known information processing subdivisions, and that blood flow 'activity' and neural activity share a wide range of local regulatory mechanisms, are obviously not arguments that compel an additional role for blood flow. Rather, they suggest that the anatomy and physiology of these two networks are positioned to function synergistically in information processing. As discussed in the next section, changes in blood flow correlate strongly with neural activity, but these correlations are not closely tied to fine-scale metabolic need.

Functional Hyperemia: Spatial and Temporal Correlation with Information Processing

Spatial Precision

The spatial resolution of functional hyperemia is widely debated, and likely varies as a function of context and brain area. In the somatosensory and visual neocortex, a general consensus exists that the pattern of increased blood flow is similar to that of subthreshold neural activity, with a peak in signal that is localized to a cortical column ($\sim$400 μm), and an extent spanning several columns (Dunn et al. 2005; Hess et al. 2000; Lauritzen 2001; Sheth et al. 2004; Vanzetta et al. 2004; Yang et al. 1998). This correlation is strongest when better localized comparisons are made between the flow delivered to the neocortical layers through small arterioles and capillaries. Large vessels that run over the surface of the cortical mantle, which contribute prominently to many imaging techniques, will typically provide artifactually large estimates of the spread of blood delivered to the tissue (Disbrow et al. 2000; Dunn et al. 2005; Duong et al. 2001; Sheth et al. 2004; Vanzetta et al. 2004).

Vertical specificity in the cortical pattern of functional hyperemia has also been observed. In the somatosensory neocortex, the peak flow rate evoked by sensory stimulation is localized to specific laminae (Gerrits et al. 2000; Norup Nielsen and Lauritzen 2001; Silva and Koretsky 2002). Evoked response amplitude and peak flow have also been correlated within cerebellar laminae (Akgoren et al. 1997). In other brain areas, evidence for more precise delivery has also been observed, as flow can be localized to a single glomerulus in the olfactory bulb during stimulus presentation (i.e., $\leq$ 100μm) (Chaigneau et al. 2003; Yang et al. 1998). Several potential mechanisms exist for fast and localized regulation of this type, ranging from direct neural control due to interneuron activation (Cauli et al. 2004; Hamel 2006) to pericyte control of vascular diameter in capillaries (Peppiatt et al. 2006).

Temporal Precision

Functional hyperemia is also temporally locked to neural activity onset. In the somatosensory neocortex, blood flow increases measured using laser Doppler have been observed less than 200 milliseconds after the onset of sensory-evoked neural responses (Matsuura et al. 1999; Norup Nielsen and Lauritzen 2001). Similarly, optical imaging techniques that integrate over local volumes at somewhat slower temporal resolution typically record a significant increase in flow within $\leq$500 msec of sensory stimulus presentation (Dunn et al. 2005; Malonek et al. 1997; Martin et al. 2006). The subsequent duration of these increases is often viewed as 'poorly correlated' with neural activity, as functional hyperemia can sustain for seconds after the onset and offset of a stimulus. As discussed in a later section, this sustained temporal pattern may not be a mismatch between activity and flow, but rather may be consistent with the information processing role of blood flow.

Functional Hyperemia is not Well Correlated with Oxygen Consumption

This increased supply of blood during functional hyperemia does not match most estimates of metabolic need. As first shown by Raichle, Fox and colleagues (Fox and Raichle 1986), the increase in oxygenated hemoglobin recruited by neural activity exceeds the oxygen delivery needs of the tissue. While there is ongoing debate as to the mechanisms of energy use during

neural activity, and as to the role that glucose demand plays in setting blood flow levels, there is general consensus that functional hyperemia, as the name suggests, overshoots the oxygen requirements of the tissue several fold (see (Kida and Hyder 2006) and (Raichle and Mintun 2006) for recent reviews).

Several hypotheses have been proposed to account for this significant 'uncoupling' between the predicted metabolic need for blood and the actual levels observed, ranging from temperature regulation to metabolite (waste) removal (Hayward and Baker 1968; Woolsey et al. 1996; Yablonskiy et al. 2000; Zhu et al. 2006). While these alternative physiological processes may be one role of functional hyperemia, several recent reviews have concluded, in concurrence with the original conclusions of (Fox and Raichle 1986), that a much stronger correlation exists between processes associated with signal processing, such as neurotransmitter release and subthreshold electrophysiological activity, than with other metabolic or physiologic ends (see (Lauritzen 2005; 2001; Peppiatt and Attwell 2004)).

Potential Mechanisms Linking Functional Hyperemia and Neural Activity

We propose an alternative explanation for functional hyperemia, beyond an exclusively metabolic account. This spatially and temporally directed process may play an active role in modulating neural activity, and the observed changes in blood flow and volume may not be overly exuberant, but rather may meet a different goal. Under this hypothesis, functional hyperemia is not the over-delivery of oxygenated blood for metabolism, but rather the targeted regulation of neural processing.

We emphasize that while uncoupling of metabolic need and functional hyperemia is an argument for positing an alternative hypothesis, the proposed information processing role of blood flow is not exclusive of other physiological roles for increased blood flow. Even if oxygen supply were proportional to need in the brain, the localized process of functional hyperemia could still shape neural activity and impact representation, and would still need to be included in any complete account of the processing machinery that supports information processing.

In this section, we discuss a variety of mechanisms through which functional hyperemia could impact neural activity. We have grouped these into two broad categories, *indirect* mechanisms, where astrocytes play a mediating role between vascular and neural networks, and *direct* mechanisms, in which astrocytes do not play an explicit role.

Direct Hemo-Neural Interactions

Diffusible Factors

Diffusible messengers that freely cross the blood-brain barrier represent one class of agent that can directly impact neural activity and that likely increase in concentration with increased blood volume. Within this class of modulators, nitric oxide (NO) is the best understood. This molecule diffuses across cellular membranes and can likely freely traverse the blood brain barrier (Kitagami et al. 2003). There are at least two vascular sources of NO that could impact neural activity: transport from the blood and production in vascular tissue. The blood carries NO, much of which is bound to oxygenated hemoglobin. With deoxygenation under physiologic conditions, the affinity of hemoglobin for NO decreases, leading to its release (Pawloski and Stamler 2002; Singel and Stamler 2005). While the impact of the blood-derived NO concentration on vasodilation is a topic of ongoing debate (Pawloski and Stamler 2002; Stamler et al. 1997), an increase in blood flow and/or blood volume should lead to an increase in the NO concentration in the surrounding tissues (Kitagami et al. 2003; Kubes et al. 1991; Vallance et al. 1989). Further, NO is produced in endothelial cells which could be stimulated to release this factor by shear stress due to enhanced flow (Charles 1999; Garthwaite et al. 2006; Iadecola et al. 1993).

The impact of increased NO concentration on neural activity could take many forms. In the presence of increased NO concentration, thalamic sensory relay neurons *in vitro* show depolarization and modulation of voltage-dependent metabotropic G-protein coupled channels, leading to dampened oscillatory activity and a more tonic mode of transmission (Budde et al. 1992). In the somatosensory and visual thalamus *in vivo*, increased NO concentration leads to enhanced stimulus-evoked firing rate, thought to occur through a distinct, NMDA-dependent mechanism (Cudeiro et al.; Do et al. 1994; Shaw and Salt 1997). In the primary visual cortex,

both suppression and facilitation of evoked firing rate have been observed following local increases in NO concentration, potentially indicating sub-populations of neurons with distinct responses in V1 (Kara and Friedlander 1999). Analyses based in signal detection theory suggest that the cumulative effect of these interactions is an enhanced signal to noise ratio of sensory transmission (Kara and Friedlander 1999). Various forms of synaptic plasticity such as long-term potentiation and depression are also modulated by NO (see (Hardingham and Fox 2006) for a recent review). The presence of enhanced blood flow, when coupled with specific patterns of spike timing or bursting activity, could combine to induce modifications of synaptic efficacy.

Direct support for the view that vascular NO impacts neural activity comes from recent findings by Garthwaite and colleagues (Garthwaite et al. 2006). They provide evidence that endothelial NO production leads to a net depolarization in proximal nerve fibers. This tonic depolarization is thought to be mediated by guanylyl-cyclase coupled receptors in the axons, whose production of cGMP engages hyperpolarization-dependent depolarizing ion channel receptors, leading to an increase in membrane potential. While these observations have yet to be tested *in vivo*, they provide strong initial reinforcement for the NO aspect of the Hemo-Neural hypothesis.

Mechanical Engagement

Functional hyperemia within a local region of cortex (e.g., a cortical column) could shape neural responses through its mechanical impact on the tissue. Increased flow, volume, pressure and the local expansion or motion of vascular processes may lead to the deformation of neural membranes. In somatosensory cortex, sensory afferent stimulation evokes a 30-40% increase in the diameter of single pial arterioles, on average a net increase of 10-15 microns, with individual examples showing expansion in excess of 15 microns (Hughes and Barnes 1980; Koralek et al. 1990; Ngai and Winn 1996).

These local mechanical signals could modulate neural activity through the engagement of mechano-sensitive ion channels. Two channels positioned to translate hyperemia into depolarized membrane potentials are the amiloride sensitive Na+ channel and stretch-activated cation channel, as both types are present in high concentration in the rodent neocortex (Lein et al.

24

2007). A further example of a neural channel positioned to sense these events in the neocortex is TRAAK, a stretch-activated potassium channel (Honore et al. 2006; Maingret et al. 1999). This channel is present in high concentrations across all neocortical layers, and shows peak density in the soma and proximal dendrites of neurons (Reyes et al. 2000; Talley et al. 2001). Mechanical engagement of this potassium channel would lead to hyperpolarization, presumably inducing a net suppression of the firing probability across a local neural population, or modulating firing modes of neurons, e.g., bursting in a subset of pyramidal cells (Silva et al. 1991).

Temperature Change

Almost all cellular processes are sensitive to temperature. Ion channels show several varieties of temperature dependence, and the impact of temperature on the driving force across a membrane is predicted by the Nernst equation. Blood flow largely dictates brain temperature, transmitting changes in core body temperature to the brain and maintaining temperature in the context of the cooler extracranial environment (Baker et al. 1994; Hayward et al. 1966; Zhu et al. 2006). While there is substantial species-specific variation in the regulation of brain temperature (Baker et al. 1994), changes in behavioral and metabolic state regularly induce fluctuations in mammalian brain temperature of $>2^0$ C (Andersen and Moser 1995; Kiyatkin 2004; Kiyatkin et al. 2002). A dorso-ventral gradient of temperature (from cooler to warmer) exists across the brain, with higher temperatures in the ventral regions determined by the large basal arteries (Melzack and Casey 1967; Serota and Gerard 1938), and a steeper gradient in the neocortex (Zhu et al. 2006).

One hypothesis invoked to explain functional hyperemia is that it provides temperature regulation of the brain, removing heat due to neural activity (Hayward and Baker 1968; Yablonskiy et al. 2000). Preliminary studies suggest that tactile stimulation (e.g., of vibrissae or skin) can induce increases in temperature from an unidentified source in somatotopically appropriate cortex or thalamus of $>.1°$ C (Gorbach 1993; Melzack and Casey 1967; Trubel et al. 2006), while different dynamics (and cooling) can be observed with sustained sensory stimulation (McElligott and Melzack 1967; Trubel et al. 2006; Yablonskiy et al. 2000). While a potentially important role for enhanced flow, the effects of functional hyperemia on temperature in a local region (e.g., a cortical column) have not been directly measured, and these effects may

vary as a function of relative depth (Zhu et al. 2006). Recent studies using magnetic resonance imaging as a probe for temperature change have reported decreases in temperature correlated with sensory-enhanced flow on the order of 1^0 C in visual cortices (Yablonskiy et al. 2000). Direct measurements of brain temperature changes during hypercapnia, a condition that transiently increases flow and arterial blood pressure, have shown decreased brain temperature, on the order of $.25^0$ C, in the non-human primate (Hayward and Baker 1968).

If functional hyperemia has even a relatively small impact on local temperature, there are several mechanisms through which it could affect neural activity. Evoked hippocampal field potential responses show increased latency with decreasing temperature changes of less than 2^0 C (see (Andersen and Moser 1995) for a review), and decreasing temperature from 37 to 32^0 C doubles the amplitude of the after-hyperpolarization and enhances spike frequency adaptation (Thompson et al. 1985; Thompson and Prince 1986). Neurons in rodent parietal cortex show substantial temperature dependence in the physiological range. Decreases of 1^0 C from 36^0 to 35^0 C can lead to a complete suppression of ACh-induced action potential firing (Mednikova and Pasikova 2005). In layer II pyramidal neurons in the primary somatosensory cortex, a 2^0 C decrease in temperature (from 35^0 to 33^0 C) induces a 50% decrease in the mini-EPSC rate, a 50% increase in the input resistance, and a decrease in the current-injection evoked firing rate (Simkus and Stricker 2002).

The changes in synaptic response observed with small changes in temperature in the physiological range in parietal cortices suggest that these effects could have a substantial impact on the net output of a cortical column. For example, within the rat barrel cortex, a difference in the rise time of excitatory conductances on the order of 1 millisecond can determine whether or not a vibrissa deflection will evoke a spike (Moore and Nelson 1998; Moore et al. 1999; Simons and Carvell 1989; Wilent and Contreras 2005). Many of these changes associated with temperature could modulate conductance and evoked release on this time scale, altering sensory signal transmission.

Indirect Mechanisms: Astrocyte-Mediated Hemo-to-Neural Signaling

Anatomically, astrocytes are positioned between neurons and vasculature, and play a key role in neural-to-hemodynamic signaling. However, many recent studies have demonstrated that astrocytes also modulate neural activity (for reviews, see (Araque et al. 2001; Nedergaard et al. 2003; Newman 2003; Volterra and Meldolesi 2005)). In this section, we propose that glia may mediate hemo-to-neural interactions, translating functional hyperemia-related vascular signals into changes in neural activity and, in turn, information processing.

The Anatomical Interconnectivity and Range of Impact of Astrocytes

Astrocytes have multiple processes that are interconnected with glial, neural and vascular elements. Astrocytes are densely interconnected with other astrocytes, communicating through gap junctions and chemical signals. As first observed by Golgi ((Golgi 1885)), astrocytic end-feet form a dense net of multiple discrete contacts with vessels (Nedergaard et al. 2003). Astrocytic end-feet also overlap axonal-dendritic connections in the central nervous system, forming the 'tripartite synapse' (Araque et al. 1999; Nedergaard 1994; Nedergaard et al. 2003). In the hippocampus, 57% of synapses form this kind of anatomical and functional unit (Lehre and Danbolt 1998).

Individual astrocytes are proposed to have physiological impact over 'micro-domains' spanning ~ 300 - 400 microns in diameter (Nedergaard et al. 2003; Oberheim et al. 2006). Within this extent, a given astrocyte contacts up to thousands of neurons (Fellin et al. 2004; Oberheim et al. 2006), and their end-feet line microvessels at the 'border' of a putative microdomain (Simard et al. 2003). Signal transmission in astrocytes is triggered by traveling calcium oscillations that induce the release of several factors (Charles et al. 1991; Cornell-Bell et al. 1990). One support for the 'microdomain' view is that spreading calcium waves and the related process of ATP diffusion extend approximately this distance. Evidence also exists for the selective induction of calcium waves in sub-zones within an astrocyte. Spontaneous calcium oscillations in hippocampal slices can occur in single astrocytic processes (Pasti et al. 1997; Taylor-Clarke et al. 2002) and electrical stimulation of the cerebellum can recruit activation in sub-regions of glia

(Grosche et al. 2002; Grosche et al. 1999). Local expression of calcium waves may provide a more precise and more rapid means of communication between vasculature and neurons via astrocytes.

Role of Astrocytes in Neural-to-Hemodynamic Communication

Several theories predict that astrocytes play a major role in translating neural activity into enhanced blood flow (Araque et al. 1998a; Paulson and Newman 1987; Pellerin and Magistretti 1994; Rossi 2006; Takano et al. 2006; Zonta et al. 2003). Calcium signaling in astrocytes can be induced by a variety of factors released by neurons, including glutamate, GABA and ACh (Fellin et al. 2006), and this increased calcium signal may trigger enhanced blood flow through vascular end foot contacts. Initial support for this view came from the observation that glutamate application in culture induces the production of vasodilatory substances in astrocytes (Fellin et al. 2006). Direct support comes from *in vitro* and *in vivo* studies, in which either electrical stimulation of local neurons or direct stimulation of astrocytes causes dilation of local vessels in a fashion correlated with increased astrocytic calcium concentration (Filosa et al. 2004; Mulligan and MacVicar 2004; Takano et al. 2006; Zonta et al. 2003).

Astrocyte-to-Neuron Communication

Astrocytes can regulate neural activity through a variety of mechanisms. A prominent mechanism is the release of neuro-active factors, including but not limited to steroids, neuropeptides, growth factors, aspartate, prostaglandin E2, and D-serine (Haydon and Carmignoto 2006; Volterra and Meldolesi 2005). The potentially most important member of this class is glutamate. In culture and slice preparations, glutamate release from astrocytes can cause large, NMDA-dependent depolarizations in adjacent neurons (Araque et al.; Hassinger et al. 1995; Parpura et al. 1994; Parri et al. 2001; Pasti et al. 1997). Further, direct stimulation of adjacent astrocytes enhances the rate of spontaneous miniature excitatory post-synaptic currents (EPSCs) and net depolarization in neighboring neurons (Araque et al. 1998a). In some circumstances, the net effect of astrocytic stimulation is the potentiation of presynaptic neural inputs (Jourdain et al. 2007), while in others the effect of the astrocyte-induced increase in spontaneous release is synaptic depression, decreased evoked response amplitudes and increased

failure rate (Araque et al. 1998a). At the neuromuscular junction, glial regulation is responsible for ~50% of the synaptic depression observed during repetitive stimulation (Newman 2003; Rochon et al. 2001). Similarly, astrocytic release of adenosine is believed to play a role in heterosynaptic suppression of transmission (Manzoni et al. 1994; Zhang et al. 2003). Some evidence also suggests a role for astrocytic glutamate release in maladaptive excitatory activity, specifically in the generation of epileptogenic-like activity in pyramidal neurons (Kang et al. 2005).

Astrocytic glutamate release can also impact local circuit function through influence on inhibitory interneurons. Release of caged calcium in hippocampal astrocytes increases the rate of spontaneous activity in inhibitory interneurons, and the rate of inhibitory post-synaptic currents observed in neighboring neurons (Liu et al. 2004). Further, activation of interneurons by astrocytic glutamate facilitates the potentiation of inhibitory input to pyramidal neurons, leading to a decrease in the failure rate of presynaptic release from interneurons (Kang et al. 1998).

In addition to the direct release of factors onto neurons, other astrocytic mechanisms have been shown to modulate neural activity. The uptake of glutamate is a well-established role of astrocytes, and provides a complementary mechanism for neural regulation. In the retina, the amplitude and duration of ganglion cell EPSCs are significantly increased when the glial glutamate transporter is blocked (Higgs and Lukasiewicz 1999), suggesting that glia can act to regulate the duration of excitatory signal transmission.

The Impact of Functional Hyperemia on Astrocyte Activity

While it is accepted that astrocytes can impact neural activity, thereby providing a key step in the hemo-astro-neural progression proposed here, the second essential process, the impact of functional hyperemia on signaling in astrocytes, has not been established. Functional hyperemia could cause signaling in astrocytes relevant to neural information processing through a variety of mechanisms, including all of those described above for *direct* hemo-neural modulation.

Diffusible messengers carried by blood may modulate astrocytic function. Application of NO to astrocytes *in vitro* induces an influx of calcium (Li et al. 2003) and glutamate and ATP release (Bal-Price et al. 2002). Astrocytes and endothelial cells are known to interact closely in development, in cell signaling and in the maintenance of the blood-brain barrier (see (Abbott 2002) for a review). The dense apposition of astrocytic endfeet over capillary endothelial cells (Kacem et al. 1998) positions them to be modulated by endothelial NO release, which can be triggered by increased hemodynamic activity (Charles 1999; Garthwaite et al. 2006; Iadecola 1993).

Mechanical interactions are also a potential mechanism for vascular to astrocytic signaling leading to neural modulation. Several studies have demonstrated the induction of calcium waves with mechanical deformation in astrocytes (Charles et al. 1991; Islas et al. 1993; Niggel et al. 2000; Stout and Charles 2003). Astrocytic end feet are, as described above, in an ideal position to detect the mechanical impact of functional hyperemia, as they ensheath cerebral microvessels, and endfeet have a high density of mechano-sensitive connexin channels that trigger intracellular calcium release (Simard et al. 2003).

The Impact of Hemo-to-Astrocytic Activation on Neural Processing

As described in the above review, neural activity is modulated by astrocytic activity, and astrocytes are in a key position to be modulated by changes in blood flow and volume. As such, functional hyperemia should, through this *indirect* mechanism, modulate neural activity. Anatomical and physiological considerations suggest that these proposed interactions will occur at least within a microdomain of $\leq$ 300-400 microns (Anderson and Nedergaard 2003; Oberheim et al. 2006). The calcium waves in astrocytic processes move slowly, on the order of microns per second (Mulligan and MacVicar 2004; Wang et al. 2006): However, calcium waves can occur in astrocytic processes locally opposed to neurons, and sensory stimulation recruits astrocytic processes on a faster time course (<1s) than cell bodies (Takano et al. 2006). These findings suggest that local interactions (<10 micron) may be crucial if *indirect* mechanisms contribute significantly to a more rapid hemodynamic impact on ongoing neural activity, and more

generally that the hemo-astro-neural pathway may impact longer time course state-related phenomena.

Summary

The pathways and time courses predicted by the Hemo-Neural hypothesis, and the related interactions between neurons, vasculature and astrocytes, are summarized in **Figure 1**. In the diagram, the gray arrows represent accepted interactions or those for which primary data currently exists. As reviewed above, neural activity is believed to induce functional hyperemia through direct contact with vasculature, and/or through astrocytic intermediaries. Astrocytic activity, in turn, has been shown to be able to drive vascular dilation and contraction, and also to alter neural processing.

The darker arrows in Figure 1 constitute the present hypothesis. They represent the direct and indirect pathways through which hemodynamic modulation of neural information processing is proposed to occur. The time course at the bottom of Figure 1 shows the predicted evolution of these effects. The direct pathway (black arrow) is predicted to cause rapid neuromodulation, occurring milliseconds to seconds after the onset of

Figure 1

functional hyperemia. The indirect pathway that requires astrocytic transduction (dark gray arrows) is predicted to show delayed modulation, occurring seconds to tens of seconds after the onset of functional hyperemia.
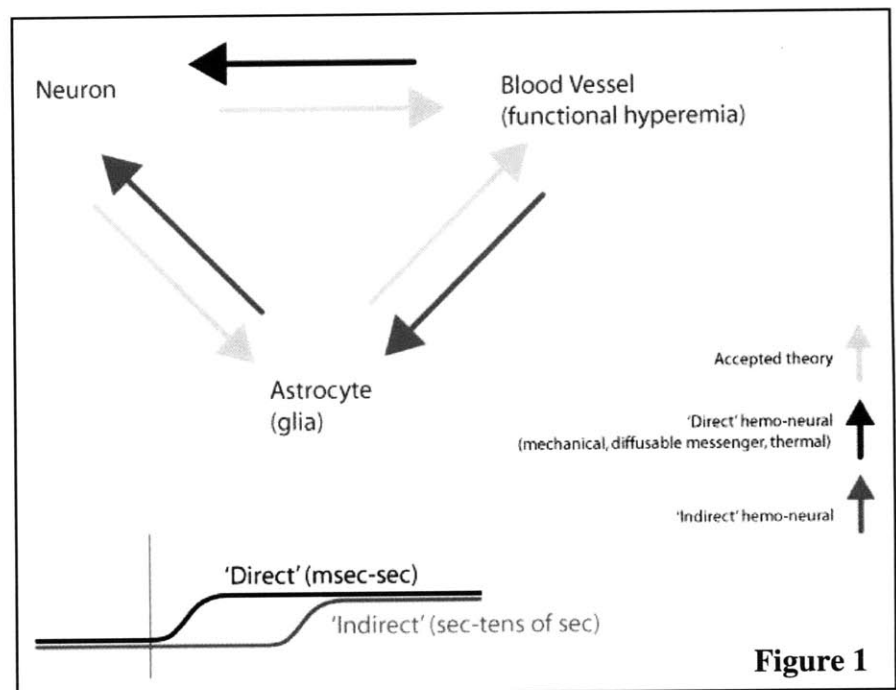
31

One Impact of Blood Flow on Information Processing: Cortical Dynamics

The above evidence suggests that both direct and indirect mechanisms exist through which functional hyperemia can modulate neural activity. In the current section, we propose one kind of impact of functional hyperemia on neural information processing, the dynamic modulation of neural excitability in sensory neocortex.

With regards to the primary somatosensory cortex, functional hyperemia has spatial structure on the order of a single cortical column ($\leq$ 400 microns), its onset follows neural activity by $\leq$ 200 msec, and enhanced blood flow and volume sustain for seconds after the onset of neural activity. We predict that this signal provides a spatio-temporally targeted modulator of the gain state of neural transmission. The mechanisms defined above suggest that either enhancement or suppression of spontaneous and evoked activity can occur, and that the directionality of modulation depends on brain area and context. Facilitation of neural activation could be engaged through recruitment of mechano-sensitive cation channels, through modulation by NO or through astrocyte-mediated depolarization.

Depolarization or hyperpolarization of this type will impact the response of cortical neurons to a sensory stimulus, and dynamics of this kind have been proposed as a means of optimizing cortical function for perception. One hypothesis suggests that the transition from high cortical gain to low cortical gain represents a transition from states optimal for detection to those optimal for discrimination of sensory stimuli, respectively (see Moore et al., 1999; Moore, 2004 for reviews). High gain modes in which a broader region of a cortical map is activated by a sensory stimulus are predicted to facilitate the detection of input, but may be sub-optimal for precise stimulus representation. In contrast, low gain modes with sharper, more delimited lateral spread of signal are predicted to facilitate the precise representation and discrimination of sensory stimuli, but are less optimal for detection of weaker sensory signals. This transition could be modulated by either the pattern of ongoing sensory stimulation, reflecting the information context in which processing is occurring. For example, high-frequency sensory input leading to an adapted state is predicted to impair detection and facilitate discrimination. Similarly, internal

state properties may also modulate cortical activity levels and information processing, such as ongoing activity in the thalamo-cortical loop at alpha-band frequencies (Worden et al. 2000).

Perhaps the most important context in which to consider the Hemo-Neural hypothesis is during natural behavior. In many active sensing contexts, preparatory motor or cognitive behaviors will lead to an increase in blood flow in the cortical representation that is about to process incoming signals, and may 'pre-condition' neural processing by inducing enhanced blood flow prior to the receipt of meaningful information. One example of a motor behavior that is correlated with a shift to an attentive perceptual state is the 'whisking' engaged by rodents during active sensing with the vibrissae. When a rat searches its environment, looking for an object to contact and identify, it actively whisks its vibrissae forward and backwards at a rate of 5-12 Hz (Carvell and Simons 1990; Kleinfeld et al. 2006; Welker 1964). During search, whisking can begin up to seconds prior to contact with the surface. During whisking in air, both sensory feedback and input of signals from the motor system drive activity in SI (Fee et al. 1997; Ferezou et al. 2006; Kleinfeld et al. 2002), activity that should produce enhanced blood flow within 2-3 cycles of the onset of vibrissa motions (or ~250 msec). Under the present hypothesis, blood flow would 'anticipate' the acquisition of information, helping transform cortical circuits to more optimally represent the incoming signals prior to surface contact.

This kind of anticipatory change in blood flow is not limited to cases where active motor exploration precedes acquisition. In many 'cognitive' paradigms, blood flow modulation occurs in anticipation of or independent of the receipt of sensory input. One example of a context in which hemo-neural modulation of cortical dynamics may impact information processing is through enhancement of evoked responses during selective attention. A wide variety of studies have demonstrated that attention to a region of input space (e.g., a retinotopic position or body area) is correlated with enhanced evoked action potential firing of cortical neurons with receptive fields overlapping the attended region (Bichot and Desimone 2006). These effects typically emerge 100-500 milliseconds after the onset of attentional focus (Khayat et al. 2006; Khoe et al. 2006; Worden et al. 2000).

33

Functional hyperemia is positioned to modulate activity during attention, as enhanced blood flow is often localized to regions of the cortical map corresponding to the attended region of space. For example, in area V1, selective and divided attention to specific quadrants of the visual field is correlated with increased BOLD signal in the attended sub-regions of the retinotopic map (McMains and Somers 2004). Similarly, anticipation of contact in a specific body region is correlated with relatively greater blood volume in the corresponding part of the SI homunculus (e.g., the hand area if finger contact is predicted) as compared to non-cued body regions prior to stimulation onset (Drevets et al. 1995).

Ongoing blood flow and volume levels that impact representation may be determined by any of the many mechanisms that control functional hyperemia. Of particular interest given the current proposal is the regulation of hyperemia by neuromodulators already implicated in regulation of attention, such as acetylcholine. A wide variety of studies have suggested that ACh release may be essential to the cortical dynamics mediating attention and working memory (Feldman et al. 2005; Furey et al. 2000; Robbins et al. 2000; Sarter et al. 2005). Under the current hypothesis, ACh would have synergistic neuromodulatory and hemodynamic influences during enhanced attentional states, modulating the local vascular and neural network in the service of a common information processing goal.

Why Engage Functional Hyperemia for Neural Modulation?

This proposal begs the question as to why functional hyperemia is a 'necessary' aspect of neural modulation, given that other mechanisms are known to exist that recruit these dynamics. Put another way, why would such a mechanism evolve if it appears redundant to existing processes? There are several responses to this kind of teleological question applied to biology.

The emergence of a neuroregulatory role for functional hyperemia is not difficult to conceive. If one presumes any of the several possible metabolic needs for activity-driven increases in blood flow, in agreement with the existing theories for this phenomenon, then a correlation is present

between blood flow and neural activity. If an 'overflow' of this supply also proved adaptive for the functionality of neural representation, then one would predict its evolutionary emergence through the reinforcement of this correlation. Further, there is strong evidence from invertebrates for the vascular transmission of neuromodulatory substances that regulate neural firing, neural oscillations and behavior, e.g., in control of the stomatogastric ganglion (Marder et al. 2005; Nusbaum and Beenhakker 2002).

There are also important physiological reasons why functional hyperemia may be employed to suppress neural activity. Unchecked neural activation following stimulation is a hallmark of forms of epilepsy and schizophrenia (Blum and Mann 2002), and in the limit becomes the cause of excitotoxic cell death (Tsuang et al. 2000). Metabolic 'control systems' such as the hemodynamic pathways could, therefore, have evolved mechanisms for neural regulation targeted to the basic health of the system that have additional benefit for the efficient representation of information. The existence of severe maladies characterized by failed neural suppression suggests, further, that mechanisms of neural gain regulation are not sufficient in a significant fraction of the population. As such, the addition of a novel mechanism (functional hyperemia) is not redundant.

A further argument for a role for functional hyperemia in information processing is its unique character. While there are several possible mechanisms through which functional hyperemia may differentially impact different neuron or synapse classes, a distinctive feature of this mechanism is that it acts on the neurons throughout a local area, 'binding' their function. This kind of impact would be predicted to be of particular significance in representations, like a sensory map, where spatial position within a local network is important to representation. High-resolution sensory cortices such as primary visual cortex (Hubel and Wiesel 1977) and the vibrissa barrel cortex (Andermann and Moore 2006; Andermann et al. 2004; Moore and Andermann 2005) are characterized by clustering of neurons with similar tuning in an overlapping set of columns. These interdependent columnar systems may be ideally positioned to be regulated by a modulator acting on the spatial scale currently ascribed to hyperemia.

Recent hypotheses have emphasized that energetic efficiency in brain operation is a paramount constraint, and therefore leads to sparse coding through the dynamic restriction of activity and the adaptability of networks (Laughlin and Sejnowski 2003). In such a situation, the interdependence of computation and metabolism would be adaptive. The synergistic engagement of the metabolic supply network to regulate coding is, in this context, a consistent proposal.

Perhaps the most appropriate answer to the question of why functional hyperemia 'needs' to exist as an information processing mechanism is that this question is ill-posed. The attempt to delineate the evolutionary necessity of any given mechanism in an existing organism is almost always an open-ended endeavor. This practice is particularly difficult when judging the importance of a newly proposed mechanism, where the nature of its interactions is only hypothesized. Analysis of the neuromodulatory role of functional hyperemia is, at present, best focused on the study of the observable impact of hemodynamics on neural processing, reserving a further discussion of the evolutionary 'necessity' of this mechanism until more is known about its basic biology and its impact on behaviorally-relevant information processing.

Clinical Implications of the Hemo-Neural Hypothesis

There are several potential clinical implications of the prediction that functional hyperemia modulates neural activity. Diseases that impact the vasculature and impact cognitive function may in part be operating through a failure in the hemo-neural interactions, and the loss or alteration of neuromodulatory function that results.

The negative outcomes of stroke are commonly believed to arise only from localized cell death in the focus of the lesion and the metabolic losses and stresses associated with deprived flow. Under the current hypothesis, the altered blood supply in itself, and the subsequent loss of normal functionality in a given neural circuit, may be causal in behavioral symptoms even if downstream neurons are viable. One cause of cell death in stroke is hyper-excitation of the tissue resulting from a variety of factors (Mattson 2003). A direct prediction of the hemoneural

hypothesis is that decreased blood flow could induce an increase in the excitability of neural tissue, and that this loss of a suppressive mechanism could contribute to this post-traumatic response. The loss of suppression also predicts a period of enhanced hyper-excitability at the edge of the lesioned area, sustained until homeostatic mechanisms can be engaged, and leaving the tissue beyond the predicted penumbra of obvious damage in a maladaptive state for normal information processing.

Recent advances suggest that Alzheimer's disease is initially expressed as a vascular phenomenon, with impaired cholinergic dilation of blood vessels implicated in its pathophysiology (Cauli et al. 2004; de la Torre and Mussivand 1993; Geaney et al. 1990; Iadecola 2004; Sato and Sato 1995). As such, the Hemo-Neural hypothesis would predict an impact of vascular decline on hemo-neural interactions, taxing the information processing capacity of the system through loss of one form of normal modulatory control. A specific prediction is that pre-diagnosis Alzheimer's patients could show enhanced facilitation and/or the failure of tonic and phasic levels of intracortical suppression, in agreement with recent transcranial magnetic stimulation studies (Liepert et al. 2001; Pierantozzi et al. 2004).

Epilepsy can arise through a broad variety of mechanisms, including a failure in the normal mechanisms of neural suppression (Duncan et al. 2006). The Hemo-Neural hypothesis predicts that hemodynamic abnormalities could lead to these symptoms. In agreement with this prediction, abnormal vascular anatomy is a hallmark of seizure disorders (Leutmezer et al. 2003; Zaidi et al. 2000) and a compromised blood-brain barrier predicts seizure onset (Oby and Janigro 2006). Further, vagal nerve stimulation has recently been successfully employed to suppress the onset of epileptic seizures (DeGiorgio et al. 2000; Schachter 2002) and could operate at least in part through vascular regulation.

A failure in cortical dynamics is also widely predicted to be a causal factor in schizophrenia. Schizophrenic subjects show several indications of failed cortical suppressive mechanisms, including decreased prominence of gamma oscillations (Lee et al. 2003; Spencer et al. 2003). While this symptomatology has many proposed neural causes (Lewis et al. 2005; Woo and Lu

2006), vascular abnormalities in resting blood volume distribution and presumed vascular anatomy have also been observed in schizophrenic subjects (Cohen et al. 1995), and could contribute.

Other Links Between Hemodynamics and Information Processing

The interdependent nature of vascular and neural interactions suggests other hypotheses as to their combined function in information processing, beyond the suggestion that functional hyperemia regulates neural dynamics. The role of hemodynamics in shaping oscillatory behaviors—such as those expressed in EEG and MEG signals—should be considered. This suggestion is particularly salient given the potential role of NO in regulating thalamic rhythms (Pape and Mager 1992), and astrocytes in unifying activity across disparate neurons (Angulo et al. 2004; Fellin et al. 2004). Vascular oscillations are also prominent features of the cerebral vasculature (van Helden et al. 2006), and changes in these hemodynamic state properties may interact with neural state properties. A further prediction mentioned above is that the combination of functional hyperemia and patterns of neural activity may facilitate the induction of longer-term neural plasticity. On a longer time-scale, selective regulation of the blood-brain barrier, shaped by the recent history of flow to the region, could also serve an integrative role (Krizanac-Bengez et al. 2004; Leybaert 2005).

A more radical aspect of the Hemo-Neural hypothesis than the one elaborated above is that the vasculature also plays a direct role in carrying information, beyond just modulation of neurons. If neural activity in one region (for example, a specific layer of the neocortex) were to produce a signal that was taken up by the vasculature, it could be selectively transmitted to a downstream target (e.g., other layers of the neocortex). At least two mechanisms could support this kind of communication. Peripheral and central vascular tissue is capable of electrical coupling (Segal and Duling 1987; Yamazaki and Kitamura 2003). Electrical signals can be transmitted, putatively through gap junction connections in endothelial and/or smooth muscle cells, from capillaries to their feeding arterioles, and may condition a vasodilatory response. These changes in membrane potential in vascular cells can be driven by neuromodulators (e.g., ACh) (McGahren et al. 1998) and by local changes in flow (e.g., the occlusion of a neighboring

arteriole) (McGahren et al. 1997). These signals generated 'downstream' could induce voltage dependent interactions in upstream targets, from a capillary bed and the granular layers of the cortex, for example, to an arteriole and the supragranular layers. Moving in the other direction, the transport of diffusible messengers is also a possibility. Diffusible messengers produced in a superficial cortical layer could be transported down an arteriole and released in deeper layers. This view, while even further from currently accepted models of information processing, similarly bears further investigation.

Future Directions

The ideas presented have several direct implications for future research. The Hemo-Neural hypothesis argues that any computational model or broader theory that seeks an accurate and biophysical account of information processing in the brain should include hemodynamics as an explicit component. This view also suggests that the wealth of studies that have investigated hemodynamic patterns and neural-to-vascular coupling are not only informative with regards to the metabolic functioning of the brain, but are also descriptions of signals that impact representation. As such, fMRI and related techniques are not simply second-order localization tools, but probes of part of the process of information representation. If true, there are important considerations as to the logical interpretation of these hemodynamic signals, and of how they synergistically interact with the variable that most of these studies would like to track, neural activity.

The Hemo-Neural hypothesis suggests several lines of experimentation to systematically test this proposal. Understanding the impact of hemodynamics on neural activity requires the independent regulation of blood flow *in vivo*. This kind of probe is essential for systematically dissociating these effects from alternative explanations, and for ultimately addressing these predictions during active behavior. An informative frustration in attempting these experiments is the extensive overlap in factors that regulate hemodynamics that also directly or indirectly regulate neural activity through other pathways. The interdependent modulation of these two systems, while a strong argument for the Hemo-Neural hypothesis, also makes the discrete investigation of these predictions difficult. This challenge underscores the inter-related nature of central neural and

hemodynamic processes, and the likelihood that they function in tandem in the modulation of information processing.

References

Abbott NJ. Astrocyte-endothelial interactions and blood-brain barrier permeability. *J Anat* 200: 629-638, 2002.

Akgoren N, Mathiesen C, Rubin I, and Lauritzen M. Laminar analysis of activity-dependent increases of CBF in rat cerebellar cortex: dependence on synaptic strength. *Am J Physiol* 273: H1166-1176, 1997.

Andermann ML, and Moore CI. A somatotopic map of vibrissa motion direction within a barrel column. *Nat Neurosci* 9: 543-551, 2006.

Andermann ML, Ritt J, Neimark MA, and Moore CI. Neural correlates of vibrissa resonance; band-pass and somatotopic representation of high-frequency stimuli. *Neuron* 42: 451-463, 2004.

Andersen P, and Moser EI. Brain temperature and hippocampal function. *Hippocampus* 5: 491-498, 1995.

Anderson CM, and Nedergaard M. Astrocyte-mediated control of cerebral microcirculation. *Trends Neurosci* 26: 340-344; author reply 344-345, 2003.

Angulo MC, Kozlov AS, Charpak S, and Audinat E. Glutamate released from glial cells synchronizes neuronal activity in the hippocampus. *J Neurosci* 24: 6920-6927, 2004.

Araque A, Carmignoto G, and Haydon PG. Dynamic signaling between astrocytes and neurons. *Annu Rev Physiol* 63: 795-813, 2001.

Araque A, Parpura V, Sanzgiri RP, and Haydon PG. Glutamate-dependent astrocyte modulation of synaptic transmission between cultured hippocampal neurons. *Eur J Neurosci* 10: 2129-2142, 1998a.

Araque A, Parpura V, Sanzgiri RP, and Haydon PG. Tripartite synapses: glia, the unacknowledged partner. *Trends Neurosci* 22: 208-215, 1999.

Araque A, Sanzgiri RP, Parpura V, and Haydon PG. Calcium elevation in astrocytes causes an NMDA receptor-dependent increase in the frequency of miniature synaptic currents in cultured hippocampal neurons. *J Neurosci* 18: 6822-6829, 1998b.

Baker KZ, Young WL, Stone JG, Kader A, Baker CJ, and Solomon RA. Deliberate mild intraoperative hypothermia for craniotomy. *Anesthesiology* 81: 361-367, 1994.

Bal-Price A, Moneer Z, and Brown GC. Nitric oxide induces rapid, calcium-dependent release of vesicular glutamate and ATP from cultured rat astrocytes. *Glia* 40: 312-323, 2002.

Bichot NP, and Desimone R. Finding a face in the crowd: parallel and serial neural mechanisms of visual selection. *Prog Brain Res* 155: 147-156, 2006.

Blum BP, and Mann JJ. The GABAergic system in schizophrenia. *Int J Neuropsychopharmacol* 5: 159-179, 2002.

Borowsky IW, and Collins RC. Metabolic anatomy of brain: a comparison of regional capillary density, glucose metabolism, and enzyme activities. *J Comp Neurol* 288: 401-413, 1989.

Budde T, Mager R, and Pape HC. Different Types of Potassium Outward Current in Relay Neurons Acutely Isolated from the Rat Lateral Geniculate Nucleus. *Eur J Neurosci* 4: 708-722, 1992.

Carmeliet P. Blood vessels and nerves: common signals, pathways and diseases. *Nat Rev Genet* 4: 710-720, 2003.

Carvell GE, and Simons DJ. Biometric analyses of vibrissal tactile discrimination in the rat. *J Neurosci* 10: 2638-2648, 1990.

Cauli B, Tong XK, Rancillac A, Serluca N, Lambolez B, Rossier J, and Hamel E. Cortical GABA interneurons in neurovascular coupling: relays for subcortical vasoactive pathways. *J Neurosci* 24: 8940-8949, 2004.

Chaigneau E, Oheim M, Audinat E, and Charpak S. Two-photon imaging of capillary blood flow in olfactory bulb glomeruli. *Proc Natl Acad Sci U S A* 100: 13081-13086, 2003.
Charles A. Nitric oxide pumps up calcium signalling. *Nat Cell Biol* 1: E193-195, 1999.

Charles AC, Merrill JE, Dirksen ER, and Sanderson MJ. Intercellular signaling in glial cells: calcium waves and oscillations in response to mechanical stimulation and glutamate. *Neuron* 6: 983-992, 1991.

Cohen BM, Yurgelun-Todd D, English CD, and Renshaw PF. Abnormalities of regional distribution of cerebral vasculature in schizophrenia detected by dynamic susceptibility contrast MRI. *Am J Psychiatry* 152: 1801-1803, 1995.

Cornell-Bell AH, Finkbeiner SM, Cooper MS, and Smith SJ. Glutamate induces calcium waves in cultured astrocytes: long-range glial signaling. *Science* 247: 470-473, 1990.

Cudeiro J, Grieve KL, Rivadulla C, Rodriguez R, Martinez-Conde S, and Acuna C. The role of nitric oxide in the transformation of visual information within the dorsal lateral geniculate nucleus of the cat. *Neuropharmacology* 33: 1413-1418, 1994.

de la Torre JC, and Mussivand T. Can disturbed brain microcirculation cause Alzheimer's disease? *Neurol Res* 15: 146-153, 1993.

DeGiorgio CM, Schachter SC, Handforth A, Salinsky M, Thompson J, Uthman B, Reed R, Collins S, Tecoma E, Morris GL, Vaughn B, Naritoku DK, Henry T, Labar D, Gilmartin R, Labiner D, Osorio I, Ristanovic R, Jones J, Murphy J, Ney G, Wheless J, Lewis P, and Heck C. Prospective long-term study of vagus nerve stimulation for the treatment of refractory seizures. *Epilepsia* 41: 1195-1200, 2000.

Disbrow EA, Slutsky DA, Roberts TP, and Krubitzer LA. Functional MRI at 1.5 tesla: a comparison of the blood oxygenation level-dependent signal and electrophysiology. *Proc Natl Acad Sci U S A* 97: 9718-9723, 2000.

Do KQ, Binns KE, and Salt TE. Release of the nitric oxide precursor, arginine, from the thalamus upon sensory afferent stimulation, and its effect on thalamic neurons in vivo. *Neuroscience* 60: 581-586, 1994.

Drevets WC, Burton H, Videen TO, Snyder AZ, Simpson JR, Jr., and Raichle ME. Blood flow changes in human somatosensory cortex during anticipated stimulation. *Nature* 373: 249-252, 1995.

Duncan JS, Sander JW, Sisodiya SM, and Walker MC. Adult epilepsy. *Lancet* 367: 1087-1100, 2006.

Dunn AK, Devor A, Dale AM, and Boas DA. Spatial extent of oxygen metabolism and hemodynamic changes during functional activation of the rat somatosensory cortex. *Neuroimage* 27: 279-290, 2005.

Duong TQ, Kim DS, Ugurbil K, and Kim SG. Localized cerebral blood flow response at submillimeter columnar resolution. *Proc Natl Acad Sci U S A* 98: 10904-10909, 2001.

Eichmann A, Le Noble F, Autiero M, and Carmeliet P. Guidance of vascular and neural network formation. *Curr Opin Neurobiol* 15: 108-115, 2005.

Fee MS, Mitra PP, and Kleinfeld D. Central versus peripheral determinants of patterned spike activity in rat vibrissa cortex during whisking. *J Neurophysiol* 78: 1144-1149., 1997.

Feekes JA, and Cassell MD. The vascular supply of the functional compartments of the human striatum. *Brain* 129: 2189-2201, 2006.

Feldman D, Wolfe J, Drew P, Pahlavan S, and Abarbanel H. Whisker resonance measured in awake behaving animals. In: *SFN 2005*. Washington, DC: 2005.

Fellin T, Pascual O, Gobbo S, Pozzan T, Haydon PG, and Carmignoto G. Neuronal synchrony mediated by astrocytic glutamate through activation of extrasynaptic NMDA receptors. *Neuron* 43: 729-743, 2004.

Fellin T, Sul JY, D'Ascenzo M, Takano H, Pascual O, and Haydon PG. Bidirectional astrocyte-neuron communication: the many roles of glutamate and ATP. *Novartis Found Symp* 276: 208-217; discussion 217-221, 233-207, 275-281, 2006.

Ferezou I, Bolea S, and Petersen CC. Visualizing the cortical representation of whisker touch: voltage-sensitive dye imaging in freely moving mice. *Neuron* 50: 617-629, 2006.

Filosa JA, Bonev AD, and Nelson MT. Calcium dynamics in cortical astrocytes and arterioles during neurovascular coupling. *Circ Res* 95: e73-81, 2004.

Fox PT, and Raichle ME. Focal physiological uncoupling of cerebral blood flow and oxidative metabolism during somatosensory stimulation in human subjects. *Proc Natl Acad Sci U S A* 83: 1140-1144, 1986.

Furey ML, Pietrini P, and Haxby JV. Cholinergic enhancement and increased selectivity of perceptual processing during working memory. *Science* 290: 2315-2319, 2000.

Garthwaite G, Bartus K, Malcolm D, Goodwin D, Kollb-Sielecka M, Dooldeniya C, and Garthwaite J. Signaling from blood vessels to CNS axons through nitric oxide. *J Neurosci* 26: 7730-7740, 2006.

Geaney DP, Soper N, Shepstone BJ, and Cowen PJ. Effect of central cholinergic stimulation on regional cerebral blood flow in Alzheimer disease. *Lancet* 335: 1484-1487, 1990.

Gerrits RJ, Raczynski C, Greene AS, and Stein EA. Regional cerebral blood flow responses to variable frequency whisker stimulation: an autoradiographic analysis. *Brain Res* 864: 205-212, 2000.

Golgi C. Sulla fina anatomia degli organi centrali del sistema nervoso. *Riv Sper Fremiat Med Leg Alienazioni Ment* 72-123, 1885.

Gorbach AM. Infrared imaging of brain function. *Adv Exp Med Biol* 333: 95-123, 1993.

Grosche J, Kettenmann H, and Reichenbach A. Bergmann glial cells form distinct morphological structures to interact with cerebellar neurons. *J Neurosci Res* 68: 138-149, 2002.

Grosche J, Matyash V, Moller T, Verkhratsky A, Reichenbach A, and Kettenmann H. Microdomains for neuron-glia interaction: parallel fiber signaling to Bergmann glial cells. *Nat Neurosci* 2: 139-143, 1999.

Gross CG. *Brain Vision Memory: Tales in the History of Neuroscience*. Cambridge: The MIT Press, 1998, p. 247.

Grubb RL, Jr., Hernandez-Perez MJ, Raichle ME, and Phelps ME. The effects of iodinated contrast agents on autoregulation of cerebral blood flow. *Stroke* 5: 155-160, 1974.

Hamel E. Perivascular nerves and the regulation of cerebrovascular tone. *J Appl Physiol* 100: 1059-1064, 2006.

Hardingham N, and Fox K. The role of nitric oxide and GluR1 in presynaptic and postsynaptic components of neocortical potentiation. *J Neurosci* 26: 7395-7404, 2006.

Hassinger TD, Atkinson PB, Strecker GJ, Whalen LR, Dudek FE, Kossel AH, and Kater SB. Evidence for glutamate-mediated activation of hippocampal neurons by glial calcium waves. *J Neurobiol* 28: 159-170, 1995.

Haydon PG, and Carmignoto G. Astrocyte control of synaptic transmission and neurovascular coupling. *Physiol Rev* 86: 1009-1031, 2006.

Hayward JN, and Baker MA. Role of cerebral arterial blood in the regulation of brain temperature in the monkey. *Am J Physiol* 215: 389-403, 1968.

Hayward JN, Smith E, and Stuart DG. Temperature gradients between arterial blood and brain in the monkey. *Proc Soc Exp Biol Med* 121: 547-551, 1966.

Hess A, Stiller D, Kaulisch T, Heil P, and Scheich H. New insights into the hemodynamic blood oxygenation level-dependent response through combination of functional magnetic resonance imaging and optical recording in gerbil barrel cortex. *J Neurosci* 20: 3328-3338, 2000.

Higgs MH, and Lukasiewicz PD. Glutamate uptake limits synaptic excitation of retinal ganglion cells. *J Neurosci* 19: 3691-3700, 1999.

Hirase H, Creso J, Singleton M, Bartho P, and Buzsaki G. Two-photon imaging of brain pericytes in vivo using dextran-conjugated dyes. *Glia* 46: 95-100, 2004.

Hoge RD, Franceschini MA, Covolan RJ, Huppert T, Mandeville JB, and Boas DA. Simultaneous recording of task-induced changes in blood oxygenation, volume, and flow using diffuse optical imaging and arterial spin-labeling MRI. *Neuroimage* 25: 701-707, 2005.

Honore E, Patel AJ, Chemin J, Suchyna T, and Sachs F. Desensitization of mechano-gated K2P channels. *Proc Natl Acad Sci U S A* 103: 6859-6864, 2006.

Hubel DH, and Wiesel TN. Ferrier lecture. Functional architecture of macaque monkey visual cortex. *Proc R Soc Lond B Biol Sci* 198: 1-59., 1977.

Hughes M, and Barnes C. *Neural Control of Circulation*. New York: Academic Press, 1980.
Iadecola C. Neurovascular regulation in the normal brain and in Alzheimer's disease. *Nat Rev Neurosci* 5: 347-360, 2004.

Iadecola C. Regulation of the cerebral microcirculation during neural activity: is nitric oxide the missing link? *Trends Neurosci* 16: 206-214, 1993.

Iadecola C, Beitz AJ, Renno W, Xu X, Mayer B, and Zhang F. Nitric oxide synthase-containing neural processes on large cerebral arteries and cerebral microvessels. *Brain Res* 606: 148-155, 1993.

Islas L, Pasantes-Morales H, and Sanchez JA. Characterization of stretch-activated ion channels in cultured astrocytes. *Glia* 8: 87-96, 1993.

Jourdain P, Bergersen LH, Bhaukaurally K, Bezzi P, Santello M, Domercq M, Matute C, Tonello F, Gundersen V, and Volterra A. Glutamate exocytosis from astrocytes controls synaptic strength. *Nat Neurosci* 10: 331-339, 2007.

Kacem K, Lacombe P, Seylaz J, and Bonvento G. Structural organization of the perivascular astrocyte endfeet and their relationship with the endothelial glucose transporter: a confocal microscopy study. *Glia* 23: 1-10, 1998.

Kang J, Jiang L, Goldman SA, and Nedergaard M. Astrocyte-mediated potentiation of inhibitory synaptic transmission. *Nat Neurosci* 1: 683-692, 1998.

Kang N, Xu J, Xu Q, Nedergaard M, and Kang J. Astrocytic glutamate release-induced transient depolarization and epileptiform discharges in hippocampal CA1 pyramidal neurons. *J Neurophysiol* 94: 4121-4130, 2005.

Kara P, and Friedlander MJ. Arginine analogs modify signal detection by neurons in the visual cortex. *J Neurosci* 19: 5528-5548, 1999.

Khayat PS, Spekreijse H, and Roelfsema PR. Attention lights up new object representations before the old ones fade away. *J Neurosci* 26: 138-142, 2006.

Khoe W, Freeman E, Woldorff MG, and Mangun GR. Interactions between attention and perceptual grouping in human visual cortex. *Brain Res* 1078: 101-111, 2006.

Kida I, and Hyder F. Physiology of functional magnetic resonance imaging: energetics and function. *Methods Mol Med* 124: 175-195, 2006.

Kitagami T, Yamada K, Miura H, Hashimoto R, Nabeshima T, and Ohta T. Mechanism of systemically injected interferon-alpha impeding monoamine biosynthesis in rats: role of nitric oxide as a signal crossing the blood-brain barrier. *Brain Res* 978: 104-114, 2003.

Kiyatkin EA. Brain hyperthermia during physiological and pathological conditions: causes, mechanisms, and functional implications. *Curr Neurovasc Res* 1: 77-90, 2004.

Kiyatkin EA, Brown PL, and Wise RA. Brain temperature fluctuation: a reflection of functional neural activation. *Eur J Neurosci* 16: 164-168, 2002.

Kleinfeld D, Ahissar E, and Diamond ME. Active sensation: insights from the rodent vibrissa sensorimotor system. *Curr Opin Neurobiol* 16: 435-444, 2006.

Kleinfeld D, Sachdev RN, Merchant LM, Jarvis MR, and Ebner FF. Adaptive filtering of vibrissa input in motor cortex of rat. *Neuron* 34: 1021-1034., 2002.

Kong Y, Zheng Y, Johnston D, Martindale J, Jones M, Billings S, and Mayhew J. A model of the dynamic relationship between blood flow and volume changes during brain activation. *J Cereb Blood Flow Metab* 24: 1382-1392, 2004.

Koralek KA, Olavarria J, and Killackey HP. Areal and laminar organization of corticocortical projections in the rat somatosensory cortex. *J Comp Neurol* 299: 133-150, 1990.

Krimer LS, Muly EC, 3rd, Williams GV, and Goldman-Rakic PS. Dopaminergic regulation of cerebral cortical microcirculation. *Nat Neurosci* 1: 286-289, 1998.

Krizanac-Bengez L, Mayberg MR, and Janigro D. The cerebral vasculature as a therapeutic target for neurological disorders and the role of shear stress in vascular homeostatis and pathophysiology. *Neurol Res* 26: 846-853, 2004.

Kubes P, Suzuki M, and Granger DN. Nitric oxide: an endogenous modulator of leukocyte adhesion. *Proc Natl Acad Sci U S A* 88: 4651-4655, 1991.

Laughlin SB, and Sejnowski TJ. Communication in neuronal networks. *Science* 301: 1870-1874, 2003.

Lauritzen M. Reading vascular changes in brain imaging: is dendritic calcium the key? *Nat Rev Neurosci* 6: 77-85, 2005.

Lauritzen M. Relationship of spikes, synaptic activity, and local changes of cerebral blood flow. *J Cereb Blood Flow Metab* 21: 1367-1383, 2001.

Lee KH, Williams LM, Breakspear M, and Gordon E. Synchronous gamma activity: a review and contribution to an integrative neuroscience model of schizophrenia. *Brain Res Brain Res Rev* 41: 57-78, 2003.

Lehre KP, and Danbolt NC. The number of glutamate transporter subtype molecules at glutamatergic synapses: chemical and stereological quantification in young adult rat brain. *J Neurosci* 18: 8751-8757, 1998.

Lein ES, Hawrylycz MJ, Ao N, Ayres M, Bensinger A, Bernard A, Boe AF, Boguski MS, Brockway KS, Byrnes EJ, Chen L, Chen L, Chen TM, Chin MC, Chong J, Crook BE, Czaplinska A, Dang CN, Datta S, Dee NR, Desaki AL, Desta T, Diep E, Dolbeare TA, Donelan MJ, Dong HW, Dougherty JG, Duncan BJ, Ebbert AJ, Eichele G, Estin LK, Faber C, Facer BA, Fields R, Fischer SR, Fliss TP, Frensley C, Gates SN, Glattfelder KJ, Halverson KR, Hart MR, Hohmann JG, Howell MP, Jeung DP, Johnson RA, Karr PT, Kawal R, Kidney JM, Knapik RH, Kuan CL, Lake JH, Laramee AR, Larsen KD, Lau C, Lemon TA, Liang AJ, Liu Y, Luong LT, Michaels J, Morgan JJ, Morgan RJ, Mortrud

MT, Mosqueda NF, Ng LL, Ng R, Orta GJ, Overly CC, Pak TH, Parry SE, Pathak SD, Pearson OC, Puchalski RB, Riley ZL, Rockett HR, Rowland SA, Royall JJ, Ruiz MJ, Sarno NR, Schaffnit K, Shapovalova NV, Sivisay T, Slaughterbeck CR, Smith SC, Smith KA, Smith BI, Sodt AJ, Stewart NN, Stumpf KR, Sunkin SM, Sutram M, Tam A, Teemer CD, Thaller C, Thompson CL, Varnam LR, Visel A, Whitlock RM, Wohnoutka PE, Wolkey CK, Wong VY, Wood M, Yaylaoglu MB, Young RC, Youngstrom BL, Yuan XF, Zhang B, Zwingman TA, and Jones AR. Genome-wide atlas of gene expression in the adult mouse brain. *Nature* 445: 168-176, 2007.

Leutmezer F, Podreka I, Asenbaum S, Pietrzyk U, Lucht H, Back C, Benda N, and Baumgartner C. Postictal psychosis in temporal lobe epilepsy. *Epilepsia* 44: 582-590, 2003.

Lewis DA, Hashimoto T, and Volk DW. Cortical inhibitory neurons and schizophrenia. *Nat Rev Neurosci* 6: 312-324, 2005.

Leybaert L. Neurobarrier coupling in the brain: a partner of neurovascular and neurometabolic coupling? *J Cereb Blood Flow Metab* 25: 2-16, 2005.

Li N, Sul JY, and Haydon PG. A calcium-induced calcium influx factor, nitric oxide, modulates the refilling of calcium stores in astrocytes. *J Neurosci* 23: 10302-10310, 2003.

Liepert J, Bar KJ, Meske U, and Weiller C. Motor cortex disinhibition in Alzheimer's disease. *Clin Neurophysiol* 112: 1436-1441, 2001.

Liu QS, Xu Q, Kang J, and Nedergaard M. Astrocyte activation of presynaptic metabotropic glutamate receptors modulates hippocampal inhibitory synaptic transmission. *Neuron Glia Biol* 1: 307-316, 2004.

Maingret F, Fosset M, Lesage F, Lazdunski M, and Honore E. TRAAK is a mammalian neuronal mechano-gated K+ channel. *J Biol Chem* 274: 1381-1387, 1999.

Malonek D, Dirnagl U, Lindauer U, Yamada K, Kanno I, and Grinvald A. Vascular imprints of neuronal activity: relationships between the dynamics of cortical blood flow, oxygenation, and volume changes following sensory stimulation. *Proc Natl Acad Sci U S A* 94: 14826-14831., 1997.

Manzoni OJ, Manabe T, and Nicoll RA. Release of adenosine by activation of NMDA receptors in the hippocampus. *Science* 265: 2098-2101, 1994.

Marder E, Bucher D, Schulz DJ, and Taylor AL. Invertebrate central pattern generation moves along. *Curr Biol* 15: R685-699, 2005.
Martin C, Martindale J, Berwick J, and Mayhew J. Investigating neural-hemodynamic coupling and the hemodynamic response function in the awake rat. *Neuroimage* 32: 33-48, 2006.

Matsuura T, Fujita H, Seki C, Kashikura K, Yamada K, and Kanno I. CBF change evoked by somatosensory activation measured by laser-Doppler flowmetry: independent evaluation of RBC velocity and RBC concentration. *Jpn J Physiol* 49: 289-296, 1999.

Mattson MP. Excitotoxic and excitoprotective mechanisms: abundant targets for the prevention and treatment of neurodegenerative disorders. *Neuromolecular Med* 3: 65-94, 2003.

McElligott JG, and Melzack R. Localized thermal changes evoked in the brain by visual and auditory stimulation. *Exp Neurol* 17: 293-312, 1967.

McGahren ED, Beach JM, and Duling BR. Capillaries demonstrate changes in membrane potential in response to pharmacological stimuli. *Am J Physiol* 274: H60-65, 1998.

McGahren ED, Dora KA, Damon DN, and Duling BR. A test of the role of flow-dependent dilation in arteriolar responses to occlusion. *Am J Physiol* 272: H714-721, 1997.

McMains SA, and Somers DC. Multiple spotlights of attentional selection in human visual cortex. *Neuron* 42: 677-686, 2004.

Mednikova YS, and Pasikova NV. The temperature sensitivity of the cholinergic responses of cortical neurons in the guinea pig brain. *Neurosci Behav Physiol* 35: 615-621, 2005.

Melzack R, and Casey KL. Localized temperature changes evoked in the brain by somatic stimulation. *Exp Neurol* 17: 276-292, 1967.

Michaloudi H, Grivas I, Batzios C, Chiotelli M, and Papadopoulos GC. Areal and laminar variations in the vascularity of the visual, auditory, and entorhinal cortices of the developing rat brain. *Brain Res Dev Brain Res* 155: 60-70, 2005.

Moore CI, and Andermann ML. The vibrissa resonance hypothesis. In: *Neural Plasticity in Adult Somatic Sensory-Motor Systems*, edited by Ebner FFTaylor & Francis Publishing Group, CRC Press, 2005, p. 21-59.

Moore CI, and Nelson SB. Spatio-temporal subthreshold receptive fields in the vibrissa representation of rat primary somatosensory cortex. *J Neurophysiol* 80: 2882-2892., 1998.

Moore CI, Nelson SB, and Sur M. Dynamics of neuronal processing in rat somatosensory cortex. *Trends Neurosci* 22: 513-520. 511_00001452 00001451_00001452, 1999.

Mulligan SJ, and MacVicar BA. Calcium transients in astrocyte endfeet cause cerebrovascular constrictions. *Nature* 431: 195-199, 2004.

Nedergaard M. Direct signaling from astrocytes to neurons in cultures of mammalian brain cells. *Science* 263: 1768-1771, 1994.

Nedergaard M, Ransom B, and Goldman SA. New roles for astrocytes: redefining the functional architecture of the brain. *Trends Neurosci* 26: 523-530, 2003.

Newman EA. New roles for astrocytes: regulation of synaptic transmission. *Trends Neurosci* 26: 536-542, 2003.

Ngai AC, and Winn HR. Estimation of shear and flow rates in pial arterioles during somatosensory stimulation. *Am J Physiol* 270: H1712-1717, 1996.

Niggel J, Sigurdson W, and Sachs F. Mechanically induced calcium movements in astrocytes, bovine aortic endothelial cells and C6 glioma cells. *J Membr Biol* 174: 121-134, 2000.

Norup Nielsen A, and Lauritzen M. Coupling and uncoupling of activity-dependent increases of neuronal activity and blood flow in rat somatosensory cortex. *J Physiol* 533: 773-785, 2001.

Nusbaum MP, and Beenhakker MP. A small-systems approach to motor pattern generation. *Nature* 417: 343-350, 2002.

Oberheim NA, Wang X, Goldman S, and Nedergaard M. Astrocytic complexity distinguishes the human brain. *Trends Neurosci* 29: 547-553, 2006.

Oby E, and Janigro D. The blood-brain barrier and epilepsy. *Epilepsia* 47: 1761-1774, 2006.

Palmer RM, Ferrige AG, and Moncada S. Nitric oxide release accounts for the biological activity of endothelium-derived relaxing factor. *Nature* 327: 524-526, 1987.

Pape HC, and Mager R. Nitric oxide controls oscillatory activity in thalamocortical neurons. *Neuron* 9: 441-448, 1992.

Parpura V, Basarsky TA, Liu F, Jeftinija K, Jeftinija S, and Haydon PG. Glutamate-mediated astrocyte-neuron signalling. *Nature* 369: 744-747, 1994.

Parri HR, Gould TM, and Crunelli V. Spontaneous astrocytic Ca2+ oscillations in situ drive NMDAR-mediated neuronal excitation. *Nat Neurosci* 4: 803-812, 2001.

Pasti L, Volterra A, Pozzan T, and Carmignoto G. Intracellular calcium oscillations in astrocytes: a highly plastic, bidirectional form of communication between neurons and astrocytes in situ. *J Neurosci* 17: 7817-7830, 1997.

Patel U. Non-random distribution of blood vessels in the posterior region of the rat somatosensory cortex. *Brain Res* 289: 65-70, 1983.

Paulson OB, and Newman EA. Does the release of potassium from astrocyte endfeet regulate cerebral blood flow? *Science* 237: 896-898, 1987.

Pawloski JR, and Stamler JS. Nitric oxide in RBCs. *Transfusion* 42: 1603-1609, 2002.

Pellerin L, and Magistretti PJ. Glutamate uptake into astrocytes stimulates aerobic glycolysis: a mechanism coupling neuronal activity to glucose utilization. *Proc Natl Acad Sci U S A* 91: 10625-10629, 1994.

Peppiatt C, and Attwell D. Neurobiology: feeding the brain. *Nature* 431: 137-138, 2004.

Peppiatt CM, Howarth C, Mobbs P, and Attwell D. Bidirectional control of CNS capillary diameter by pericytes. *Nature* 443: 700-704, 2006.

Pierantozzi M, Panella M, Palmieri MG, Koch G, Giordano A, Marciani MG, Bernardi G, Stanzione P, and Stefani A. Different TMS patterns of intracortical inhibition in early onset Alzheimer dementia and frontotemporal dementia. *Clin Neurophysiol* 115: 2410-2418, 2004.

Raichle ME, and Mintun MA. Brain work and brain imaging. *Annu Rev Neurosci* 29: 449-476, 2006.

Ramon y Cajal, S.. *Recollections of My Life*. translated Craigie, EH. Cambridge: The MIT Press, 1996, p. 630.

Reyes R, Lauritzen I, Lesage F, Ettaiche M, Fosset M, and Lazdunski M. Immunolocalization of the arachidonic acid and mechanosensitive baseline traak potassium channel in the nervous system. *Neuroscience* 95: 893-901, 2000.

Riddle DR, Gutierrez G, Zheng D, White LE, Richards A, and Purves D. Differential metabolic and electrical activity in the somatic sensory cortex of juvenile and adult rats. *J Neurosci* 13: 4193-4213, 1993.

Robbins TW, Mehta MA, and Sahakian BJ. Neuroscience. Boosting working memory. *Science* 290: 2275-2276, 2000.

Rochon D, Rousse I, and Robitaille R. Synapse-glia interactions at the mammalian neuromuscular junction. *J Neurosci* 21: 3819-3829, 2001.

Rossi DJ. Another BOLD role for astrocytes: coupling blood flow to neural activity. *Nat Neurosci* 9: 159-161, 2006.

Roy CS, and Sherrington CS. On the Regulation of the Blood-supply of the Brain. *J Physiol* 11: 85-158 117, 1890.

Sarter M, Hasselmo ME, Bruno JP, and Givens B. Unraveling the attentional functions of cortical cholinergic inputs: interactions between signal-driven and cognitive modulation of signal detection. *Brain Res Brain Res Rev* 48: 98-111, 2005.

Sato A, and Sato Y. Cholinergic neural regulation of regional cerebral blood flow. *Alzheimer Dis Assoc Disord* 9: 28-38, 1995.

Schachter SC. Vagus nerve stimulation: where are we? *Curr Opin Neurol* 15: 201-206, 2002.

Segal SS, and Duling BR. Propagation of vasodilation in resistance vessels of the hamster: development and review of a working hypothesis. *Circ Res* 61: II20-25, 1987.

Serota HM, and Gerard RW. Localized thermal changes in the cat's Brain. *J Neurophysiol* 1: 115-124, 1938.

Shaw PJ, and Salt TE. Modulation of sensory and excitatory amino acid responses by nitric oxide donors and glutathione in the ventrobasal thalamus of the rat. *Eur J Neurosci* 9: 1507-1513, 1997.

Sheth SA, Nemoto M, Guiou M, Walker M, Pouratian N, Hageman N, and Toga AW. Columnar specificity of microvascular oxygenation and volume responses: implications for functional brain mapping. *J Neurosci* 24: 634-641, 2004.

Silva AC, and Koretsky AP. Laminar specificity of functional MRI onset times during somatosensory stimulation in rat. *Proc Natl Acad Sci U S A* 99: 15182-15187, 2002.

Silva LR, Amitai Y, and Connors BW. Intrinsic oscillations of neocortex generated by layer 5 pyramidal neurons. *Science* 251: 432-435, 1991.

Simard M, Arcuino G, Takano T, Liu QS, and Nedergaard M. Signaling at the gliovascular interface. *J Neurosci* 23: 9254-9262, 2003.

Simkus CR, and Stricker C. Properties of mEPSCs recorded in layer II neurones of rat barrel cortex. *J Physiol* 545: 509-520, 2002.

Simons DJ, and Carvell GE. Thalamocortical response transformation in the rat vibrissa/barrel system. *J Neurophysiol* 61: 311-330., 1989.

Singel DJ, and Stamler JS. Chemical physiology of blood flow regulation by red blood cells: the role of nitric oxide and S-nitrosohemoglobin. *Annu Rev Physiol* 67: 99-145, 2005.

Spencer KM, Nestor PG, Niznikiewicz MA, Salisbury DF, Shenton ME, and McCarley RW. Abnormal neural synchrony in schizophrenia. *J Neurosci* 23: 7407-7411, 2003.

Stamler JS, Jia L, Eu JP, McMahon TJ, Demchenko IT, Bonaventura J, Gernert K, and Piantadosi CA. Blood flow regulation by S-nitrosohemoglobin in the physiological oxygen gradient. *Science* 276: 2034-2037, 1997.

Stout C, and Charles A. Modulation of intercellular calcium signaling in astrocytes by extracellular calcium and magnesium. *Glia* 43: 265-273, 2003.

Takano T, Tian GF, Peng W, Lou N, Libionka W, Han X, and Nedergaard M. Astrocyte-mediated control of cerebral blood flow. *Nat Neurosci* 9: 260-267, 2006.

Talley EM, Solorzano G, Lei Q, Kim D, and Bayliss DA. Cns distribution of members of the two-pore-domain (KCNK) potassium channel family. *J Neurosci* 21: 7491-7505, 2001.

Taylor-Clarke M, Kennett S, and Haggard P. Vision modulates somatosensory cortical processing. *Curr Biol* 12: 233-236, 2002.

Thompson SM, Masukawa LM, and Prince DA. Temperature dependence of intrinsic membrane properties and synaptic potentials in hippocampal CA1 neurons in vitro. *J Neurosci* 5: 817-824, 1985.

Thompson SM, and Prince DA. Activation of electrogenic sodium pump in hippocampal CA1 neurons following glutamate-induced depolarization. *J Neurophysiol* 56: 507-522, 1986.

Trubel HK, Sacolick LI, and Hyder F. Regional temperature changes in the brain during somatosensory stimulation. *J Cereb Blood Flow Metab* 26: 68-78, 2006.

Tsuang MT, Stone WS, and Faraone SV. Toward reformulating the diagnosis of schizophrenia. *Am J Psychiatry* 157: 1041-1050, 2000.

Turing AM. Computing Machinery and Intelligence. *Mind: A Quarterly Review of Psychology and Philosophy* 59: 433-460, 1950.

Vallance P, Collier J, and Moncada S. Nitric oxide synthesised from L-arginine mediates endothelium dependent dilatation in human veins in vivo. *Cardiovasc Res* 23: 1053-1057, 1989.

van Helden DF, Hosaka K, and Imtiaz MS. Rhythmicity in the microcirculation. *Clin Hemorheol Microcirc* 34: 59-66, 2006.

Vanzetta I, Slovin H, Omer DB, and Grinvald A. Columnar resolution of blood volume and oximetry functional maps in the behaving monkey; implications for FMRI. *Neuron* 42: 843-854, 2004.

Vaucher E, Tong XK, Cholet N, Lantin S, and Hamel E. GABA neurons provide a rich input to microvessels but not nitric oxide neurons in the rat cerebral cortex: a means for direct regulation of local cerebral blood flow. *J Comp Neurol* 421: 161-171, 2000.
Vesalius. De Humani Corporis Fabrica. 1543.

Volterra A, and Meldolesi J. Astrocytes, from brain glue to communication elements: the revolution continues. *Nat Rev Neurosci* 6: 626-640, 2005.
Wang X, Lou N, Xu Q, Tian GF, Peng WG, Han X, Kang J, Takano T, and Nedergaard M. Astrocytic Ca2+ signaling evoked by sensory stimulation in vivo. *Nat Neurosci* 9: 816-823, 2006.

Welker WI. Analysis of Sniffing in the Albino Rat. *Behavior* 12: 223-244, 1964.

Wilent WB, and Contreras D. Dynamics of excitation and inhibition underlying stimulus selectivity in rat somatosensory cortex. *Nat Neurosci* 8: 1364-1370, 2005.

Woo NH, and Lu B. Regulation of cortical interneurons by neurotrophins: from development to cognitive disorders. *Neuroscientist* 12: 43-56, 2006.

Woolsey TA, Rovainen CM, Cox SB, Henegar MH, Liang GE, Liu D, Moskalenko YE, Sui J, and Wei L. Neuronal units linked to microvascular modules in cerebral cortex: response elements for imaging the brain. *Cereb Cortex* 6: 647-660., 1996.

Worden MS, Foxe JJ, Wang N, and Simpson GV. Anticipatory biasing of visuospatial attention indexed by retinotopically specific alpha-band electroencephalography increases over occipital cortex. *J Neurosci* 20: RC63, 2000.

Yablonskiy DA, Ackerman JJ, and Raichle ME. Coupling between changes in human brain temperature and oxidative metabolism during prolonged visual stimulation. *Proc Natl Acad Sci U S A* 97: 7603-7608, 2000.

Yamazaki J, and Kitamura K. Intercellular electrical coupling in vascular cells present in rat intact cerebral arterioles. *J Vasc Res* 40: 11-27, 2003.

Yang X, Renken R, Hyder F, Siddeek M, Greer CA, Shepherd GM, and Shulman RG. Dynamic mapping at the laminar level of odor-elicited responses in rat olfactory bulb by functional MRI. *Proc Natl Acad Sci U S A* 95: 7715-7720, 1998.

Zaidi A, Clough P, Cooper P, Scheepers B, and Fitzpatrick AP. Misdiagnosis of epilepsy: many seizure-like attacks have a cardiovascular cause. *J Am Coll Cardiol* 36: 181-184, 2000.

Zhang JM, Wang HK, Ye CQ, Ge W, Chen Y, Jiang ZL, Wu CP, Poo MM, and Duan S. ATP released by astrocytes mediates glutamatergic activity-dependent heterosynaptic suppression. *Neuron* 40: 971-982, 2003.

Zheng D, LaMantia AS, and Purves D. Specialized vascularization of the primate visual cortex. *J Neurosci* 11: 2622-2629, 1991.

Zhu M, Ackerman JJ, Sukstanskii AL, and Yablonskiy DA. How the body controls brain temperature: the temperature shielding effect of cerebral blood flow. *J Appl Physiol* 101: 1481-1488, 2006.

Zonta M, Angulo MC, Gobbo S, Rosengarten B, Hossmann KA, Pozzan T, and Carmignoto G. Neuron-to-astrocyte signaling is central to the dynamic control of brain microcirculation. *Nat Neurosci* 6: 43-50, 2003.

Chapter 3

Pinacidil Induces Vascular Dilation and Hyperemia *in vivo* and Does Not Impact Biophysical Properties of Neurons and Astrocytes *in vitro*[b]

Abstract

Vascular and neural systems are highly interdependent, as indicated by the wealth of intrinsic modulators shared by the two systems. We tested the hypothesis that pinacidil, a selective agonist for the SUR2B receptor found on smooth muscles, could serve as an independent means of inducing vasodilation and increased local blood volume to emulate functional hyperemia. Application of pinacidil induced vasodilation and increased blood volume in the *in vivo* neocortex in anesthetized rats and awake mice. Direct application of this agent to the *in vitro* neocortical slice had no direct impact on biophysical properties of neurons or astrocytes assessed with whole-cell recording. These findings suggest that pinacidil provides an effective and selective means for inducing hyperemia *in vivo*, and may provide a useful tool in directly testing the impact of hemodynamics on neural activity, as recently predicted by the Hemo-Neural hypothesis.

Introduction

Interactions between the brain and blood are essential to health. Metabolic supply of the brain is provided through the vasculature, and disruptions of this relationship, in extreme cases such as stroke, is a key characteristic of neurologic disease. Neuro-Hemodynamic coupling is also demonstrated in healthy individuals on faster time scales in functional hyperemia, the local increase in blood flow and volume that accompanies neural activity (Sherrington 1890, Raichle 1998).

---

[b] Portions of this chapter were previously published under the same title in *Cleve Clin J. Med, 2009 Apr; 76 Suppl 2:S80-5*, authors Cao R, Higashikubo BT, Cardin J, Knoblich U, Ramos R, Nelson MT, Moore CI, Brumberg JC.

We have recently proposed a further level of interdependence between the two systems, the Hemo-Neural hypothesis, which predicts that hemodynamic events such as functional hyperemia will modulate neural activity (Moore 2008). An impact of hemodynamics on neurons could occur through a number of mechanisms including the activation of mechanoreceptors on astrocytes or neurons, a thermal impact of increased blood flow on ion channels and vesicle release, and the local increase and diffusion of blood-borne factors such as nitric oxide (Garthwaite 2006, Kozlov 2006). Astrocytes are predicted to play a key role in hemo-neural modulation, as they are tightly coupled to the vascular system and participate in a number of neural functions (Nedergaard 2003, Haydon 2006). Through these mechanisms and others, hemodynamics could shift the 'state' of the local neural circuit, thereby impacting information processing. This regulation of neural dynamics could also provide a homeostatic mechanism for promoting healthy brain function (e.g., prevention of kindling).

To study the impact of hyperemia on neural and astrocytic activity *in vivo*, it is essential to independently control blood flow in the brain with means that do not directly impact neurons or astrocytes. Pinacidil is a sulfonylurea receptor agonist that opens the SUR2B potassium-sensitive ATP channel (Ashcroft 2000). In the telencephalon, SUR1 receptors are localized to neurons and glia (Levin 2001, Zawar 1999). In contrast, SUR2 receptors are localized to vasculature, with SUR2A in cardiac and skeletal muscle, and SUR2B in vascular smooth muscle, with primary expression in smaller arteries, arterioles and capillaries (Li 2003). By opening the SUR2B channel, pinacidil hyperpolarizes and relaxes smooth muscle, causing vasodilation. Pinacidil is a potent and selective SUR2B agonist, with a dissociation constant of 135nM and EC50 value of 680nM (Schwanstecher 1998) . This agonist is ~5 times more specific for SUR2B than SUR2A, and shows ~5 orders of magnitude lower affinity for SUR1 (in the mM range) (Schwanstecher 1998; Shindo 1998; Russ 2003; Higdon 1997). Previous studies have demonstrated the efficacy of this agent as a vasodilator (Wahl 1989, Hempelmann 1995, Quayle 1997)

In the present study, we systematically examined the utility of pinacidil as an agent for the selective induction of hyperemia. First, we quantified the vasodilation induced by pinacidil *in vivo*, and examined local increases in blood volume in the parenchyma. These studies were conducted in anesthetized rats and awake mice. Second, we used *in vitro* slice recordings to

examine whether direct application of relatively high concentrations of pinacidil would have any impact on the physiology of neurons and astrocytes. We found that *in vivo*, pinacidil induces a level of vasodilation and increased local blood volume consistent with natural functional hyperemia across a variety of preparations, and that there was no detectable impact of this agent on intrinsic biophysical measures in neurons and astrocytes *in vitro*.

Methods

Animal Preparation *in vivo*

To probe the impact of pinacidil on arterial diameter and parenchymal blood volume *in vivo*, we measured the effects of topical application to the primary somatosensory cortex (SI) of rats and mice. Rats and mice (Sprague-Dawley, 250–500 grams, CD57 BL/6 mice, ~25 grams) were anaesthetized with Nembutal (50 mg/kg IP initial dose, followed by 5mg supplements as needed for maintenance). Animals were maintained at ~ 37°C by a heating blanket. A craniotomy (~2mm diameter in rats, ~1mm in mice) and durotomy were performed over SI, and the cortex protected with Kwik-Cast silastic elastomer (WPI) while an imaging chamber was attached with dental cement. Kwik-Cast was removed, and the chamber filled with 0.9% saline and sealed with a round coverglass (avoiding bubbles) secured with cyanoacrylate.

Controlling Visualization During Drug Delivery *in vivo*

To minimize brain motion and flow artifacts during visualization of hemodynamics in the rat preparation, we constructed a customized, pressurized chamber with inflow and outflow for constant perfusion. The volume of the chamber was ~0.3 ml, and the flow through the system averaged about 2ml/minute. The chamber consisted of a 1cm diameter, 3mm high plastic ring with a flat top profile and a base shaped to the angle of the lateral skull edge over SI. In the wall of this chamber, three large holes were drilled and patched with pieces cut from rubber NMR septa (VWR) to create re-sealable ports for drug application and bubble removal. Three additional permanent holes were drilled in the chamber walls, through which blunted 1cm lengths of 18-gauge stainless steel needles were wedged and affixed with superglue: one for ACSF inflow, one for combined outflow, and the third for pressure regulation. The overall pressure of the chamber was regulated by a small vertical tube whose height (and thus fluid

level) could be adjusted on a manipulator stand, and whose other end was open to the atmosphere. Inflow and outflow were controlled via regulators on a gravity feed system. In the mouse preparation, the need to control visualization was addressed by maintaining a constant rate of wicking in a smaller-profile open chamber, and a microfluidic switch with 12μL of dead space was added to minimize propulsive impact and delay due to switching between solutions. Drug and ethanol solutions were delivered to rat and mouse chambers after being heated to physiological temperature, 37°C degrees.

Optical Measurement of Hemodynamics *in vivo*

We used a charge-coupled device (CCD) camera (the Roper 512B, Princeton Instruments) to image the cortical surface at a frame rate of ~4Hz, with illumination from a voltage-regulated xenon arc lamp. A green band-pass filter (550nm) was employed to maximize imaging near the isobestic point of hemoglobin, providing optimal vessel contrast and a surrogate measure for blood volume change in the parenchyma. Lenses (50 and 125mm) were arranged in series to form a macroscope.

We measured the impact of pinacidil on the diameter of the middle cerebral artery (MCA) and on parenchymal blood volume. Arteries were distinguished from veins by their lighter color, lower tortuosity and/or the inability to follow individual movement of red blood cells (indicating high flow rate). To measure arterial diameter, we took a cross section. We calculated the borders in each frame as the point 50% between the pixel brightness of the lightest part of the profile (over parenchymal tissue) and the darkest part (over the vessel). In **Figure 1A**, the green bar bisecting an artery indicates the point at which we obtained data that went into the width plot at the top of **Figure 1B**, which shows a line scan of darkness around the artery as a function of time. For parenchymal measurements, we summed all pixels in a region without detectable vessels (such as the red enclosed region in **Figure 1A**) and measured the change in darkness over successive frames.

Pinacidil Administration *in vivo*

Pinacidil is hydrophobic and was therefore dissolved in ethanol at ~12 mg/kg and then diluted 1:100 in ACSF to achieve a 400μM solution in 1% ethanol. Stock solutions were stored at -20°C

and diluted in fresh ACSF for each experiment. For each run, the cortex was imaged for 3 minutes to establish baseline. For the pressurized rat chamber, at the end of the baseline period, 0.1-0.3mls of 400μM pinacidil in 1% ethanol in ACSF or saline would be pumped (taking about 1s) into the 0.3ml volume chamber. Simultaneously, an equivalent volume was drawn out to balance pressure by a push-pull pump with access through two of the resealable rubber ports.

Pinacidil Administration *in vitro*

Coronal slices were prepared from post-natal day 14-40 Sprague-Dawley rats and maintained in a submersion chamber at $27^{\circ}C$ for recording. Solutions were prepared in artificial cerebral spinal fluid (ACSF (in mM): 125 NaCl, 2.5 KCl, 1 MgCl$_2$, 1.25 NaH$_2$PO$_4$, 2 CaCl$_2$, 25 NaHCO$_3$, and 25 d-glucose). The applied solutions were 1% ethanol, ~400 μM pinacidil in 1% ethanol, and ACSF, all perfused with 5% CO$_2$ in 95% O$_2$ (carbogen).

For astrocyte recordings, slices were incubated immediately after cutting for 20 minutes in ACSF containing 50μM SR101, a water soluble fluorescent dye specifically taken up by astrocytes (Nimmerjahn 2004). The slices were then allowed to rest for an hour before intracellular recordings with a 3-5MΩ pipette. For fluorescence visualization, the light source was a 100 W Hg arc lamp, with excitation and barrier filters and dichroic mirrors tailored to the spectral characteristics of SR101 (excitation ~ 586nm, emission ~ 605nm)

Slices were imaged under differential interference contrast optics with IR illumination. Cells in layers 2/3 and in the same field and plane of view as a blood vessel of >20μm diameter were targeted, and vessel expansion was monitored during intracellular recording at ~4Hz with a cooled charge coupled device camera (cCCD) from Q-imaging (Retiga EX) connected to the microscope via a parfocal C-mount. This configuration also enabled imaging of neurons and astrocytes in the slice.

Drug/control solutions were switched every 90–180 seconds. Recording pipettes were filled with (in mM) 120 KGlu, 10 NaCl, 20 KCl, 10 HEPES, 2 Mg-ATP, 0.3 Na-GTP, 0.5 EGTA, and 0.3-1% biocytin (wt/vol) for subsequent visualization of the neurons.

Results

Pinacidil Induces Vasodilation in Anesthetized Rats and Awake Mice

The image in **Figure 1A** shows the cortical surface over SI. The green bisection line over the MCA shows the point of sampling for the darkness plot in **Figure 1B** shown in the rectangular box below the vascular image. The width of this dark band is the width of the MCA over time, showing expansion after pinacidil addition (gray bar). The point at which dilation is observed
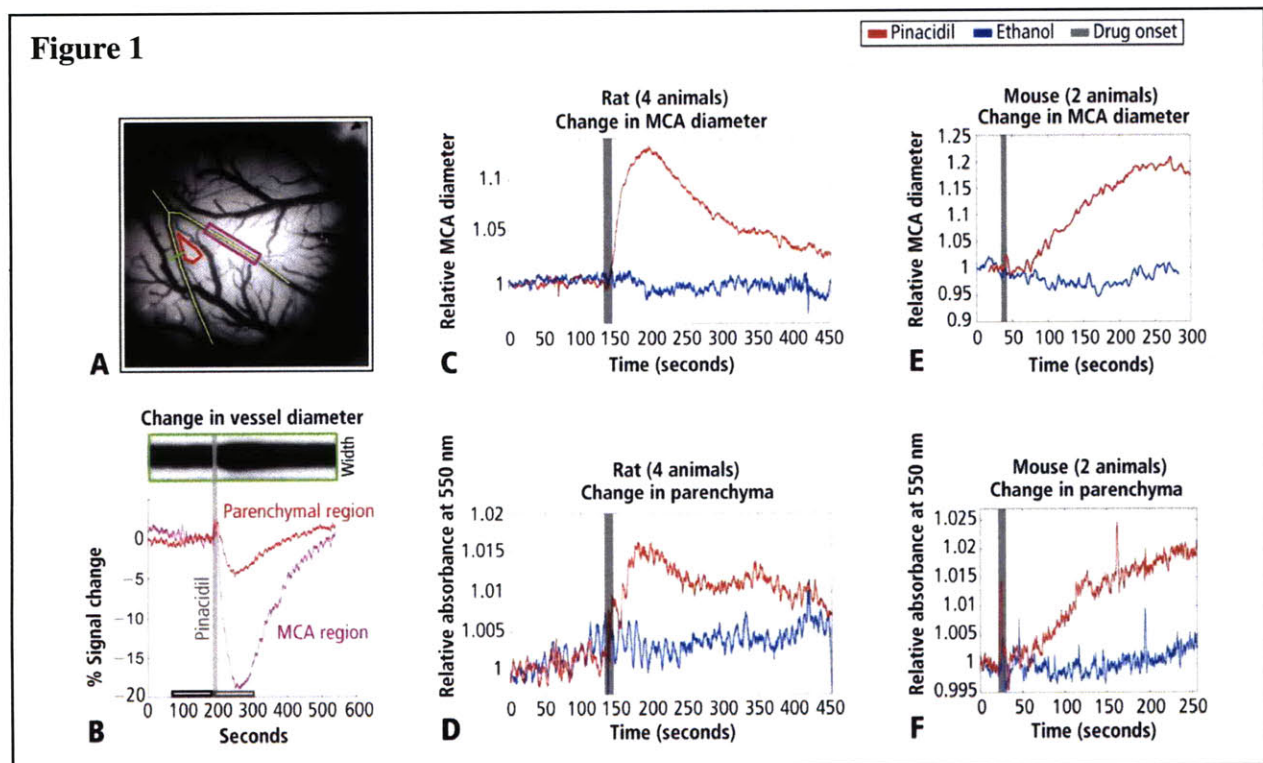

Figure 1: *In vivo responses to pinacidil application. (**A**) Cortical surface over the somatosensory cortex in a rat: yellow lines indicate course of the middle cerebral artery (MCA); purple box indicates area of subsequent analysis following pinacidil application; red outline indicates the parenchymal region. (**B**) Inset reveals change in MCA diameter over time (at green line in panel A); graph shows normalized changes in absorption measured in the MCA and parenchymal regions over the same time period, with the gray line indicating the onset of pinacidil application. (**C**) Average change in MCA diameter in rats in response to pinacidil (red) and ethanol (blue). (**D**) Changes in parenchymal absorbance in rats over time. (**E**) In mice, MCA diameter increases in response to pinacidil (red) but not ethanol (blue). (**F**) Changes in parenchymal absorbance in mice over time.*

corresponds to a darkening in a parenchymal region (red triangle in the image) and over the

MCA and surrounding cortex (purple rectangle, reflecting expansion). Vasodilation and parenchymal signal increases were consistently observed on the first trial in all experiments (N = 4 first runs from 4 anesthetized rats, **Figure 1C** and **D**). Dilation initiated <10s after drug arrival, with maximal dilation and parenchymal darkening at a ~50-60 second latency. Ethanol in a 1:100 solution with ACSF under the same conditions evoked a non-significant reduction in vessel diameter and no change in parenchymal darkening. Following the first presentation, subsequent pinacidil effects were less reliable.

As shown in **Figure 1E** and **F**, the hemodynamic impact of pinacidil in anesthetized rats was replicated in awake, head-posted mice (N = 2 mice, 2 runs each). Presentation of 220 or 440μM pinacidil evoked comparable mean increases in arterial diameter (peak diameter increase of ~20%) and parenchymal darkening (peak increase of ~2%), effects that were repeatable within subjects in a single session (N = 2).

Pinacidil Does Not Have a Direct Effect on Non-Vascular Tissue

Vessels in slice only rarely responded to pinacidil application, with no significant changes in vessel diameter over 14 vessels in 14 distinct slices *in vitro* (**Figure 2A**). Presumably pinacidil succeeds in inducing smooth muscle hyperpolarization under these conditions, but because unpressurized vessels in slice do not have a source of dilatory force against vessel walls, no expansion is observed.

Pinacidil Does Not Impact Spiking Probability or Input Resistance in Neurons or Membrane Potential in Neurons and Astrocytes

In recordings from regular-spiking neurons of pyramidal shape (N=30), we saw no change in any metric measured. At 50s post-application, approximately the time of peak vasodilatory effects *in vivo*, the membrane potential did not change (variation of -0.5 ± 0.9mV standard deviation; **Figure 2E**), spike rate induced by current injection did not change (variation of 0.1 ± 1.1 spikes/stim **Figure 2F**), and input resistance did not change (variation of -0.7 ± 6.5MΩ **Figure 2D**). In a limited subset of recordings from fast-spiking interneurons, we similarly did not observe any impact of pinacidil application (N=3). All significance tests were paired t-tests (*p* > 0.1).
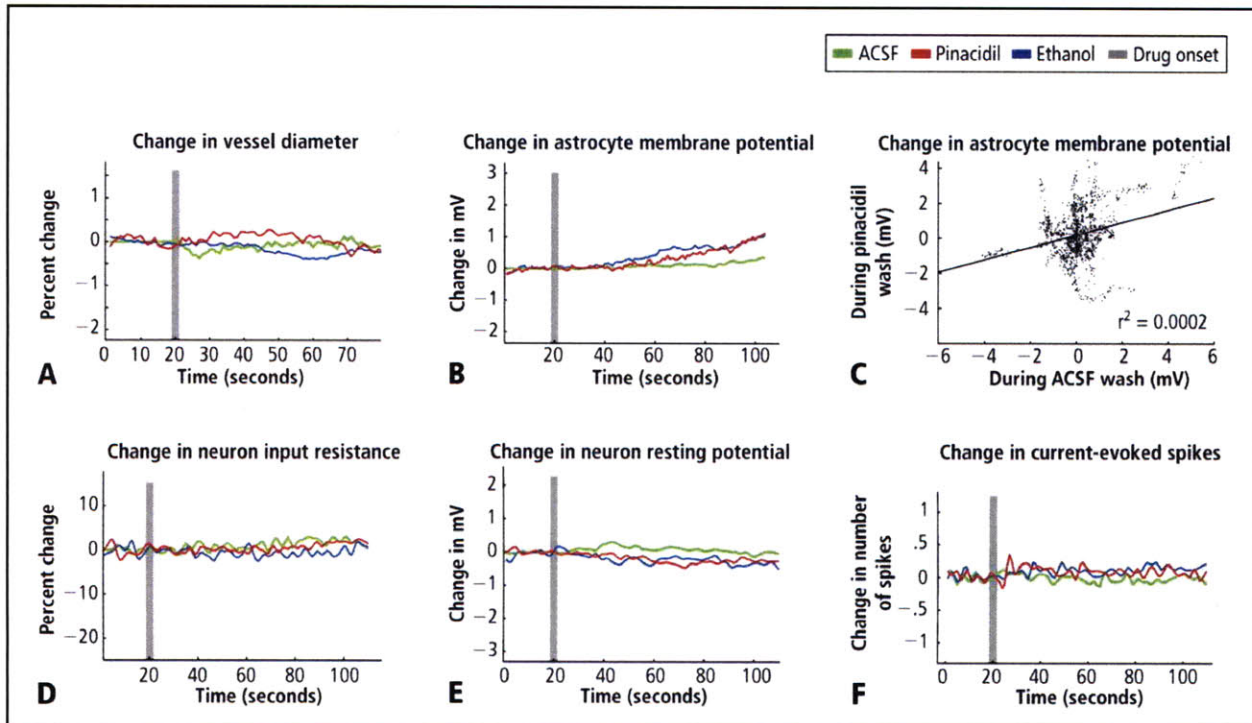
Figure 2

Figure 2*: (A) Pinacidil at a dose of 400 µM does not show a significant effect on vessel diameters in slice (14 vessels). (B) Astrocytes depolarize slightly in response to 1% ethanol in artificial cerebrospinal fluid (ACSF). Depolarization was about 1 mV, on average (30 cells). (C) Depolarization of astrocytes in response to pinacidil and ethanol is not significant. (D, E, F) Layer 2/3 neurons showed no response to pinacidil or ethanol in input resistance, resting membrane potential, or spikes evoked by depolarizing current injection (30 cells), with no additional effect observed in response to application of pinacidil in 1% ethanol.*

Astrocytes (N=35) also showed no significant effects of pinacidil application, demonstrating only a slow depolarization during ethanol (1.3mV +- 1.7mV at 50s post-drug application) and pinacidil with ethanol (0.5 $\pm$ 2.1mV) application (**Figure 2B**). When we plotted the change in membrane potential at 10 second intervals since drug application (0 to 80 seconds post-drug), we found no trends in astrocytic response to either ACSF or pinacidil (**Figure 2C**).

Astrocytes are Sensitive to Changes in Chamber Flow Pressure

In preliminary experiments, we observed 2 astrocytes that depolarized on switching to the pinacidil solution. These 2 recordings were obtained prior to placing an inline pressure meter in

the flow pathway that allowed us to monitor and exclude trials that showed flow changes. In the 35 subsequent recordings that did not have flow changes, we never observed a detectable impact of either ethanol or pinacidil on astroctyes or neurons. We also note that neurons and astrocytes were more likely to die and/or to lose recording quality during a cycle of ethanol or pinacidil presentation, as opposed to ACSF presentation.

During recordings at double our typical application dose (800µM), we observed 2 pyramidal cells (out of 8) that showed depolarization (10-15 mV peak) and a loss of spike initiation capability. Following washout, these cells recovered membrane potential but spiking responses to current injection remained impaired. We did not evaluate the impact of this dose on vascular tone or rhythmic vasomotion.

Figure 3
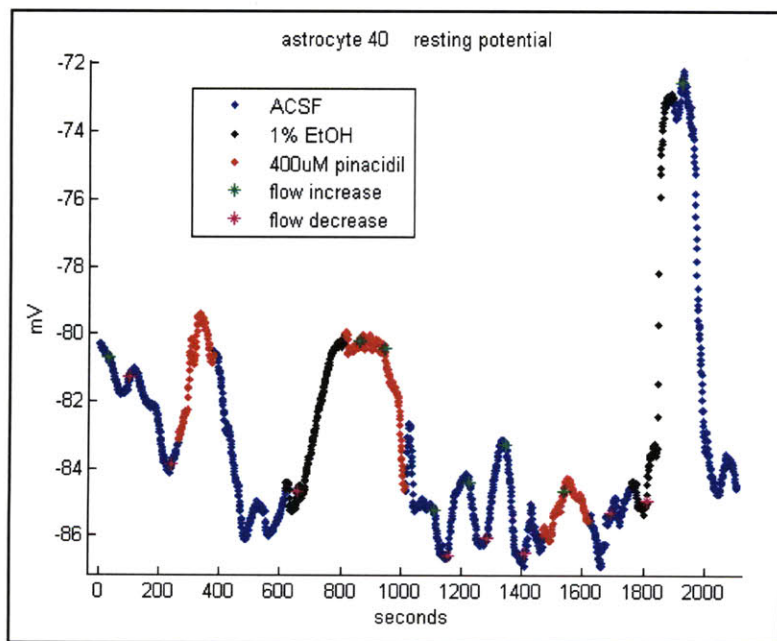
Figure 3: Example of an astrocyte sensitive to flow rate into slice recording chamber. Flow increases (higher flow pressure, green asterisks) resulted in lower membrane potentials while flow decreases (lower flow pressure, pink asterisks) resulted in more depolarized membrane potentials. Changes in flow rate generally corresponded to a change in solution (e.g. from ACSF to ethanol, blue to red just after 600 seconds). The impact of changes in pressure without changes in solution can be seen between 1000 and 1400 seconds, where ACSF at higher pressure alternates with flow of ACSF at lower pressure.

In contrast to the absence of a detectable impact of pinacidil, we found that the membrane potentials of neurons and astrocytes were sensitive to flow rate. In several astrocytes, decreasing flow rate caused a depolarization of up to ~10 mV that showed an immediate onset, reaching a

new baseline within 2-5 seconds, and increasing flow rate had the opposite effect. These effects can be seen most clearly in the period from ~100-~1450 seconds (**Figure 3**) The effect was observed in every astrocyte probed with flow changes (N = 10), though the magnitude of the effect varied.

Changes in flow rate generally corresponded to a change in solution (e.g. from ACSF to ethanol) because of the gravity-drip system, which was sensitive to the level of fluid in the reservoir tubes upstream. These varied depending on how much of each solution remained at the time of switching.

Discussion

Pinacidil provides an effective means of creating vasodilation *in vivo*. At concentrations $\leq$ 400μM, pinacidil is also selective for cortical vascular smooth muscle, exhibiting no direct effect on intrinsic properties of neurons or astrocytes. As an independent means to induce increased vasodilation and blood volume in a manner analogous to that seen in functional hyperemia, pinacidil provides a viable technique for testing the impact of hyperemic events on neural or astrocytic activity. Pinacidil may also be a selective means of emulating other normal hemodynamic phenomena and could have therapeutic applications, such as targeted administration of pinacidil in response to acute vessel obstruction to maintain sufficient perfusion.

The hemodynamic effects induced by pinacidil are similar to natural functional hyperemia. In SI during sensory stimulation in rodents, increases in total oxygenated hemoglobin during sensory stimulation—analogous to our measurement of cortical darkening at 550 nm—peak in a range of 2-5% (Jones 2008; Martin 2006, Kong 2004), and arteries/arterioles dilate 10-20% (Woolsey, 1996). The time course of pinacidil effects also parallels the sustained response to continued sensory drive. Arterial diameter in rodent SI and the fMRI Blood Oxygen Level Dependent (BOLD) response in humans and rodents remains high when tactile input is sustained for periods lasting tens of seconds (Woolsey 1996, Moore 2000), as it does under pinacidil application.

While pinacidil represents an important step forward in our ability to control blood flow while probing the impact of hemodynamics in cortex, it has limitations. The drug is only capable of producing vasodilation—drugs in the same family that block the SUR2B channels to create vasoconstriction (such as diazoxide or glibenclamide) or thromboxane receptor agonists (Crepel 1993, Lovick 2005, Quayle 1997) are unfortunately known to be non-specific, affecting neurons as well as blood vessels. Pinacidil is also non-water-soluble, necessitating its dissolution in ethanol or DMSO, agents that can have confounding impacts on the system. Applied *in vivo*, pinacidil also does not appear to wash out fully, or its impact on smooth muscles persists, so that the first trial in each animal is the most consistent and effective. These limitations stated, this pharmacological approach nevertheless represents a unique means of selective hyperemia induction *in vivo*.

Perhaps the most unexpected result was the sensitivity of both neurons and astrocytic membrane potentials to the flow rate through the chamber. Flow changes were crudely controlled by changing flow-regulator position, and so not quantified, and would have been different from cell to cell. Flow changes could potentially have corresponded to changes in temperature (depending on how quickly the in-line heater adapted), pressure, or oxygenation level (as newer ACSF might be expected to have higher oxygen levels. Another possibility is that the cells were sensitive to shear stress, as experienced by flow over the cellular surface perturbing the slice. However, flow rates were not so high as to cause visible changes in the slice being imaged. In some ways, the flow rate is a proxy in slices for the role of blood flow in vivo, as it fulfills many of the same functions (oxygenation, temperature and pressure modulation, waste removal). It may be the case that only some cells (only neurons, only astrocytes, or only a subset of each) are responsive to these variables, but that they propagate the effects to nearby cells.

TRPV4 channels are responsive to temperature, membrane stretch, and shear stress, and are known to be expressed on astrocytes (see Ch 3); as such, they may play a role in transducing the flow rate effects observed.

While the mechanism of these membrane responses are not known, it is consistent with (and supportive evidence for) the hemo-neural hypothesis that physical factors such as those influenced by flow rate can impact membrane potential.

References

Roy CS, and Sherrington CS. On the Regulation of the Blood-supply of the Brain. *J Physiol* 11:85-158 117, 1890

Raichle ME Behind the scenes of functional brain imaging: a historical and physiological perspective. *Proc Natl Acad Sci* USA 95:765–772 (1998)

Garthwaite G, Bartus K, Malcolm D, Goodwin D, Kollb-Sielecka M, Dooldeniya C, and Garthwaite J. Signaling from blood vessels to CNS axons through nitric oxide. *J Neurosci* 26:7730-7740, 2006.

Kozlov AS, Angulo MC, Audinat E, Charpak S. Target cell-specific modulation of neuronal activity by astrocytes. *Proc Natl Acad Sci* U S A. 2006 Jun 27;103(26):10058-63.

Nedergaard M, Ransom B, and Goldman SA. New roles for astrocytes: redefining the functional architecture of the brain. *Trends Neurosci* 26: 523-530, 2003.

Haydon PG, and Carmignoto G. Astrocyte control of synaptic transmission and neurovascular coupling. *Physiol Rev* 86: 1009-1031, 2006.

Levin, B.E., A.A. Dunn-Meynell, and V.H. Routh, Brain glucosensing and the K(ATP) channel. *Nat Neurosci*, 2001. 4(5): p. 459-60.

Zawar, C., T.D. Plant, C. Schirra, A. Konnerth, and B. Neumcke, Cell-type specific expression of ATP-sensitive potassium channels in the rat hippocampus. *J Physiol*, 1999. 514 (Pt 2): p. 327-41.

Li, L., J. Wu, and C. Jiang, Differential expression of Kir6.1 and SUR2B mRNAs in the vasculature of various tissues in rats. *J Membr Biol*, 2003. 196(1): p. 61-9.

Schwanstecher, M., C. Sieverding, H. Dorschner, I. Gross, L. Aguilar-Bryan, C. Schwanstecher, and J. Bryan, Potassium channel openers require ATP to bind to and act through sulfonylurea receptors. *Embo J*, 1998. 17(19): p. 5529-35.

Shindo, T., M. Yamada, S. Isomoto, Y. Horio, and Y. Kurachi, SUR2 subtype (A and B)-dependent differential activation of the cloned ATP-sensitive K+ channels by pinacidil and nicorandil. *Br J Pharmacol*, 1998. 124(5): p. 985-91.

Russ, U., U. Lange, C. Loffler-Walz, A. Hambrock, and U. Quast, Binding and effect of K ATP channel openers in the absence of Mg2+. *Br J Pharmacol*, 2003. 139(2): p. 368-80.

Higdon, N.R., S.A. Khan, L.V. Buchanan, and K.D. Meisheri, Tissue and species variation in the vascular receptor binding of 3H-P1075, a potent KATP opener vasodilator. *J Pharmacol Exp Ther*, 1997. 280(1): p. 255-60.

Frances M. Ashcroft, Fiona M. Gribble, New windows on the mechanism of action of KATP channel openers, *Trends in Pharmacological Sciences,* Volume 21, Issue 11, 1 November 2000, Pages 439-445

Hempelmann, Ralf G.; Barth, Harald L.; Mehdorn, H. Maximilian; Pradel, Rainer; Ziegler, Albrecht Effects of Potassium Channel Openers in Isolated Human Cerebral Arteries. *Neurosurgery.* 37(6):1146-1153, December 1995.

Wahl M. The effects of pinacidil and tolbutamide in feline pial arteries in situ. *Pflugers Arch.* 1989 Nov;415(2):250-2.

J. M. Quayle, M. T. Nelson and N. B. Standen, ATP-sensitive and inwardly rectifying potassium channels in smooth muscle *Physiol. Rev.* 77: 1165-1232, 1997

Nimmerjahn A, Kirchhoff F, Kerr JN, Helmchen F. Sulforhodamine 101 as a specific marker of astroglia in the neocortex in vivo. *Nat Methods.* 2004 Oct;1(1):31-7

Kong Y, Zheng Y, Johnston D, Martindale J, Jones M, Billings S, and Mayhew J. A model of the dynamic relationship between blood flow and volume changes during brain activation. *J Cereb Blood Flow Metab* 24: 1382-1392, 2004.

Martin C, Martindale J, Berwick J, and Mayhew J. Investigating neural-hemodynamic coupling and the hemodynamic response function in the awake rat. *Neuroimage* 32: 33-48, 2006.

Jones M, Devonshire IM, Berwick J, Martin C, Redgrave P, Mayhew J. Alterered neurovascular coupling during information-processing states. *Eur J Neurosci.* 2008 May;27(10):2758-72.

Woolsey TA, Rovainen CM, Cox SB, Henegar MH, Liang GE, Liu D, Moskalenko YE, Sui J, and Wei L. Neuronal units linked to microvascular modules in cerebral cortex: response elements for imaging the brain. *Cereb Cortex* 6: 647-660., 1996.

Moore CI, Stern CE, Corkin S, Fischl B, Gray AC, Rosen BR, Dale AM. Segregation of somatosensory activation in the human rolandic cortex using fMRI. *J Neurophysiol.* 2000 Jul;84(1):558-69.

Lovick TA, Brown LA, Key BJ. Neuronal activity-related coupling in cortical arterioles: involvement of astrocyte-derived factors. *Exp Physiol.* 2005 Jan;90(1):131-40.

Crépel V, Krnjević K, Ben-Ari Y. Sulphonylureas reduce the slowly inactivating D-type outward current in rat hippocampal neurons.*J Physiol.* 1993 Jul;466:39-54.

Chapter 4

Astrocytic Calcium Changes in Response to Vasodilation Measured with 2-Photon Laser Scanning Microscopy

Introduction: Mechanical sensitivity of astrocytes and neurons

Astrocytes have long been known to be sensitive to mechanical stimulation (Charles 1991). Mechanical stimulation of astrocytes in culture and slice results in a rapid increase in intracellular calcium, subsequent oscillations and spreading calcium waves. These mechanical effects are typically demonstrated using glass beads or pipette touches. These stimuli, while subtle, are obviously non-physiological, begging the question of whether astrocytes are driven by biologically-generated intrinsic mechanical forces.

The vasodilation and constriction that accompany changes in blood flow are one potential source of physiological mechanical deformation. As mechanical impingements on the mechanosensitive endfeet, vascular perturbations are a candidate for modulation of astrocytic activation.

The mechanism of astrocytic mechanical sensitivity is still not conclusively determined, but likely candidates are mechano-sensitive channels that either directly pass calcium or indirectly activate other mechanisms (e.g. voltage-gated Ca channels, release from internal stores) by passing other cations. At least 5 mechanosensitive channels have been shown to be expressed mammalian neocortical astrocytes, including TREK and TRAAK family potassium channels. (Kirischuk 2009).

Perhaps the most promising candidate is the non-selective cation TRPV4 channel, which has been shown to be expressed in rat cortical astrocytes, and highly enriched in layer 1 in astrocytic processes near large vessels. These channels are sensitive to membrane stretch as well as shear stress and temperature (O'Neil 2005). They co-localize with aquaporin channels in astrocytic

endfeet enwrapping blood vessels. Treating cultured astrocytes with Ruthenium Red (RR), a non-specific TRPV channel antagonist, blocks the Ca response to hypo-osmotically induced cell swelling (Benfenati 2007).

As described in **Chapter 3**, Charpak and colleagues have shown that mechanically pressurizing and depressurizing a vessel in slice can give rise to slow inward (granule cells and pyramidal cells) and slow outward currents (mitral cells) in nearby neurons in hippocampus (Angulo 2004) and olfactory bulb (Kozlov 2006), through the activation of astrocytes via their sensitive endfeet.

As a preliminary test of whether such mechanisms were also present in neocortex, we similarly applied mechanical pressure waves to arterioles *in vitro.*

Part 1: Effects of vascular pressurization in slice

Abstract

To look for mechanosensitive effects of changes in vascular diameter on nearby astrocytes, I used a similar method to that described by Charpak's group to pressurize the blood vessels, but recorded directly from nearby astrocytes likely to have endfeet on the stimulated vessel. Rapid mechanical inflation of blood vessels caused rapid depolarization in nearby astrocytes, where larger increases in pressure resulted in larger depolarizations. A similar response was seen in neurons, where depolarization often led to spiking.

Methods

Fresh cortical slices were prepared from P16-P24 rats. Slices were incubated in ACSF with carbogen, and stained with SR101 to label astrocytes. To gain access to the interior of an intact vessel in slice, a quartz pipette connected to a syringe full of 0.9% saline was driven through the wall of a pial vessel significantly upstream of the recording site (> 300μm away) at high speed. The pipette was pulled as for patch clamp recording, then broken to create a sharp edge. A second pipette was used to record in current clamp mode from layer 2/3 neurons or astrocytes near the threaded vessel, while the saline syringe was manipulated by hand to increase and decrease pressure in the vessel.

Figure 1
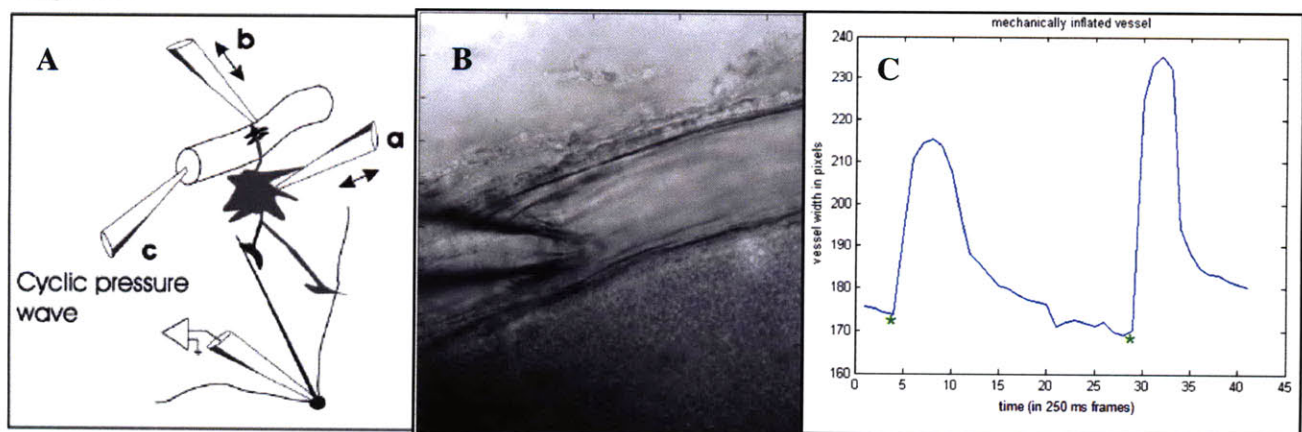
Figure 1: (A) Schematic of set-up (from Kozlov 2006). (B) Quartz pipette in pial vessel. (C) Dilation of vessel caused by pressure injection. Pressure applied upstream at times indicated by green asterisks.

Results

A typical inflation event dilated the vessel between 20% and 40% from baseline (which we would expect to be slightly below the baseline dilation *in vivo*, as the vessels are unpressurized in slice. The time to maximum dilation from baseline would be around 1 second, and the time to recover halfway to baseline between 500 and 800 ms (camera imaging at 4 Hz).
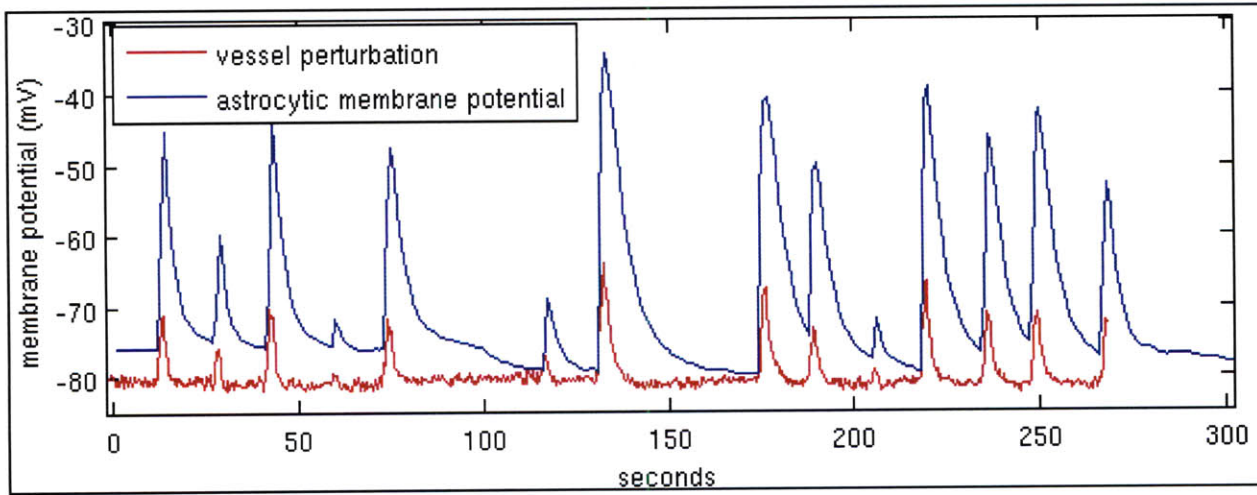
Figure 2

Figure 2: *Example of induced vessel dilation and changes in astrocytic membrane potential*

In this example (Fig 2), observation indicated that larger pressure increases resulted in larger depolarizations of the astrocyte, and there was 100% reliability in pressure events evoking depolarizations. This cell took ~200 ms to depolarize to half-maximum for each event, ~ 1 sec to reach maximum, and ~ 3 sec to decay to half max, and ~ 15 sec to recover to baseline. All 5 astrocytes probed in this way showed sensitivity to applied vascular pressure.
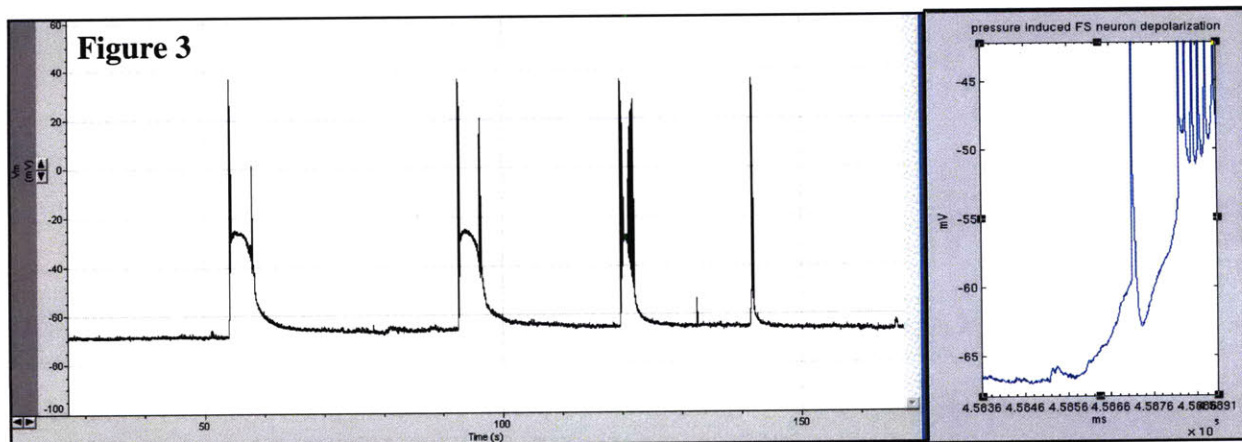
Figure 3 *(A) Example neuron trace (fast-spiking cell). (B) Zoom of a rise event.*

This fast spiking cell (one of two recorded from) depolarized and spiked, then stopped spiking until pressure decrease started and membrane repolarized to below -35mV. The time course of depolarization from resting potential (~-69 mV) to spike threshold (-56 mV) was between 50 and 100 ms, (e.g. 63 ms, 72 ms, for first two instances above). Burst firing rates in this neuron were ~50 Hz. Decay time to half-maximum after the pressure was released ranged from 50 ms to 250 ms, and may have depended on the response time of the vessel wall as well (Fig 3).

A subpopulation of pyramidal cells (N = 4, example Fig 4) behaved similarly, with onset and offset spiking corresponding to pressure, but with a slower time course, taking 150 – 250 ms to depolarize, and firing repeatedly (5 Hz) rather than bursting.

Figure 4
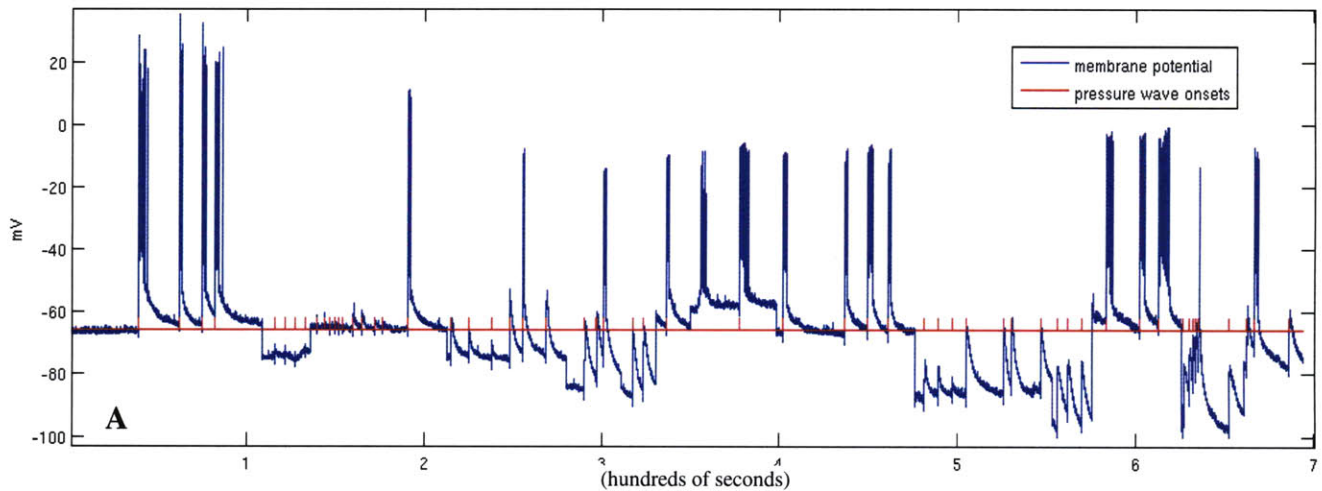
Figure 4: (A) Pyramidal cell responding to pressure waves and injected current steps (not shown).
(B) Time course of depolarization, short time scale.

In one case I was able to measure pressure onset together with membrane potential (Fig 4B). The square wave indicates pressure onset, but gives no information about shape, amplitude or duration of the pressure wave. The small initial hyperpolarization and offset transient is probably an artifact. This recording showed an almost immediate onset of depolarization, suggesting that the neural depolarization is a
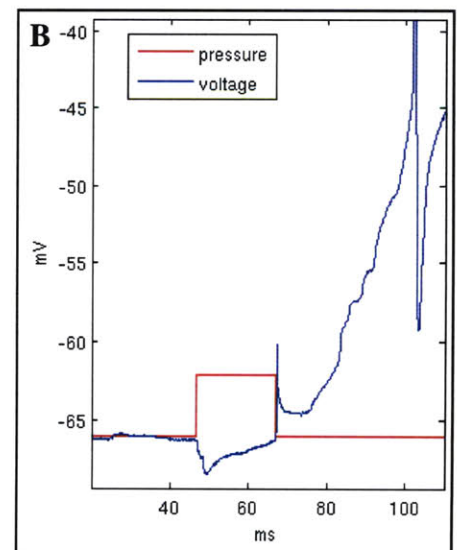
result of direct neural responsiveness to the pressure wave, rather than a slower effect mediated by astrocytes. When clamped below -80mV, the neuron depolarized up to 35mV, but did not reach threshold. However, repeated pressure waves before the cell could repolarize could depolarize the membrane to threshold.

There were a few other kinds of responses. First, there were 5 pyramidal cells that did not appear to be responsive at all to this form of mechanical stimulation. These cells were from two younger animals (P17 - P18), whereas the responsive cells were from two slightly older animals (P24 - P28). Second, there was a cell that showed an increase in sporadic spontaneous spiking in the 60 sec after a pressure pulse, but which were not aligned to the pressure pulse. Current injections in the same cells drove normal spiking. Also, the cell had a different depolarization slope from either pyramidal or FS interneurons, with either a very low threshold (-64mV) or an extremely sharp sub-threshold depolarization. Finally, there was one pyramidal cell which did not depolarize or spike, but showed an increase in the number and size of mini EPSPs in the 5 seconds after a pressure wave versus the 5 seconds before.

Table 1 – Summary of vessel pressure-induced mechanical effects on cell types

Cell Type	Effect	# of cells / total cells recorded
Astrocytes	depolarization coordinated with pressure wave	5 out of 5
FS neuron	depolarization & bursting	2 out of 3
Pyramidal	depolarization & spiking	4 out of 10
Pyramidal	increase in size & frequency of mEPSPs after pressure wave	1 out of 10
? Neuron type	increased spontaneous spiking after pressure wave	1 out of 3

These effects could not be replicated by moving the intracellular recording pipette into or away from the patched cell (however, the velocity of that manipulation was lower). Also, seal resistance did not change during pressure waves.

Discussion

The examples above show a sensitivity to mechanical perturbation in astrocytic depolarization in both neurons and astrocytes, in agreement with the previous observations in hippocampus (Angulo 2004) and olfactory bulb (Kozlov 2006). These findings implicate pressure sensitivity in both cell types, potentially mediated by mechanosensitive channels, as a mechanism by which astrocytes and/or neurons may be sensitive to vascular changes. In this preliminary *in vitro* study, astrocytes were more consistently responsive than neurons, consistent with predictions based on their association with vessels through mechanosensitive endfeet.

After this preliminary study of mechanosensitivity, we moved on to *in vivo* 2-photon imaging of astrocytes during induced vasodilation for several reasons. Most importantly, the experiments performed here, while providing initial confirmation of our hypothesis, would have required extensive development as a preparation before they would have yielded quantitative information. Going beyond these initial observations to make this investment of development time did not seem appropriate given the inherent limitations of the *in vitro* approach for making inferences about *in vivo* system.

Briefly, I list limitations of these experiments that would have needed to be overcome. The top speed setting in our micromanipulator was not fast enough to regularly lance arterioles, leading to a high failure rate. Slower speeds were adequate for normal pipette manipulation, but not for penetration of the tough pial vessel wall without distorting the rest of the slice. Further, elaboration of these studies would have required distinction between direct effects of pressure on neurons versus astrocyte-mediated effects (the 'direct' and 'indirect' pathways of Chapter 2). For this, we would have needed simultaneous recording of pressure, astrocytic activation and neuronal activation. These data could not detect any differences in the latency of astrocytes versus neurons to the vessel dilation events. Another limitation was that with the current preparation, we could not visualize calcium activity directly, though it might be inferred from the depolarization.

Perhaps the most important concern we had with making a major effort to generalizing these experiments was their physiological relevance. The pressurization events could be violent, and thus were likely aphysiological in their magnitude and velocity. Indeed, slower pressurizations were much less reliable in inducing depolarization events. Nonetheless, cells appeared to remain as healthy in these experiments as in normal slice recordings, and the quality of the recordings did not degrade over course of the recordings (up to 20 mins). Another important limitation is that the mechanical environment in a slice is significantly different from the one *in vivo* – slices and cells may deform away from the expanding vessel in ways not possible in an intact brain (with more three-dimensional constraints). Finally, because the vessels were not actually perfused with blood, any number of co-factors might have been missing that would either compensate for the depolarization effects we saw, or perhaps increase them. For example, temperature sensitive effects would not have shown themselves, even if they turn out to be important *in vivo*.

It would have been interesting to see if these effects were blocked by adding RR to the slice solution. Being non-specific, RR might have blocked any TRPV channel variants expressed in neurons as well as astrocytes. Since TRPV4 alone does not appear to be expressed in cortical neurons (Stine 2005), it might have been a good candidate to block specifically (e.g. with RN-1734, as described in Vincent 2009) as well, to see if the neuronal effects are dependent on the astrocytic ones. Alternatively, we could also see if the effects disappeared in the TRPV4 knockout (Mizuno 2003).

It may also have been the case that neuronal activation by the pressure change was responsible for the astrocytic depolarization – although that seems less likely given the shape of the astrocytic responses and their close match the shape of the vessel dilations. A related question is what role was played by the endfeet in causing the somatic depolarization, and whether endfoot involvement is necessary to propagate mechanical signals from the vasculature.

Part 2: Inducing vasodilation while imaging astrocytic calcium levels *in vivo*

The apparent sensitivity of astrocytes and neurons in slice to mechanical perturbations of the vasculature suggests that similar effects might occur *in vivo*. We therefore employed the methods described developed in Chapter 3 to independently induce vasodilation through drug administration while imaging astrocytic Ca levels using 2-photon laser scanning microscopy.

Abstract

To visualize the effects on astrocytes of physiological-scale vasodilations induced *in vivo*, we used 2-photon imaging to track the effects of pinacidil-evoked vasodilations of pial arterioles on nearby astrocytes. We found that increases in vessel diameter corresponded to increases in astrocytic calcium levels, as measured by Fluo-4 fluorescence changes. In rare cases, traveling calcium waves were evoked by large dilations, and can be seen traveling down astrocytic processes from endfeet to the soma. More commonly, these changes were slower and less discrete in onset and tracked dilation level, with washout of pinacidil and vessel recovery corresponding to a return to baseline calcium levels.

Methods

Experiments were conducted using 2-photon calcium imaging. A craniotomy was made over somatosensory cortex of adult (>4 weeks old) wild-type C57BL6/J mice anesthetized with 80mg/kg ketamine and 6mg/kg xylazine. A craniotomy over barrel cortex was performed and an open chamber made of dental cement was implanted with inflow and outflow ports for topical drug application. Fluo-4 was then bulk-loaded as calcium indicator with a picospritzer, according to established protocols (e.g. Sato 2007). For layer 1 imaging, injection was between 50 and 100 μm deep, for layer 2/3 imaging, injection around 150 μm. SR101 was co-loaded as an astrocytic marker.

Pinacidil was dissolved in 1% ethanol (170μM) in 0.9% saline for a 400μM concentration to induce vasodilation. Constant flow at 37 degrees C was maintained across the chamber throughout the run via syringe pump and in-line heater placed immediately prior to the chamber.

Different data sets had distinct order in which runs were conducted (see Fig 5 for imaging, stimulation, and vasodilation paradigm). First set of experiments: pinacidil wash in run followed by a wash out run. Second set of experiments: 1–3 runs with 1% ethanol alone, followed by pinacidil wash in and wash out. Third set of experiments: single run with 0.6% DMSO (94µM) in 0.9% saline, followed by pinacidil wash in (400µM pinacidil in 0.5% DMSO in 0.9% saline) and wash out.

Imaging runs were 6 minutes long, with pinacidil applied 120 sec after the beginning of a run. Anatomical Z-stacks of each region were taken before and after each trial for alignment purposes in case of changes in imaging plane due to brain motion. Astrocyte data were taken in layer 1, neuron data in layers 2/3.

Figure 5
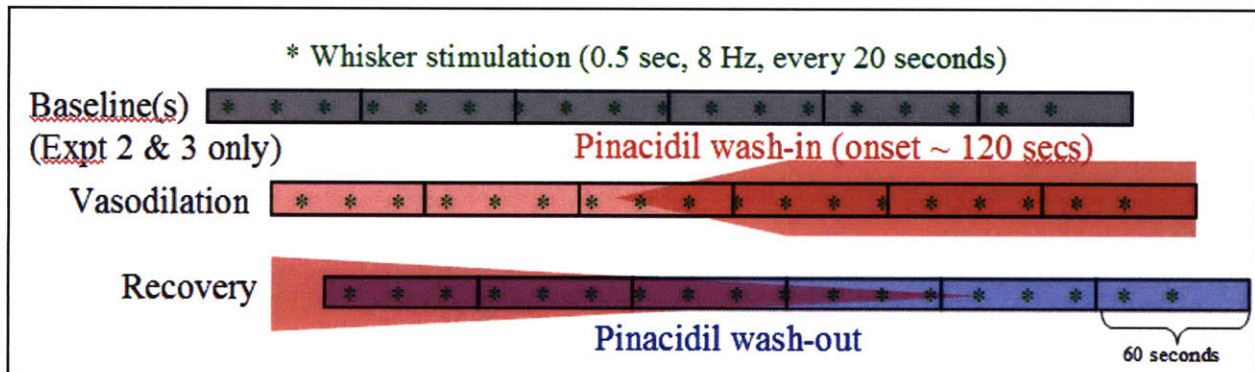
Figure 5, experimental paradigm for two photon imaging experiments. Baseline (top bar, gray) runs were not taken for the first set of experiments. Stimulation frequency also changed depending on experiment, with no sensory stimulation given in third set of experiments.

In experiments including vibrissal stimulation (1 and 2), deflections were applied for 1 sec at 8 Hz with a 30 sec inter-stimulus interval for the first data set, and for 0.5 sec at 8 Hz every 20 sec for the second data set, with 10-15 sec before onset of the first stimulus. We used a piezoelectric actuator for the first data set and electrically induced whisking through an implanted bipolar electrode wrapped around the facial nerve for the second data set. Imaging data and stimulation were coordinated through Triggersync and Prairieview software.

Image analysis

All data analysis was conducted using MATLAB. For each imaging area (set of 2 or three runs including vasodilation and washout), regions of interest (ROIs) in each image were selected by hand, circling astrocytic endfeet or soma. Endfeet were identified by their proximity and orientation parallel to vessel walls, and their curved elongated shape. ROIs ranged from 10 – 200 pixels, depending on optical zoom and imaging resolution, which were adjusted to optimize for speed and coverage with respect to each area imaged. Two measures of calcium signal were used. The first was the change in fluorescence summed over all pixels in an ROI in arbitrary units over time, compared to baseline fluorescence at the beginning of each run (F/F0). This measure is closest to the raw data, but was subject to contamination from motion caused by vasodilation, especially for endfoot ROIs, which tended to become optically obscured by the expanding vessel. The second was a thresholded measure that tracked the number of pixels in an ROI above the 90th percentile in brightness; the 90th percentile was determined with reference to the distribution of pixels in the ROI over the full time course of the run. When calcium levels increased, we found that the *number* of pixels exceeding this threshold increased. This second measure also partially compensated for motion due to expanding and recovering vessels; since pixels below threshold were discounted, the measure tracked bright endfeet as they moved laterally as the vessel expanded (ROIs were drawn so as to ensure that endfeet stayed within the ROI as they moved). To compensate for these and other sources of noise (including vertical motion of the imaging plane), we subtracted from the Fluo-4 signal signal from the SR101 channel, measured in the same two ways as described above. Since SR101 is a purely anatomical label, any changes in that channel should be due to motion or artifact that affects both channels similarly. Similar corrections have been used elsewhere (see Dombeck 2007). This allowed us to compensate both for vertical motion and overall darkening of the image due to our vasodilation manipulation. To check that the manipulation was reducing noise, we compared the standard deviations of the corrected and uncorrected signals. For Experiment 1, the standard deviation of the corrected signal was always smaller than that of the uncorrected, with a reduction of about 50%. The correction was more problematic in Experiments 2 and 3; this issue will be addressed in the results and discussion section.

Results

On two occasions, we saw vessel dilations evoke traveling calcium waves that propagated from the endfeet away from the vessel. In these two cases, the vasodilation started before the calcium wave. However, these more massive effects were unusual, observed only twice out of 89 runs with pinacidil application during imaging of astrocytes. Both examples were observed in layer 1; no waves were observed in layers 2/3 over the course of 125 imaging runs with pinacidil.
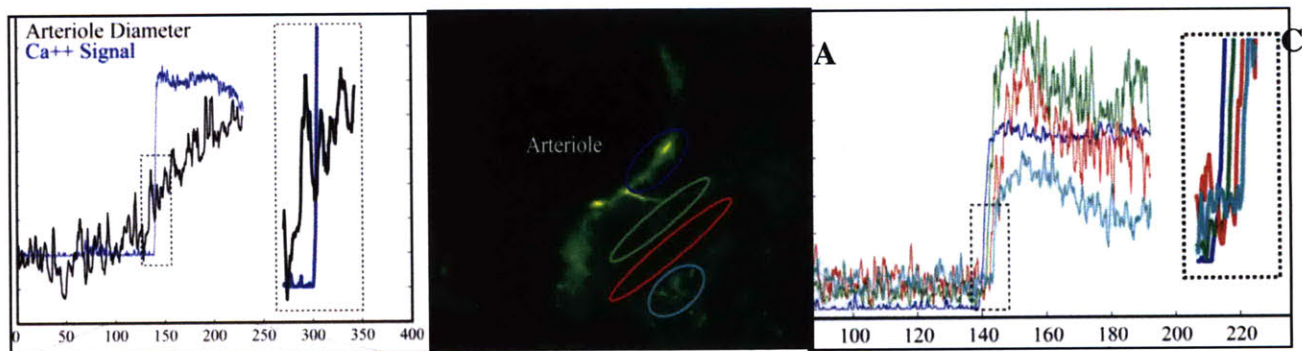
Figure 6

Figure 6 Example of a calcium wave initiated at (B) endfeet around an arteriole. (A)Time course of arteriole dilation overlaid with the time course of calcium increase in the endfeet (y-axes in arbitrary units for calcium brightness). (C) Progression of wave traveling away from arteriole, time series colored to indicate their origin in the ROIs marked in the image on the left.

More consistently, we saw a slow increase in astrocytic calcium levels across the region imaged. This increase tracked the increase in vessel diameter.

We used two measures to track changes in pixels. In the first (Fig 7B, and Fig 8A and 8C), we summed the brightness over all pixels in each ROI. The first significantly divergent time point for calcium levels (delta F/F, Fig 7B) measured in this way for vasodilation runs as compared to baseline runs was earlier for endfeet (170.8 sec) compared to all ROIs (soma and endfeet together, 172.2 sec) and much later than for the blood vessels (149.2). In the second measurement method (Fig 7C, and Fig 8B and 8D), we used a thresholded measure, where only the pixels above 90th percentile brightness in an ROI were counted, allowing us to focus analysis on the high signal-to-noise data where there was little ambiguity of sufficient calcium indicator
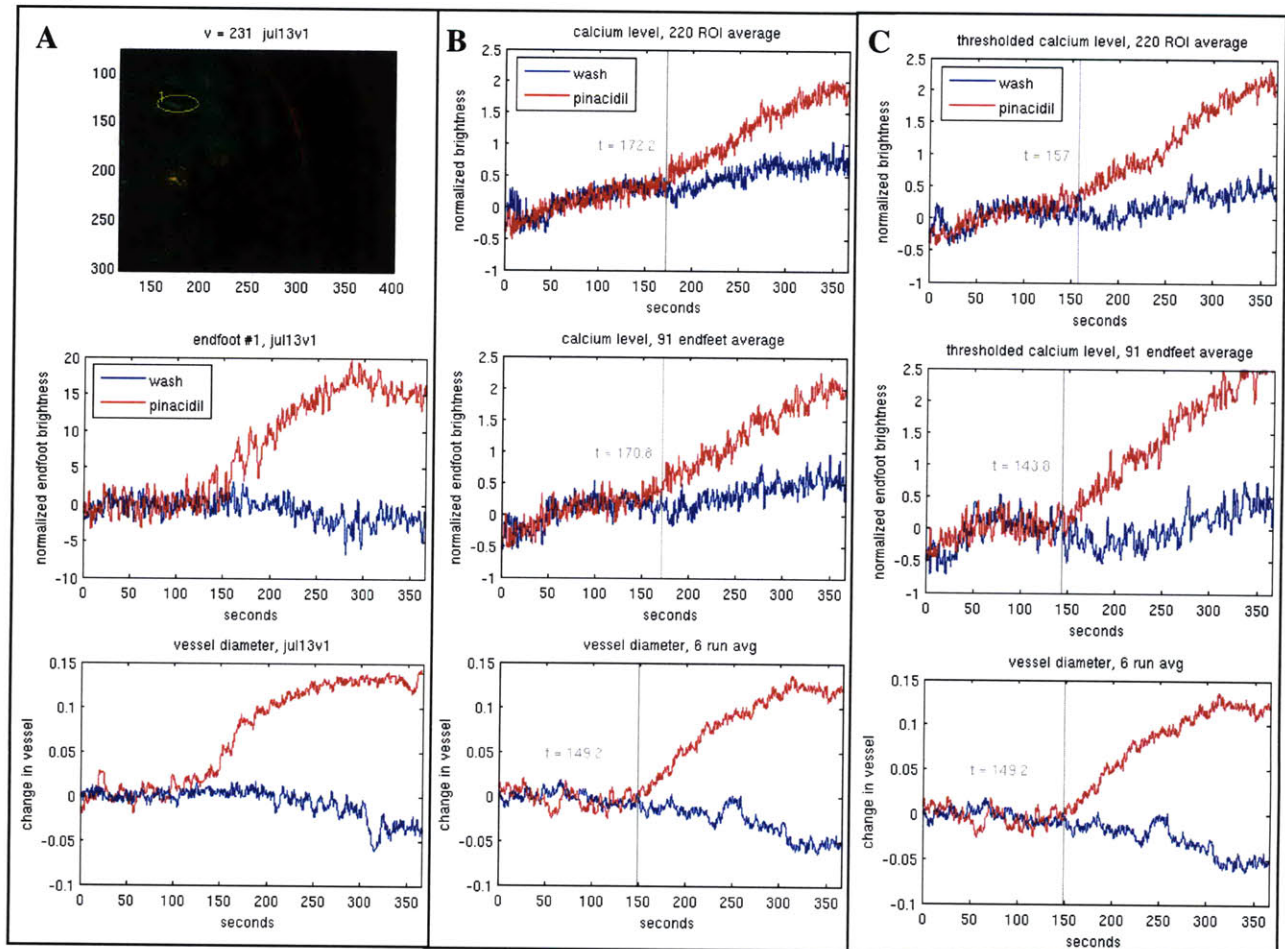
Figure 7

Figure 7 Increases in astrocytic calcium level in response to vasodilation of pial arterioles in layer I (A) Top An example image in which green fluorescence indicates Fluo-4 loading. (A) Middle Typical endfoot example of the increases observed in calcium level following vasodilation. (A) Bottom Measurement of pinacidil induced vasodilation in this example. Across these plots, pinacidil arrived to the brain surface at ~120 sec, but does not reach full concentration until about 140 sec. Calcium changes begin to diverge from wash after 140 sec. (B) Top Raw measurement of change in fluorescence (calcium indicator). The average over all astrocytic ROIs (soma and endfeet) from 4 animals and 6 runs (N = 220 ROIs). The gray vertical line indicates the first significant divergence of the two data sets. (B) Middle The average over 91 endfeet from same animals and runs. Notice the slightly earlier divergence between vasodilation (red) and wash-out runs (blue). (B) Bottom The time course of pinacidil induced vasodilation and calcium indicator brightness across this average. (C) The same data sets as in B, but using a thresholded measure of calcium signal to track only brightly labeled pixels. These traces show slightly higher signal to noise as well as an earlier statistically-significant divergence.

uptake. On this measure (Fig 7C), the first divergence came at 143.8 sec for endfeet and 157 sec for all ROIs.

For astrocytic regions of interest (as selected by SR101 labeling), we compared calcium levels in the beginning and ending of runs (first and last 60 sec). In wash in runs, this captured levels before and after dilation: In wash out runs, this allowed quantification during reconstriction. Quantifying these changes over all ROIs (N = 220), we found that a larger number of regions increased in brightness over the course of a trial when vasodilation occurred (pinacidil wash in) than when the vessel was reconstricting during pinacidil wash out. Note that in both conditions an increase was observed.
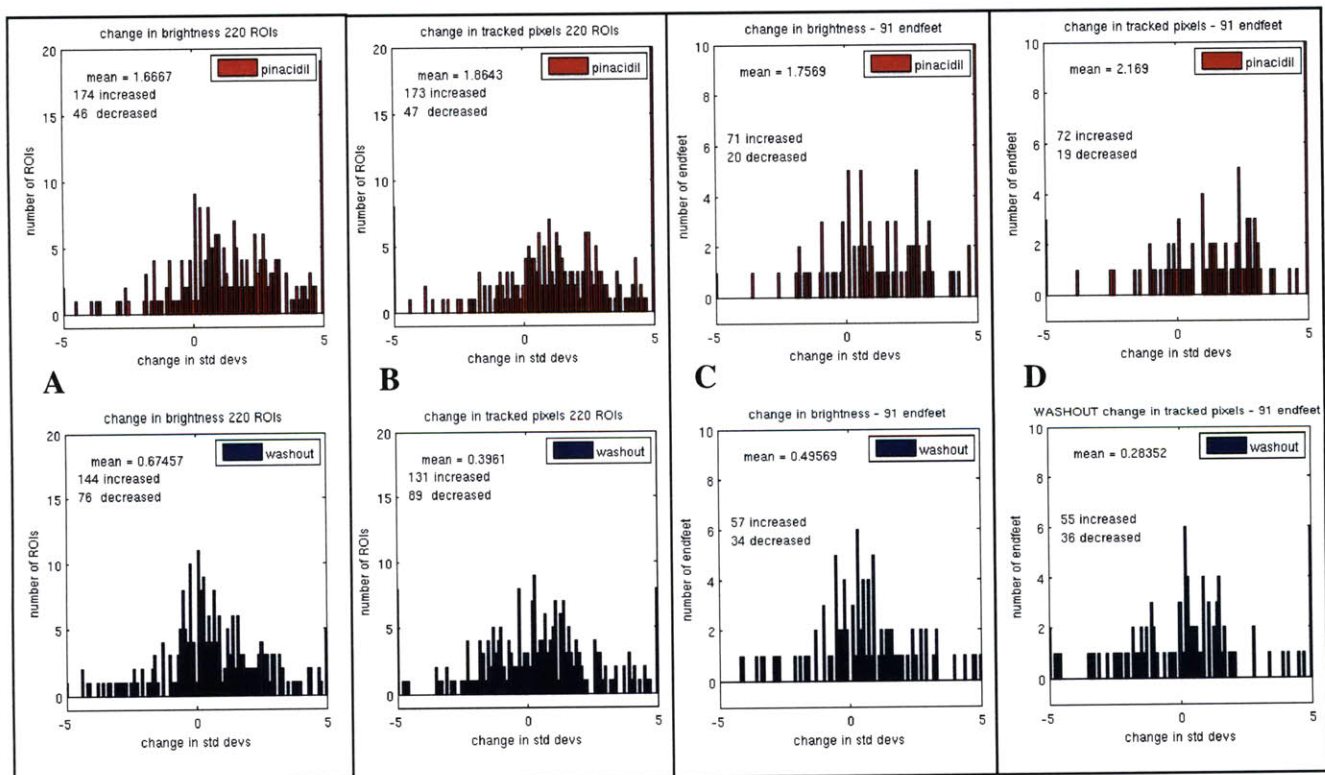
Figure 8

Figure 8 *Histograms of the change in calcium level during vasodilation vs. reconstriction. (**A**) shows change in calcium as measured by delta F/F, with the number of standard deviations from initial value on the x-axis. Delta is taken between the first 60 seconds and last 60 seconds of a run. (**B**) shows the same, but using the thresholded brightness measure. (**C**) simple delta F/F, endfeet only. (**D**) thresholded, endfeet only.*

By the delta F/F_0 measure, 79% of the astrocytic areas measured showed an increase during vasodilation when comparing the baseline period (first 60 seconds of run) to the dilated period (80 seconds from the end of the run to 20 seconds from the end of the run), 65% that showed an increase during wash-out. Also, more regions (19 in dilation run vs. 5 in washout run) showed a larger increase (more than 5 std devs above the mean) during vasodilation. A chi-squared goodness of fit test showed significant differences ($p < 0.01$) between the distribution of fluorescence changes in pinacidil runs versus both baseline and washout runs, for soma and endfeet populations.

With the thresholding measure, 35 ROIs showed increases above 5 std dev during vasodilation, as compared to 8 ROIs that showed increases as large during wash-out. The thresholding measurement also allowed us to better isolate endfoot-shaped regions (and only measure those) using elliptical ROIs. Because endfeet were often displaced by the expanding vessel, we drew larger ROIs without including non-endfoot pixels, which were less bright. Using this quantification, we saw a slightly larger difference between wash-in and wash-out runs, with < 60% of the areas showing an increase during wash out. The same quantification on endfeet alone (Fig 8C and 8D) showed 78% of the endfeet increased in brightness during dilation, and 63% increasing during reconstriction, a smaller change than in the total population. In all measures, SR101 brightness signals were subtracted from Fluo-4 signals to compensate for image motion and other noise that impacted image quality.

However, there was a steady increase in fluorescence in each case. This increase was likely partly due to the ethanol in pinacidil and washout solutions (and can also be seen in the time courses in Figure 7, as well as in the depolarization of cells in ethanol described in Chapter 3). In repeated imaging with no vascular perturbation comparing 1% ethanol in 0.9% saline with 0.9% saline alone, we found that there was a much smaller increase in overall brightness over time in the saline runs (< 1% for saline alone, as opposed to ~ 3% for ethanol in saline).
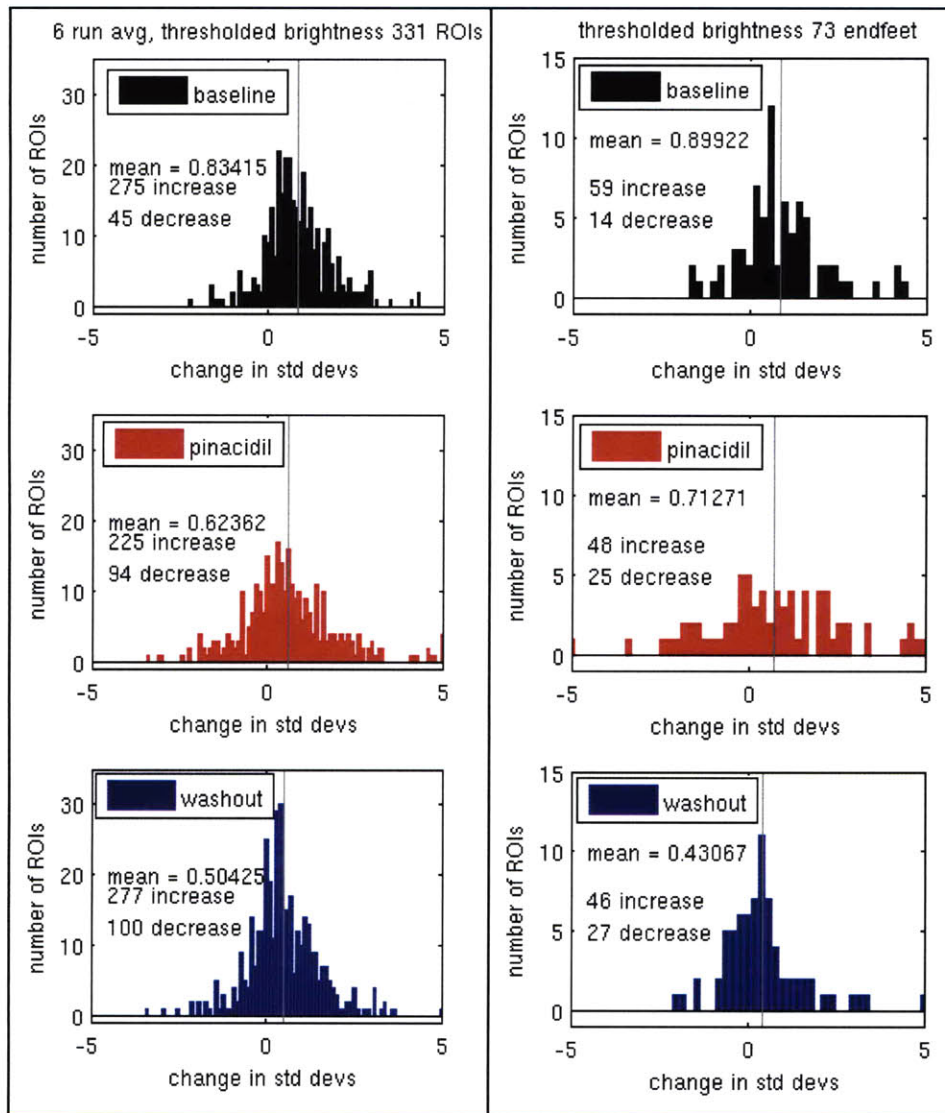
Figure 9

Figure 9: *Astrocytic calcium changes, second data set with baseline run preceding pinacidil run and thresholded measurements.*
Top: *baseline run, ethanol only. T-test shows significant difference in mean change for 331 ROIs (left), and 73 endfeet among them (right).*
Middle panels, *vasodilation run with pinacidil in ethanol vehicle. The mean increase in fluorescence measured here (mean = 0.6 total ROIs, left, and mean = 0.7, endfeet only, right) was one third the size of the increase seen in the first data set (mean = 1.9 total ROIs and mean = 2.1 endfeet only). We still see a cluster of ROIs (N = 5) that increased 5 std dev or more above the initial calcium level, compared to N=0 in the baseline or N=1 in the washout condition. That cluster is also smaller compared to 35 in the original data. **Bottom panels**, washout run, with a smaller increase than vasodilation run, but again, almost twice as large an increase as in the original data.*

A variety of factors, including period of duration of exposure to ethanol, could also have contributed to order of data acquisition effects. To balance for potential order effects, we repeated the same experiments but with 1-3 blank trials (randomized) preceding the pinacidil

trials (Experiment 2). This second set of experiments (5 animals, 5 runs, 331 ROIs total, of which 73 were endfeet) yielded noisier data, most likely because repeated imaging of the same area for > 50 min prior to collecting vasodilation data had adverse effects on the health of the cells in the area by the time of the pinacidil run, effects that may have been worsened by sustained ethanol exposure.

In this second data set, we found that brightness increased rapidly during the pre-wash-in control run, increased less rapidly during vasodilation, and continued increasing during washout (Fig 9). At no point did the mean signal for the vasodilation run become significantly different from the mean signal for the wash-out run (t-test).

This finding was puzzling, not only because of the unexpected increase in calcium during the baseline condition, but also due to the disappearance of the pinacidil-related effects seen in our initial data set. Furthermore, the increase in calcium during the vasodilation run was smaller in absolute terms that it had been in the first data set collected. The chi-squared goodness of fit test showed significant differences (p << 0.01) between the distribution of calcium changes in pinacidil runs as compared to both baseline and washout runs, for total and endfoot ROIs.

Control over vasodilation using pinacidil was unchanged, with the same time course as shown in experiment 1, and similar typical magnitudes (10-20% dilation, depending on the vessel; see Chapter 3).

We reasoned that a number of possible explanations could explain this failure to replicate, given changes made in the experimental protocol between the two data collection periods. These differences included increased astrocyte sensitivity to ethanol over prolonged exposure, differences due to changes in the pattern of whisker stimulation applied (which changed in the second data set), and artifacts due to the quality of data collected due to physiological variables, for example resulting from the introduction of a 50 minute delay before taking pinacidil data. Artifacts related to the 2-photon itself were also a possibility, as power fluctuations and pockels cell problems had begun occurring in the 6 months between collection of the two data sets.

To try to resolve these issues, I conducted a third set of experiments (2 animals, 3 runs, 220 ROIs, 61 endfeet). To control for ethanol exposure, I used DMSO as the solvent for pinacidil. To control for any impact of the pattern of sensory stimulation, I did not provide any. I also measured the imaging power output through the pockels cell simultaneously with imaging (which we did not in the second experiment) so any change in this variable could be tracked.

In this new data set, our power level recordings from the pockels cell showed a characteristic increase in power at the beginning of each day. Some periods of up to 10 minutes were stable, but overall there was a trend to significantly increased laser power over an hour of imaging time (e.g. from 1.5 to 3 milliwatts). This pattern could explain the problems in Experiment 2, where the increase in calcium indicator fluorescence in the baseline control run was much larger than any potential pinacidil-induced increase in calcium discernible in the dilation run (although the relationship between dilation runs and wash-out runs was maintained). While we cannot be sure the laser was experiencing the same problems during data collection in the second data set, we do know that the problem did not arise until several months after the collection of the initial dataset. We also found that the two-photon imaging system required increased laser power to visualize cells in the second (and third) data sets as compared to the first. The nominal difference was on average around 2 milliwatts in the later data sets vs. < 1 milliwatt in the first.

The relatively high laser power may have contributed to faster bleaching of SR101 during the baseline run (Fig 10C, most evident in left panel in black). When the calcium signal is normalized against the SR101 signal, differential bleaching of SR101 will show up as a relative increase in the corrected calcium signal, giving the appearance of a disproportionally large increase during the baseline run. Whereas the baseline period bleaching in the red channel is smooth (but stabilizing towards the end of the run), there is an inflection point around 130 seconds during the vasodilation phase. This matches the decrease in overall fluorescence (e.g. measured in the center of blood vessels in regions not directly labeled by either dye) caused by the onset of vasodilation at that same period, and ought to be corrected for in the calcium signal. The decrease stabilizes altogether by the washout run.
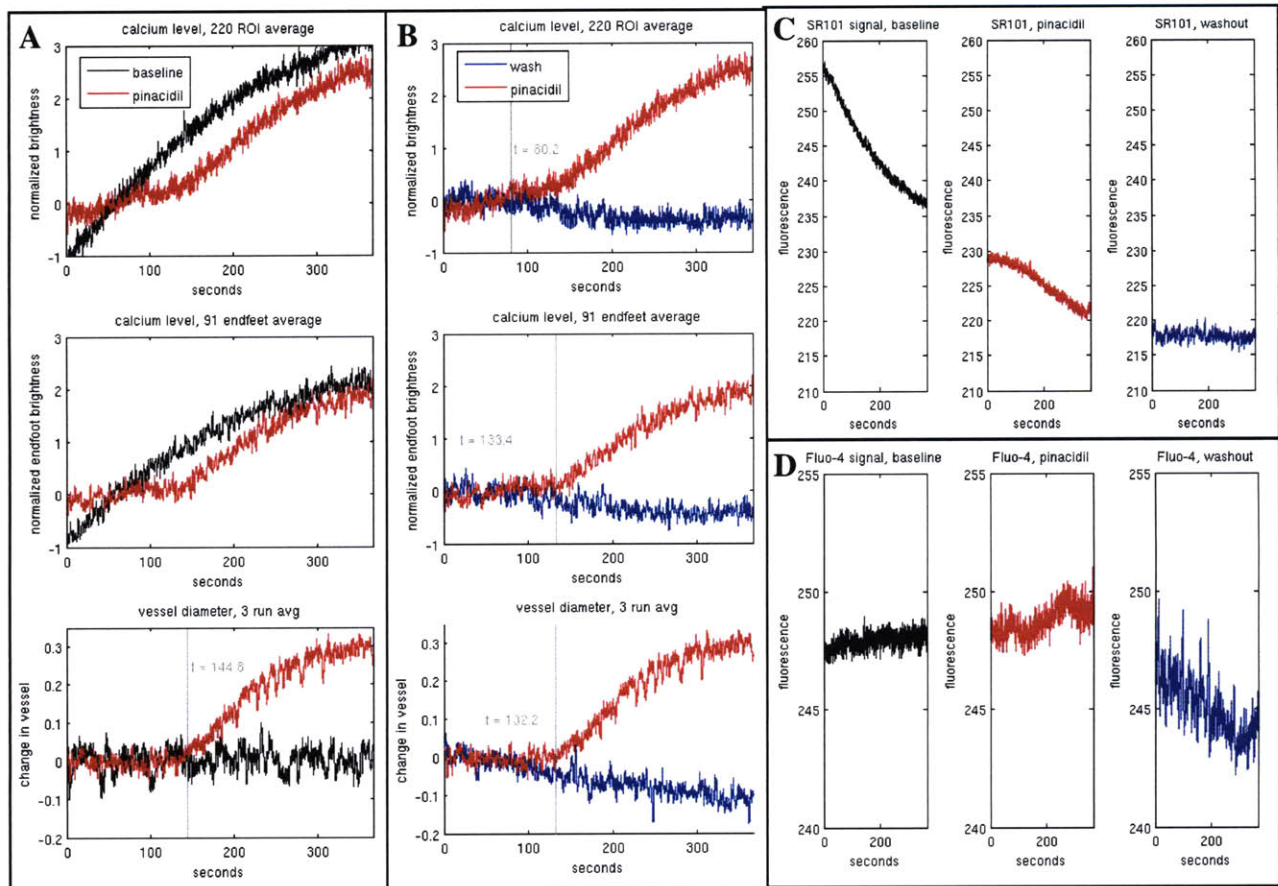
Figure 10

Figure 10 *Changes in calcium level for control, vasodilation and recovery runs in Experiment 3*

(A) *Calcium signal during baseline vs. vasodilation conditions for all ROIs (N = 220) and endfeet only (N = 61). While there is a clear flex point at which the slope of the calcium signal increases corresponding to the onset of vasodilation, the increase in the baseline condition is larger overall (similar to the counterintuitive results found in dataset 2).* ***(B)*** *Calcium signal compared between vasodilation and wash-out runs (which were taken after the transmitted laser power had stabilized; similar results to dataset 1).* ***(C)*** *Signal in SR101 channel, showing the source of artifact in differential calcium/SR101 signal.* ***(D)*** *signal in the Fluo-4 (calcium indicator) channel alone, showing a pinacidil related bump in the central column (red).*

Looking at the Fluo-4 calcium signal alone (Fig 10D), there was little or no increase in signal over the course of the non-vasodilation runs. However, we had previously found it was necessary to normalize green (active calcium signal) to red (inert measure of fluorescence) to increase

signal to noise. Because these most recent DMSO runs showed lower noise than the ethanol runs, it is possible to see an effect in the Fluo-4 channel alone. Our original data from Experiment 1 also showed an increase in uncorrected calcium signal during vasodilation.
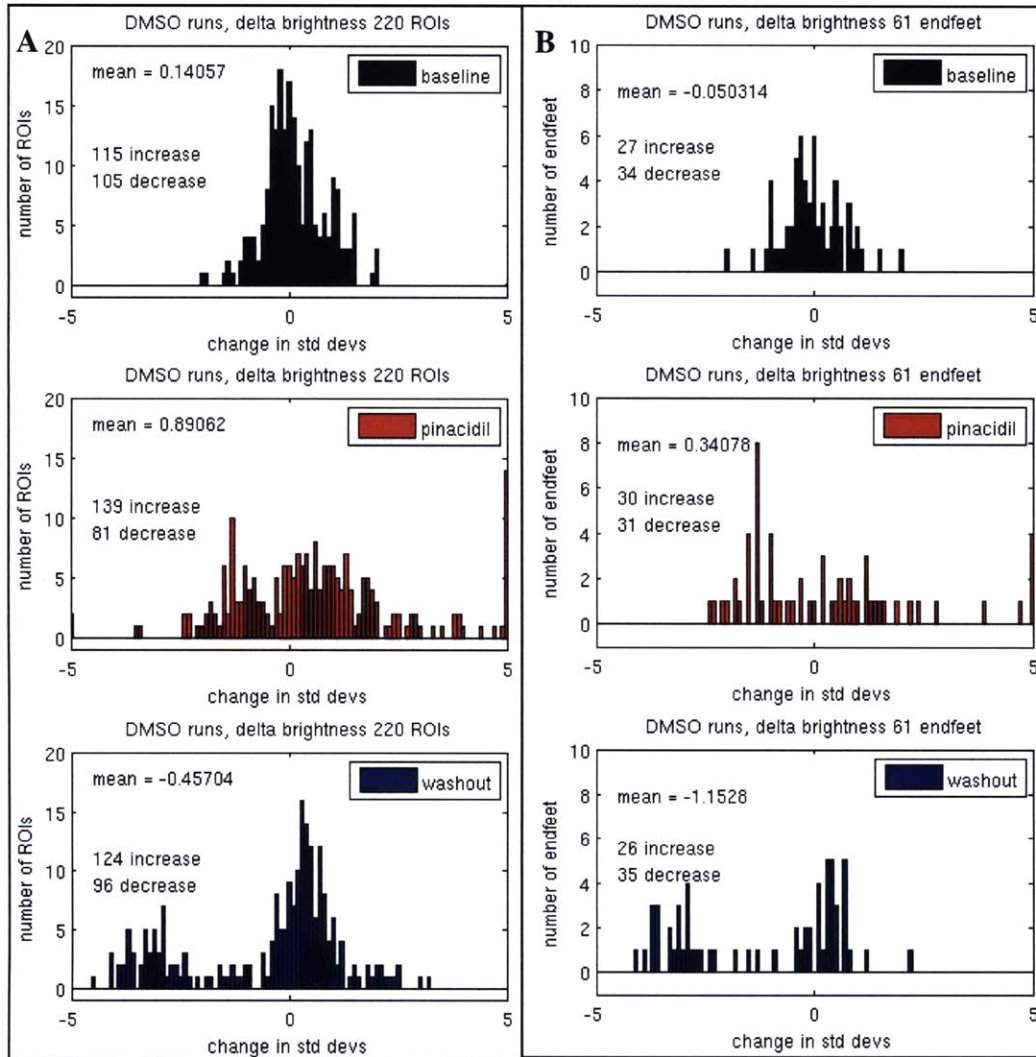
Figure 11

Figure 11: *Distribution of changes in calcium levels in individual ROIs.* **(A)** *changes in F/std(F) in normalized units for 220 ROIs (endfeet and soma).* **(B)** *Changes for endfeet alone.*

To avoid the SR101 decay artifact (Fig 10C) while correcting for the overall darkening, I used only the green signal for the baseline and washout runs. For the pinacidil run, I subtracted the normalized red signal from the green. To compensate for the additional increase in the corrected signal from this subtraction that would be expected simply from the steady SR101 signal decay

over that period, I added back an estimation of that decay based on an average of the SR101 decay during the baseline and washout runs (immediately before and after).

Looking at the distribution of responses from individual endfeet, we found once again that the largest increases in individual endfeet occurred during the vasodilation run. We found that 52% of endfeet showed an increase in calcium levels under control conditions, vs. 63% during vasodilation and 56% during washout. Looking at endfeet only, 44% increased during control, 49% during vasodilation and 43% during washout. In both cases, there were ROIs that showed a large (>= 5 std dev) increase in fluorescence during vasodilation (N = 14) but none in the other two conditions.

The mean difference between the distributions during dilation and recovery was significant only for endfoot ROIs (N = 91, p = 0.002), suggesting that more endfeet were responsive to vessel dilation than soma. A chi-squared goodness of fit test showed significant differences (p << 0.01) between distribution of fluorescence changes in pinacidil runs versus both baseline and washout runs, for soma and endfeet populations.

Discussion

In the first set of experiments, we found an increase in astrocytic calcium that correlated with the time course of pinacidil-induced vasodilation, and then decreased during recovery towards the original vessel diameter with pinacidil washout. These changes in astrocytic calcium affected the soma as well as endfeet of the cells involved.

We failed to replicate these results in the second set of experiments, which were undertaken to provide a baseline control of astrocytic calcium in layer 1 in the absence of pinacidil-induced vasodilation. Data from these experiments showed a consistent and large increase in astrocytic calcium during the baseline condition that, if anything, was damped by pinacidil-induced vasodilation. It also failed to show the divergence in calcium activation between the dilation and wash-out trials as predicted by the first set of experiments.

Results from the third set of experiments showed that a loss of signal in the SR101 channel was at least partly responsible for what we took to be an increase in calcium signal during the baseline condition. When we looked at the raw Fluo-4 signal, without using our correction for motion and other noise against the SR101 signal, the rapid increase during the baseline period was reduced, showing that the "correction" we were making for our calcium signal was adding artifact to this data set. We believe that the bleaching behavior of the SR101 may have had something to do with our laser instability, though the exact relationship is not clear yet. The shape of the SR101 signal decay is similar to the shape of the increase in laser power (inverted).

The increase may also have been partly due to sensory stimulation, which was no longer present in the third set of experiments. Although the stimulation was sparse (1 sec of 8 Hz whisker stimulation every 20 or 30 sec), we might expect it to have a greater effect during the first run of a set because of adaptation. While the first run of each pair for the first set of experiments was the vasodilation condition, the first run for each set of runs in the second experiment was the baseline condition (1 out of 3). The third set of experiments showed that the vasodilation effect on astrocytic calcium is not just an artifact of the stimulation sequence (though the effect may have been enhanced by stimulation in the first set of experiments).

The sensitivity of astrocytic calcium levels to vessel dilation provides evidence for the indirect mechanism of hem-neural action. In particular, the calcium increases, while earlier and stronger at the endfeet, are also seen in the soma, which means that they are capable of propagating down astrocytic processes, whose actions can impact neurons and synapses as well as blood vessels.

For one example relating induced vasodilation to calcium responses in neurons, please see Appendix.

Part 3: Fine timescale interactions of vasculature and endfoot calcium

Introduction

The new findings in the previous section suggest that vasodilation increases local astrocytic calcium levels. A recent literature has emerged suggesting that the reciprocal relation, the *control* of vasodilation by astrocytic endfeet, depends on current local conditions. Gordon (2006) showed that elevations of calcium in astrocytic endfeet could cause either vasoconstriction or vasodilation, depending on the local oxygenation level. Blanco (2008) showed that it also depended on the extent to which the vessel was already dilated. To further complicate the picture, Girouard (2010) shows that whether a Ca rise causes constriction or dilation depends on the size of the increase in calcium, as well as perivascular potassium levels nearby.

While we are not measuring either local oxygenation or potassium levels, *in vivo* oxygenation levels are consistent with those termed "high" by Gordon, and we can suppose that vessels at baseline are in a neutral position with respect to the Blanco measure, whereas they are in a dilated state after pinacidil application. Meanwhile, the calcium changes we observed on the time scale of seconds are small compared to those evoked in the Girouard study.

To determine the relationship between our *in vivo* data and the predictions obtained from slice in these three papers, we conducted finer time-scale analyses of the relative ability of Ca levels to predict subsequent dilation, and vice versa. To do this, we looked at the correlation between small fluctuations in astrocytic calcium and small fluctuations in vessel diameter (on the order of 1-5% each) on short time scales ($\leq$ 10 sec), using data from the three experiments described in Part 2.

Results

In individual runs, significant correlations were seen (xcorr values > 0.45)), for epochs on the order of 5-20 seconds. We saw a total of 189 epochs of high correlation (xcorr > 0.45) over 44 runs, with one epoch occurring on average once every 80 seconds. There were equal numbers of epochs showing a positive correlation between calcium and a later vessel dilation, a positive correlation between change in vessel size and change in calcium, and a negative correlation

between change in vessel size and change in calcium (38,41, and 40, respectively). The one correlation that stood out was a negative correlation between calcium level and subsequent change in vessel size, there were 70 epochs where this correlation was above 0.45, or almost twice as many epochs as for the other three categories (Table 2).

Table 2

Epochs (189 total)	Ca predicts vessel (+ correlation)	Ca predicts vessel (- correlation)	Vessel predicts Ca (+ correlation)	Vessel predicts Ca (- correlation)
Baseline	14	21	10	16
Vasodilation	14	21	15	12
Wash-out	10	28	16	12
Total	38	70	41	40

Breaking the runs down further into early, middle and late periods within each run, a clear effect of the vasodilation manipulation can be seen in the "Calcium level predicts changes in vessel dilation, negative correlation" category (Figure 12A, bin 5). A smaller but also significant effect can be seen in the "Vessel diameter predicts changes in calcium level, negative correlation" category (Figure 12C, bin 5). That is, an effect is seen at a fine scale (1-5 second correlations, changes of 1-3% in vessel diameter and calcium levels) after filtering out the slow larger-scale increase in calcium and vessel diameter that is the direct effect of the pinacidil. As with the epoch counting, more time was spent in the "negative correlation, calcium predicts vessel motion state". Notice that the periods collected in Figure 12A and 12B are consistent with the occurrence of typical "astrocytes drive vascular motion" states, while those in 12C and 12D suggest the occurrence of hemo-astro states, where vascular motion drives astrocytic calcium.

To look at the dependence of endfoot-vascular coupling on local conditions independently of the immediate history of dilation or constriction, we also divided each run into three epochs of 120 seconds each, and grouped them according to the vessel diameter at that time (baseline or dilated), and the astrocytic calcium level (baseline or increased). For these data, there were 50 runs of three epochs each from 10 animals. Data were then high-pass filtered (cutoff at 0.05 Hz)

to eliminate the large, slower time scale shifts in vessel diameter and astrocytic calcium described above in Part II.
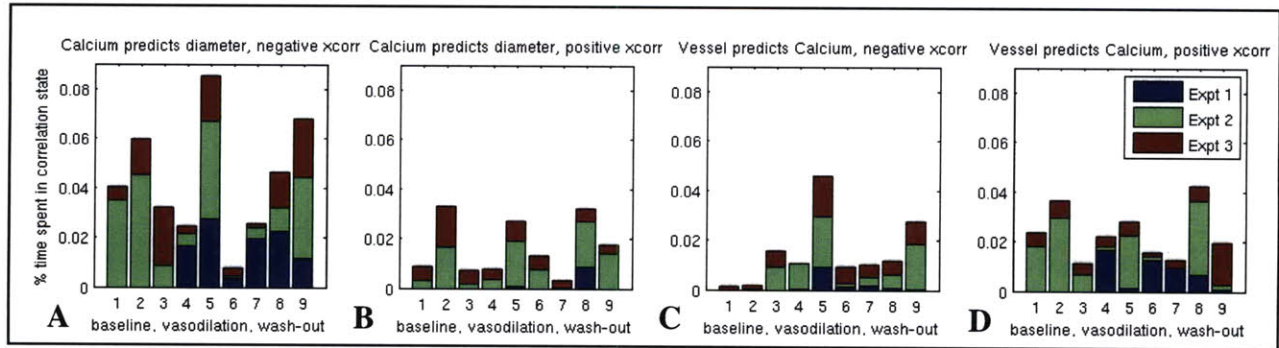
Figure 12

Figure 12 Total time spent in each of four correlated states by astrocytes and nearby vessel in area imaged. Each plot shows 9 bins in chronological order: 1- early 70 seconds of baseline run, 2- middle 70 seconds, 3 - late 70 seconds of baseline run, 4 – early 70 seconds of pinacidil run, etc. Vasodilation does not onset until bin 5.Washout begins during bin 7 for Experiments 2 and 3, and bin 8 for Experiment 1. *(A)*Negative correlation: total time spent in correlated state where an increase in calcium predicted a decrease in vessel diameter (or a decrease in calcium predicted an increase in vessel diameter) within 5 seconds. *(B)*Positive correlation: total time spend in a state where an increase in calcium predicts an increase in vessel diameter. *(C)* Negative correlation: total time spend in a state where an increase in vessel diameter predicts a decrease in astrocytic calcium levels. *(D)* Positive correlation: total time spent in a state where an increase in vessel diameter predicts a decrease in astrocytic calcium.

Cross-correlation analysis showed that changes in Ca levels preceded and predicted changes in vessel diameter in the undilated condition (in 42 out of 50 undilated epochs), a correlation that disappeared during the dilated condition (Fig 13A). This took the form of a negative correlation between calcium level and blood at short negative lag around 1 second. That is, at baseline (and after recovery), an increase in endfoot calcium predicted a decrease in vessel size a second later. It should be emphasized that this correlation was an average over many epochs of strong correlation and many epochs of no correlation, or different correlations at different lags, and so does *not* represent a static state of the system during baseline conditions.
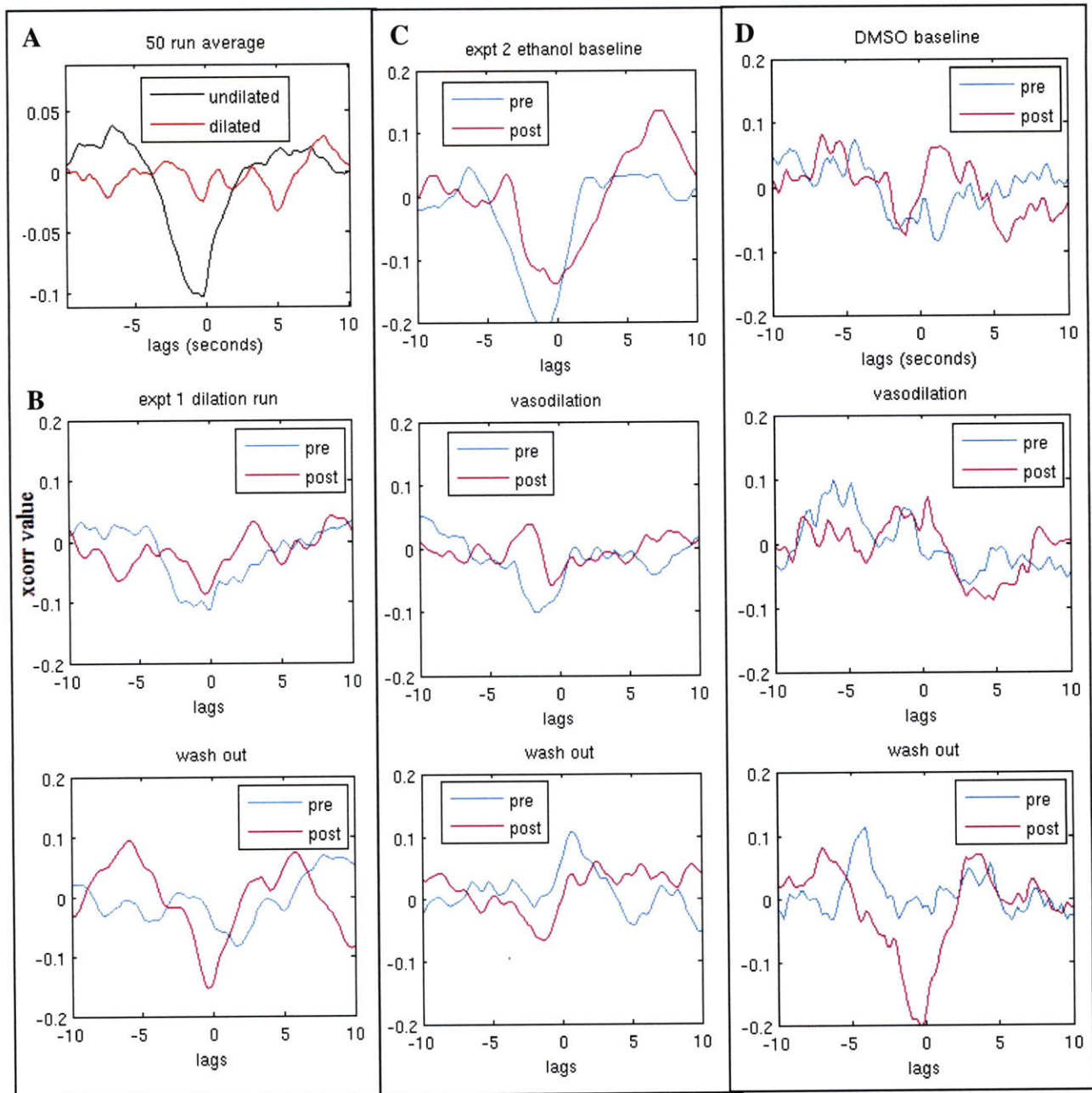
Figure 13

Figure 13 *Fine scale correlations between small fluctuations in astrocytic calcium and vessel diameter*
(A) ***Top*** *Average cross-correlation between calcium and vessel diameter during all dilated epochs (N = 34, 120 seconds each, in red), and all undilated epochs (N=50, 120 seconds each, in black). Undilated epochs include those pre-pinacidil (baseline and at the beginning of the vasodilation run) and those at the end of the washout run.* ***(B), (C), and*** *(D) average cross – correlation values between endfoot calcium and vessel diameter for B) experiment 1 data (vasodilation and wash-out runs only), C) experiment 2 data (baseline, dilation, and wash-out), and same for D) experiment 3 data. Magenta indicates the 120 seconds at the beginning of each run, while cyan indicates the 120 seconds at the end.*

Discussion

The negative correlation we found at baseline dilation is consistent with the effect described in Gordon (2008) – at high pO2 in the tissue, an increase in astrocytic endfoot calcium results in a decrease in lumen diameter. <u>The current findings are unique because they describe dependencies at a time scale of seconds (<2 sec in the averaged data), instead of minutes</u>. This finding is also consistent with the effects described by Chuquet (2007), where an increase in astrocytic calcium caused by spreading depression resulted in vasoconstriction, but the amount of constriction they observed was much larger (> 15%) and slower (~ 15 sec to reach maximum constriction from onset). On time scales closer to the ones we measured, Girouard (2010) showed an increase in vessel diameter in response to uncaging of "low" concentrations of calcium (from 100nM levels at baseline to 400nM uncaged). However, these concentrations were significantly higher than any we saw in any condition except during onset of vasodilation. In those examples, the vessel was in the process of rapidly dilating, making it harder to interpret any fluctuations riding on top as being due to endfoot calcium elevations as opposed to the vessel's response to pinacidil.

In the dilated condition, we would expect from Blanco (2006) that an increase in endfoot calcium would still cause a vasoconstriction. One reason that we may not see one is that pinacidil may have sufficiently hyperpolarized the smooth muscle so that it is unable to respond to the usual pathways that would cause a constriction, e.g. reduction of tonic BK channel current in the smooth muscle. The other pathway for vasoconstriction goes through 20-HETE, which increases calcium entry into smooth muscle, causing depolarization and thus constriction.

While there was no significant correlation over the entire 120 second dilated epoch—unlike undilated conditions where astrocytic calcium predicted dilation—there are many instances of strong coupling in the individual runs on a more local time scale (~ 10 seconds) in the vessel-endfoot direction and the endfoot-vessel direction, with positive *and* negative correlations. Epochs of strong correlation between changes in vessel diameter and changes in astrocytic calcium where vessels change at negative lag (where calcium changes lead diameter changes in time) relative to endfeet do not appear to be any more frequent or more powerful than epochs of strong correlation at positive lag (where vessel changes lead calcium changes). The magnitude of

correlation effects at positive and negative lags were similar, suggesting that the direction of influence runs as often from vessel to endfoot (as found for longer time scales in Part II above) as the more well-characterized route from endfoot to vessel.

References

Andrew C. Charles et al., "Intercellular signaling in glial cells: Calcium waves and oscillations in response to mechanical stimulation and glutamate," *Neuron* 6, no. 6 (June 1991): 983-992.

Kirischuk, S. "Mechanosensitive Channels in Neuronal and Astroglial Cells in the Nervous System" in Andre Kamkim and Irina Kiseleva, eds., *Mechanosensitivity of the Nervous System*, Ch. 1, Vol. 2 (Dordrecht: Springer Netherlands, 2009)

Roger G. O'Neil and Stefan Heller, "The mechanosensitive nature of TRPV channels," *Pflügers Archiv - European Journal of Physiology* 451, no. 1 (5, 2005): 193-203.

V. Benfenati et al., "Expression and functional characterization of transient receptor potential vanilloid-related channel 4 (TRPV4) in rat cortical astrocytes," *Neuroscience* 148, no. 4 (September 21, 2007): 876-892.

Dombeck DA, Khabbaz AN, Collman F, Adelman TL, Tank DW. Imaging large-scale neural activity with cellular resolution in awake, mobile mice. *Neuron*. Oct 4 2007; 56(1):43-57.

Gordon G., Choi, H., Rungta, R., Ellis-Davies G., & MacVicar, B., "Brain metabolism dictates the polarity of astrocyte control over arterioles," *Nature* 456, no. 7223 (December 11, 2008): 745-749.

V. M. Blanco, J. E. Stern, and J. A. Filosa, "Tone-dependent vascular responses to astrocyte-derived signals," *AJP: Heart and Circulatory Physiology* 294, no. 6 (2, 2008): H2855-H2863.

Girouard H, Bonev AD, Hannah RM, Meredith A, Aldrich RW, Nelson MT., "Astrocytic endfoot Ca2+ and BK channels determine both arteriolar dilation and constriction," *Proceedings of the National Academy of Sciences* 107, no. 8 (February 23, 2010): 3811-3816.

Julien Chuquet, Liad Hollender, and Esther A. Nimchinsky, "High-Resolution In Vivo Imaging of the Neurovascular Unit during Spreading Depression," *J. Neurosci.* 27, no. 15 (April 11, 2007): 4036-4044.

Chapter 5

Conclusion

In Chapter 2, we proposed the hypothesis that a potentially significant source of feedback regulation of brain activity may have been overlooked. The physical architecture of vasculature, astrocytes, and neurons in the brain provide circumstantial evidence for the hypothesis. We postulated that hemoneural modulation could be direct, as when neural processes are in direct functional contact with vessels (e.g. through nitric oxide or mechanoreceptors impacted by vasodilation), or indirect, through modulation of astrocytes. *In vitro* work from Garthwaite (2006) provided evidence for the direct route, while Kozlov (2008) and Angulo (2004) showed neural effects of mechanical perturbations of vasculature acting through astrocytes.

We suggested that it would be evolutionarily favorable for the information processing functions of the brain to be both integrated with and dependent on the underlying biological substrate.

Complex systems in general are likely to show a degree of "generative entrenchment" – that is, as a structure becomes more complicated over time, activities will tend to get multiplexed onto each other, with specializations building on shared cellular infrastructure simply because it is already available. Thus even specialized functions such as information processing in neurons are likely to share infrastructure with common permissive functions such as metabolism. Demonstrating this pushes us towards a more intensely *biological* view of brain function, in contrast to a functionalist view that takes the brain to be essentially like a computer, whose computational operations are only accidentally biological, rather than necessarily so.

As described in Chapter 3, we developed a method for independent control of blood flow *in vivo* to experimentally probe the impact of dilation on neocortical dynamics in astrocytes. In the course of testing the independence of pinacidil, we found that astrocytes in slice were sensitive to the rate of ACSF flow over the slice, perhaps as a result of their mechanosensitive channels.

Pursuing the mechanosensitive channels further in Chapter 4, we found that a strong dilation induced by direct injection of pressure into a vessel in slice was sufficient to induce

depolarization in all astrocytes tested, and to produce some effect in 50% of the neurons tested as well. These effects were typically 'excitatory', including depolarization, increase in minis, increase in spontaneous firing rate.

We then turned to 2-photon imaging to see if hemoneural effects like the mechanosensitivity found in slice could be seen in vivo, using pinacidil as the vasodilatory stimulus. We found that a large slow increase in vessel diameter (10-20% over 30-60 seconds) induced a corresponding increase in calcium levels in astrocytes, with the effect starting earlier at the endfeet and spreading to the soma. We also found two instances of genuine spreading calcium waves triggered by vasodilation, but this phenomenon was rare.

Focusing on shorter timescales in the same set of imaging data (Part 3), we found complicated patterns of coupling between astrocytes and vasculature that appeared to be symmetrical with respect to cross-correlational lag time. Being careful not to claim causation where we can only confirm correlation, we note that the changes in astrocytic endfoot calcium are no more likely to predict changes in vessel diameter than vice versa. We also found a strong correlation between an increase in calcium and a subsequent (~ 1 second later) decrease in vessel diameter when the vessel was undilated or mostly recovered from dilation. This correlation, which has not previously been shown *in vivo*, is consistent with the causal effects of increases in calcium on vessels at baseline dilation in well-oxygenated conditions, as described by a number of other groups working in slice.

These suggest many more experiments, leading in two directions. The first, to better characterize the fine scale dynamics of endfeet and vascular dynamics, will require more local and faster time scale control of blood flow. Ideally we would be able to control the diameter of a vessel at a single location, affecting just a few nearby endfeet, with the ability to contrast the behavior of astrocytes and neurons at that location with those nearby but closer to a non-dilated vessel. It would also be very interesting to see effects of vasoconstriction, something we have so far not attempted because there are no vasoconstrictors that do not also directly affect astrocytes and neurons. One way to solve both problems would be to use optogenetics to control vascular smooth muscle directly.

The second would be to follow the effects of the astrocytic perturbations we have seen, and ask if and how they modulate neural responses. One example is presented in the Appendix, but over the population observed, variability of the effects on evoked responses in both astrocytes and neurons is high, and no more complete characterization has been made. This may be due to differing sensitivity in different cell-types, or differential sensitivity of penetrating vessels to pinacidil-induced pial arteriole dilation. Direct control of penetrating vessels would allow us to better answer this question. Also, spontaneous firing rates are low in barrel cortex, and our evoked responses tended to vary over time even in the baseline condition. Perhaps effects of vascular changes on probability of firing would be easier to see in areas with higher firing rates.

Another question raised by our investigations is whether cells are more sensitive to *changes* in vessel diameter, or rather to the absolute state of dilation (or blood flow). Higher velocity changes were more likely to elicit spiking in the mechanical stimulation studies, and both examples of dilation-induced calcium waves in vivo happened during onset of dilation when the velocity of vessel diameter change was relatively high. Some of the neurons we observed also appeared to change their firing patterns during periods when vessel diameter was changing, whether dilating or recovering from dilation, and showed similar properties during relatively stable dilated and undilated epochs during the run.

Appendix

Effects of vasodilation on evoked responses imaged in Layer 2

We imaged neurons and astrocytes together in layer 2 to see if pinacidil had effects on sensory-evoked calcium responses in those cells. Methods were as in Chapter 4.2, but with calcium indicator OGB instead of Fluo-4. Most cells showed no obvious effect relative to baseline variability over the course of a run. However, some cells did show interesting variations depending on vessel dilation state. This example is characteristic of ~2% of the cells imaged.
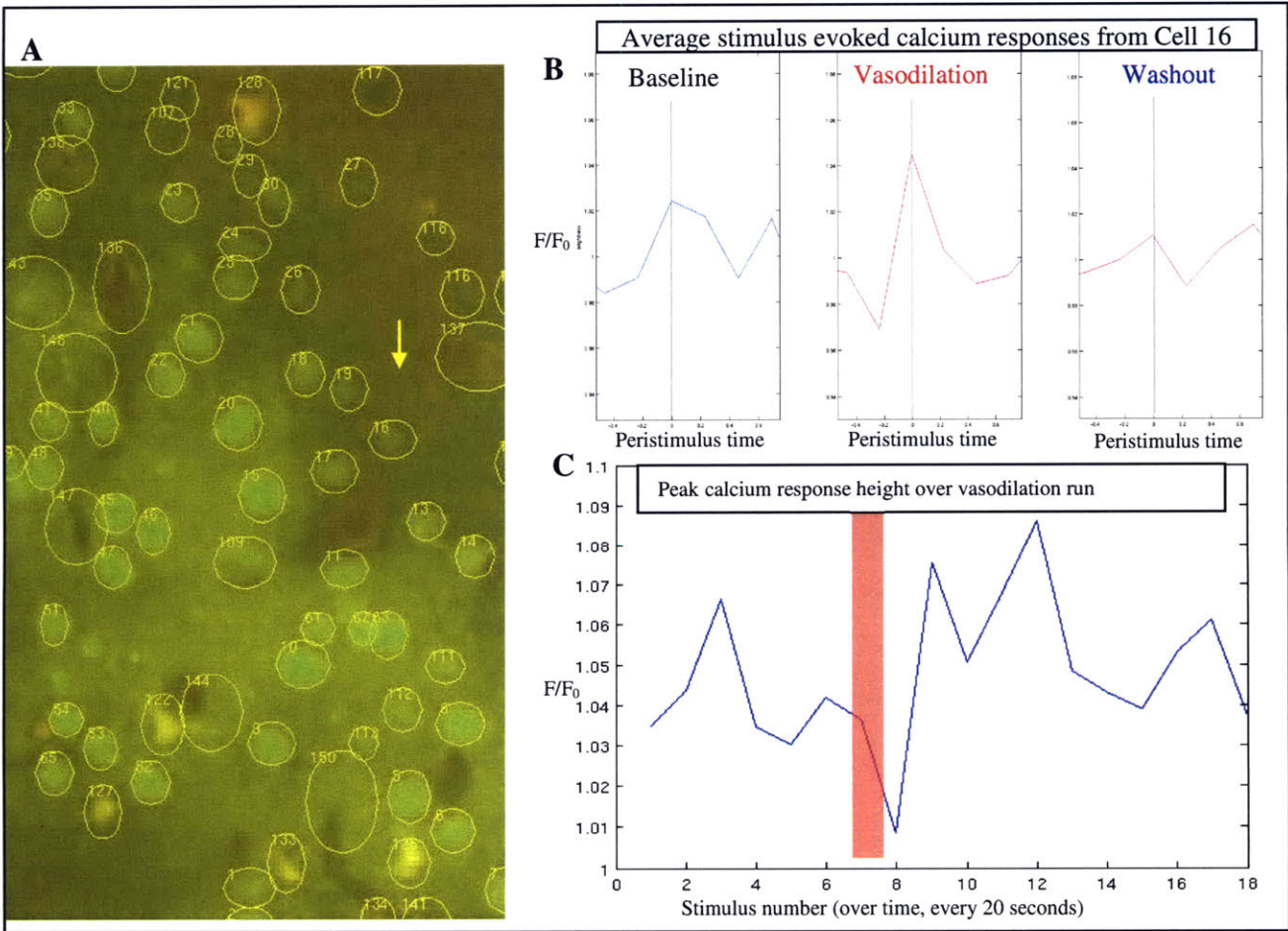
Figure 14

Figure 14 Example cell showing modulation of evoked sensory response during vasodilation. *(A) Two-photon image of area. Neurons are green (OGB), while astrocytes are yellow or orange, colabeled with SR101(red) and OGB. Arrow points to cell #16.(B) PSTH of evoked responses of cell #16 during 3 epochs of vasodilation run. Left: 0-120 sec (baseline), Middle 120-240 sec (dilation), Right: 240-360 sec (maximum dilation). Each solid colored line show the average of 6 evoked calcium responses during the epoch. Baseline (blue), mid-dilation (pink), maximum dilation (red). Stimulus onset at 0. Images were acquired at 3 Hz. (C) Evoked calcium response magnitude over vasodilation run. First stimulus was at 10 seconds into imaging run, subsequent stimuli were every 20 seconds thereafter. F/F_0 was measured during the first frame after stimulus onset (at t=0 in B)). F_0 was the average fluorescence in the 10 frames preceding each stimulus. Red bar indicates approximate onset of vasodilation.*

The example cell shown above showed an increased reliability of evoked response during the wash-in phase (center panel, **B**) as compared to the baseline period, and the period when the vessel was already dilated (and thus changing diameter more slowly). There were six vibrissal stimuli in each period, of which 3 evoked a clear response in the baseline period, 4 evoked a response in the wash-in period, and 1 evoked a response in the dilated period. There also appeared to be less spontaneous calcium fluctuation during the middle epoch, which is when the vessel would have been dilating at maximum velocity.

Other neurons showed increased evoked calcium responses during the dilated period, which decreased during wash-out, while others showed the opposite, with decreased responses upon vasodilation. We imaged over a thousand cells in 19 animals, and found that overall the responses were idiosyncratic and require further investigation to characterize with respect to cell type and the specificity of the response.